2014

Synthesis and Characterization of Coloumnar Mesophases of Novel Substituted Dibenzanthracenes and Their Donor-Acceptor Mixtures

Katie M. Psutka
Wilfrid Laurier University, psut4760@mylaurier.ca

Synthesis and Characterization of Columnar Mesophases of Novel Substituted Dibenzanthracenes and Their Donor-Acceptor Mixtures

Katie M. Psutka

Honours Bachelor of Science in Chemistry, Wilfrid Laurier University, 2012

THESIS

Submitted to the Department of Chemistry

Faculty of Science

in partial fulfillment of the requirements for

Masters of Science in Chemistry

Wilfrid Laurier University

Waterloo, Ontario, Canada, 2014

Abstract

In this thesis, the synthesis and liquid crystalline properties of a series of novel dibenz[a,c]anthracenes are reported. Specifically, two dibenzanthracenecarboxylate derivatives were prepared and were found not to exhibit a mesophase. In contrast, a series of novel *N*-substituted dibenzanthracenedicarboximides was also synthesized and found to exhibit broad columnar temperature ranges. Several dibenzanthracenedicarboximides substituted with different alkyl chains on the nitrogen atom were prepared and their mesomorphic temperature ranges were characterized. In general, it was found that having a longer, more flexible alkyl chain on the nitrogen atom resulted in a broadening of the columnar temperature range via a lowering of the melting point transition temperature.

We also prepared a novel electron donor-acceptor liquid crystal by doping a non-mesomorphic hexaalkoxydibenzanthracene with electron-poor trinitrofluorenone. In contrast to the preferred 1:1 molar ratio of donor to acceptor usually demonstrated by charge-transfer liquid crystals, this series was found to prefer a 2:1 molar ratio of donor to acceptor. Several other electron donor-acceptor series using structurally related dibenzanthracene and dibenzophenazine derivatives were found to exhibit similar behaviour suggesting that, instead of an alternating donor-acceptor stacking arrangement, more of a sandwich-like 2:1 stacking arrangement may be preferred.

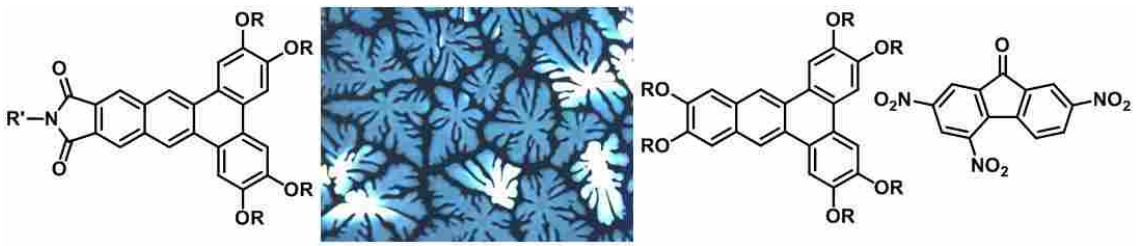

Acknowledgements

I would firstly like to thank my supervisor, Ken Maly for agreeing to take me on as his Masters student. You have been an instrumental part of both my thesis and my university experience as a whole and I will always appreciate your advice, knowledge, kindness, and belief in my abilities.

I would also like to thank everyone, past and present, with whom I worked in the Maly Lab and who contributed to my project: Josh, Joe, Michelle, Alyssa, Danielle, Laiya, Brooke, Ed, Rebecca, Matt, Willie, and Aaron. A special thanks, too, to everyone in Science Research who helped me not only with their knowledge, but also with their friendship.

I would also like to extend a special thank you to my parents for their never-ending support and encouragement - I could not have done it without you. I also can't forget my sister, Jen, who has been a great source of humour and friendship over the years. And, of course, my dogs, Indiana and Ranger, for making sure I got my daily dose of sunshine on our walks.

I would also like to acknowledge the help of Dr. Vance Williams and Kevin Bozek at SFU for their help with XRD collection and analysis. Finally, I would like to thank all of the organizations who have contributed funding for this project: Wilfrid Laurier University, NSERC, the Canada Foundation for Innovation, and the ACS Petroleum Research Fund.

Table of Contents

List of Figures

List of Tables

List of Schemes

Abbreviations

AIBN	2,2′-Azobis(2-methylpropionitrile)
ASAP	atmospheric solids analysis probe
aq.	aqueous
a.u.	absorbance units
$(Bpin)_2$	bis(pinacolato)diboron
$CDCl_3$	deuterated chloroform
Col_h	hexagonal columnar
Col_{ob}	oblique columnar
Col_r	rectangular columnar
CT	charge-transfer
d	doublet
DBA	dibenzanthracene
DBP	dibenzophenazine
DCM	dichloromethane
DMF	dimethylformamide
DMSO	dimethyl sulfoxide
DSC	differential scanning calorimetry
EtOH	ethanol
eq.	equivalents
g	grams
HAT	hexaalkoxytriphenylene
HBC	hexabenzocoronene

HEB	hexaesterbenzene
HET	hexaestertriphenylene
HOMO	highest occupied molecular orbital
HRMS	high resolution mass spectrometry
Hz	Hertz
J	coupling constant
LCD	liquid crystal display
LUMO	lowest unoccupied molecular orbital
m	multiplet
M	molar
MeOH	methanol
MHz	Megahertz
mL	milliliters
mmol	millimole
mol	mole
NBS	n-bromosuccinimide
nm	nanometer
NMR	nuclear magnetic resonance
OLED	organic light emitting diode
PAH	polycyclic aromatic hydrocarbon
POM	polarized optical microscopy
s	singlet
t	triplet

T_c	clearing temperature
TCNQ	tetracyanoquinodimethane
TCx	triphenylene carboximide
TEB	tetraesterbenzene
TGA	thermogravimetric analysis
THF	tetrahydrofuran
T_m	melting temperature
TNF	trinitrofluorenone
XRD	X-ray diffraction
δ	chemical shift

Chapter 1 Introduction

1.1 Introduction to Liquid Crystals

Liquid crystalline materials are a unique class of compounds that possess a phase of matter between that of a crystalline solid and an isotropic liquid. First discovered in the late 19th century, these compounds maintain order at the molecular level, like crystalline solids, while still exhibiting the liquid property of disordered flow.[1] The liquid crystallinity results from the interplay of two distinct constituents of the molecule: the crystalline character results from the interactions between the cores while the liquid character is derived from the saturated alkyl chains surrounding the rigid, aromatic cores.[2] These compounds are described as mesogens since they can display a mesophase, or intermediate phase, of matter.

Liquid crystals were first discovered in 1888 by Friedrich Reinitzer who, upon attempting to determine the melting point of cholesteryl benzoate, noticed two melting points: one at 145.5 ^{o}C to a cloudy liquid and a second at 178.5 ^{o}C to a clear liquid.[3] Physicist Otto Lehman studied this behaviour further, initially describing it as 'double melting'.[4] He would later coin the term 'liquid crystal' to better describe this homogenous phase of matter that shared properties of both a solid and a liquid. After their initial discovery, more research into liquid crystalline materials followed and in 1907 Daniel Vorländer reported that the liquid crystalline phase was the result of a straight molecular structure.[5] These rod-shaped compounds, known as calamitic liquid crystals (refer to Figure 1-1), quickly became the main area of research into liquid crystalline materials and currently form the basis for liquid crystalline displays.

Initially, it was thought that only these rod-shaped molecules displayed liquid crystalline properties.[6] However, several experimental studies and theoretical predictions[7-10] suggested the existence of a different type of mesogen, with a structure significantly different from the already known rod-shaped liquid crystals. In 1977 the first evidence for discotic mesogens, or disc-shaped molecules that display a liquid crystalline phase, was reported by Chandrasekhar *et al*.[11] This discovery developed into a whole new area of liquid crystal research, including new directions for research into organic electronics and photovoltaics.[12-14] Due to this, discotic liquid crystals have garnered significant attention in recent years.

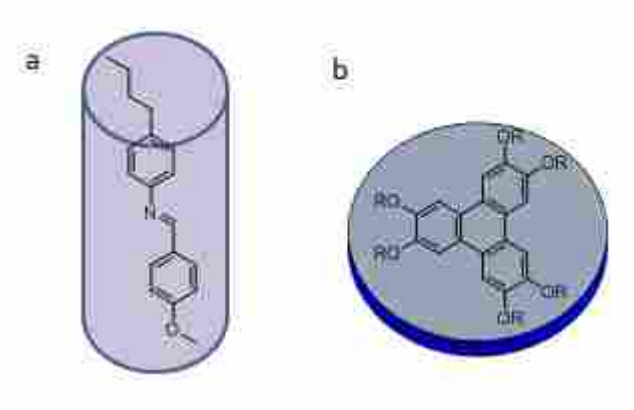

Figure 1-1: *a) A representative calamitic (rod-shaped) mesogen. b) A representative discotic (disc-shaped) mesogen.*[15]

There are two main classifications of liquid crystals: lyotropic and thermotropic. A lyotropic mesogen forms a liquid crystalline phase only in the presence of a solvent and contains both a hydrophobic group and a hydrophilic group in a structure similar to that of phospholipids.[16] In comparison, thermotropic discotic mesogens have a mesophase that is observed over a certain temperature range.[16] Modifications to the groups substituted on the aromatic core of the mesogen can affect the temperature range at which the molecule displays liquid crystallinity.

There are two important transition temperatures that occur for thermotropic liquid crystals: the melting temperature (T_m) and the clearing temperature (T_c) (Figure 1-2). The melting temperature is when the mesogen melts from a solid to a liquid crystal. Similarly, the clearing temperature is when the liquid crystal melts to an isotropic liquid. If these transitions are observed on both heating and cooling, the phases are called enantiotropic and are thermodynamically stable. If the liquid crystal phase is seen only on cooling, the phase is called monotropic and it is a metastable phase.

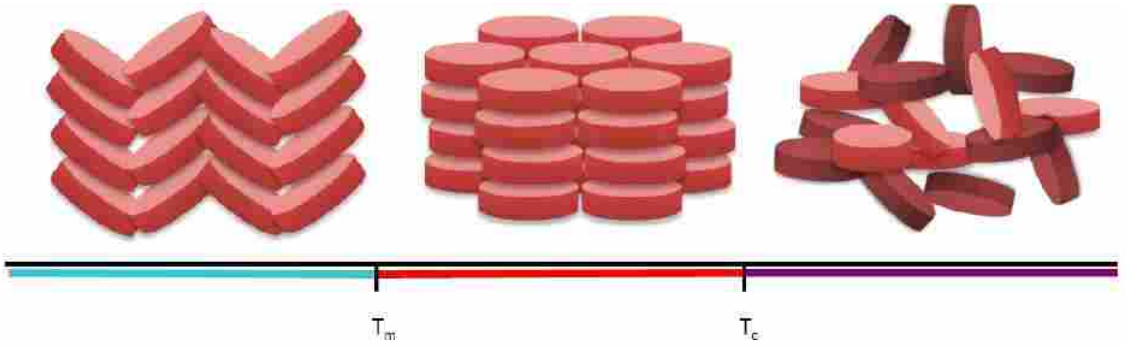

Figure 1-2: *Typical transitions for discotic liquid crystals: the crystal state, the liquid crystal state, and the isotropic liquid state.*

My thesis will focus on thermotropic discotic liquid crystals. To better understand discotic mesogens, their typical structure, commonly seen phases, and mesophase characterization will be discussed.

1.2 Discotic Liquid Crystals

Typically, discotic mesogens, such as alkoxy triphenylenes, consist of a rigid aromatic core surrounded by approximately six to eight flexible side chains (Figure 1-3). Depending on the shape and symmetry of the molecule, however, there are several liquid crystalline phases that can be observed with discotic mesogens, including nematic, smectic, cubic, and columnar phases.

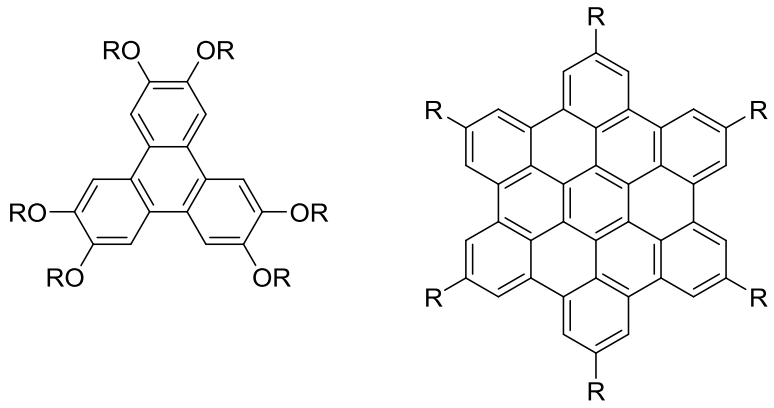

Figure 1-3: *Representative examples of discotic liquid crystals.*

1.2.1 Nematic Phases of Discotic Mesogens

The nematic phase is the least ordered mesophase, in which molecules have a high-degree of long-range orientational order, but no long-range positional order.[2] It can be further subdivided into three main categories: discotic nematic, chiral nematic, and columnar nematic (Figure 1-4).

The discotic nematic phase is the least ordered and most symmetric mesophase of the nematic mesophases.[17] In this phase, the short molecular axes of the discotic mesogens orient in a parallel manner, while the molecules still maintain full translational and rotational freedom around this axis.[2] The chiral nematic phase can occur in mixtures of discotic nematic and chiral dopants and in pure chiral discotic molecules[18] and is characterized by a helical arrangement of molecules. The columnar nematic phase is characterized by one-dimensional columnar stacking, but does not have two-dimensional ordering of the stacks.[19] Recently, a fourth nematic phase has been reported. Referred to as the nematic lateral phase, in this phase the discotic mesogens form supramolecular aggregates which then display a nematic arrangement.[20]

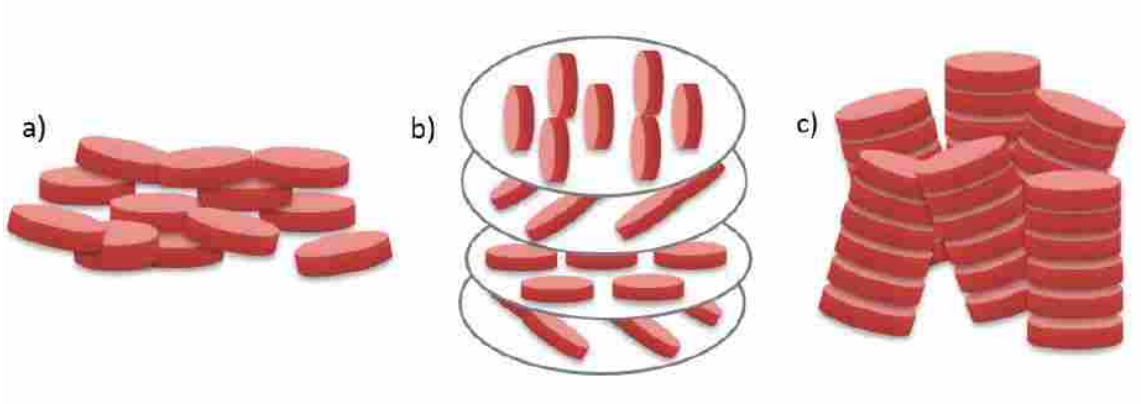

Figure 1-4: *Structures of the various nematic phases; a) discotic nematic, b) chiral nematic and c) columnar nematic.*[2]

1.2.2 Smectic Phases of Discotic Mesogens

Considered a rare phase for discotic mesogens, a smectic phase occurs when there is a reduced or uneven number of alkyl chains surrounding the core of the molecule. In this phase the disks are organized into layers that are separated by sublayers of peripheral chains.[21] In the smectic A phase, the molecules are oriented along the mesogen normal, while in the smectic C phase the molecules are tilted away from the normal.[21] An example of a discotic mesogen displaying a smectic phase is the ortho-terphenyl crown ether[22] seen in Figure 1-5.

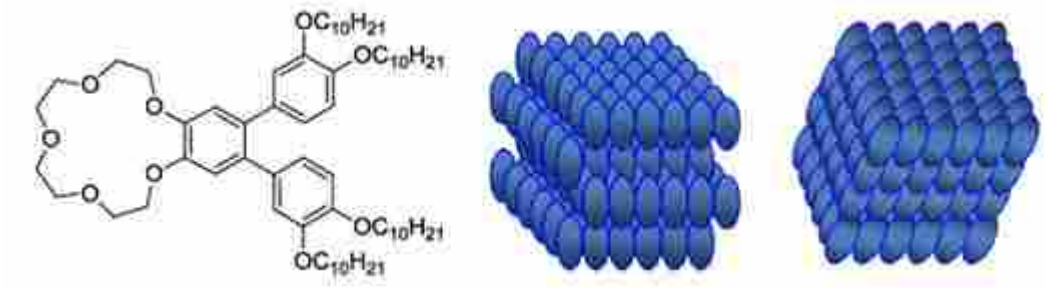

Figure 1-5: *o-terphenyl crown ether that displays a smectic discotic phase.*[22] *Schematic representations showing the smectic A and smectic C phases.*[2]

1.2.3 Cubic Phase

Although more commonly seen with lyotropic liquid crystals, some discotic phthalocyanines have been seen to demonstrate a cubic phase.[23,24] This phase consists of a network of branched columns of discotic molecules (Figure 1-6).

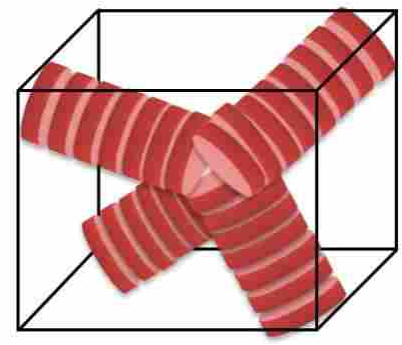

Figure 1-6: *A graphical representation of a cubic phase.*[2]

1.2.4 Columnar Phases

Columnar phases are the most common mesophases exhibited by discotic liquid crystals. In columnar phases, the discotic molecules self-assemble into extended one-dimensional columns which then arrange into one of several distinct two-dimensional lattices. Three of the most common arrangements include rectangular columnar (Col_r), oblique columnar (Col_{ob}), and hexagonal columnar (Col_h) (Figure 1-7).

The rectangular columnar phase is characterized by the rectangular packing of the columns of discotic mesogens, with each column being surrounded by disordered aliphatic chains.[2] An oblique mesophase is the result of the molecules stacking into columns with a tilted orientation.[2] The hexagonal columnar mesophase is the most common. It is characterized by the efficient hexagonal packing arrangement that the columns adopt.

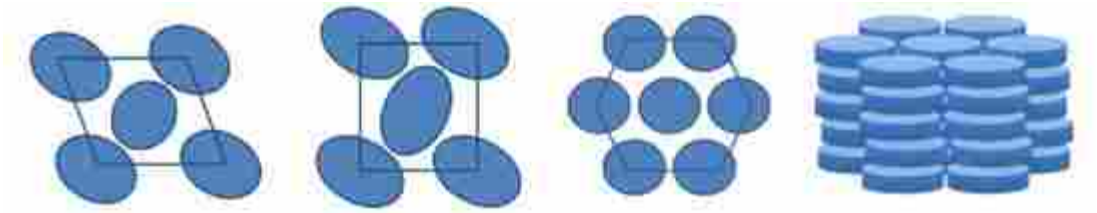

Figure 1-7: *Schematic representation of the oblique, rectangular, and hexagonal columnar mesophases.*[15]

1.3 Mesophase Characterization

1.3.1 Polarized Optical Microscopy

Polarized optical microscopy (POM) is a technique that can be used for initial characterization of liquid crystals. Liquid crystalline compounds are optically birefringent, meaning that the materials have a different refractive index depending on the orientation of the sample.[25] This distinctive property can be detected using polarized optical microscopy. With this technique, a sample of the material is placed between two linear polarizing filters that are perpendicular to each other. Since liquid crystals are birefringent, the plane polarized light is rotated as it passes through the sample and is transmitted through the cross-polarizers. Furthermore, many polarized optical microscopes are equipped with a heating stage that allows the sample to be heated or cooled, so that the presence of a liquid crystalline phase can be detected and the transition temperatures defined.

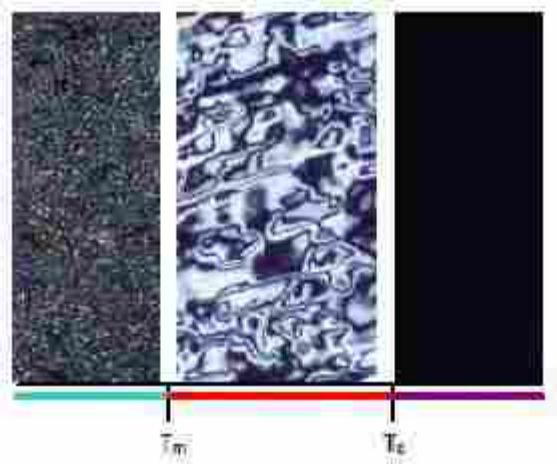

Figure 1-8: *Phase changes from crystalline solid, to liquid crystalline mesophase, to isotropic liquid, as viewed under a polarized optical microscope.*

With POM, different characteristic textures for each of the mesophase types are observed. Therefore, a polarized optical micrograph can also be used to empirically classify the observed phase; although further characterization is required to fully identify the mesophase.

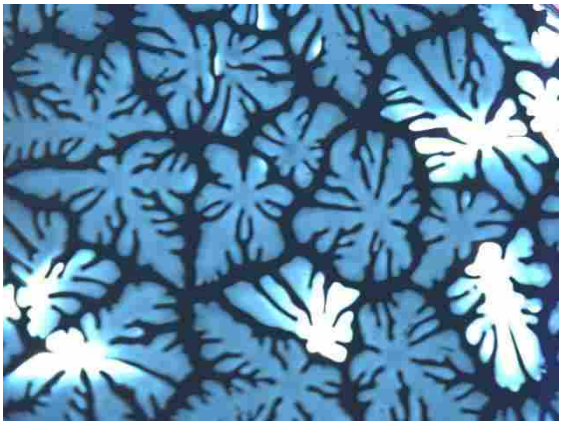

Figure 1-9: *The texture of a columnar hexagonal mesophase under a polarized optical microscope.*

1.3.2 Differential Scanning Calorimetry

Differential scanning calorimtery (DSC) is a technique that can be used to further characterize the mesophase of a liquid crystal. In this technique, the desired sample is cyclically heated and cooled alongside a reference cell. When the desired

sample undergoes a phase transition, more or less heat is required to maintain a constant temperature between the sample and the reference,[26] dependent on whether the transition is an exothermic or an endothermic process. For example, a transition from a liquid to a liquid crystal, which is an exothermic process, requires less heat to maintain a constant temperature between the sample and the reference cell; whereas a transition from a solid to a liquid crystal, which is an endothermic process, requires more heat. The difference between the sample and the reference provides both the enthalpy of the transition and the precise temperature at which the transition occurred. A typical DSC can be seen in Figure 1-10, where the peaks correspond to the phase transition temperatures and the enthalpies of these transitions are found via integration under the curve.

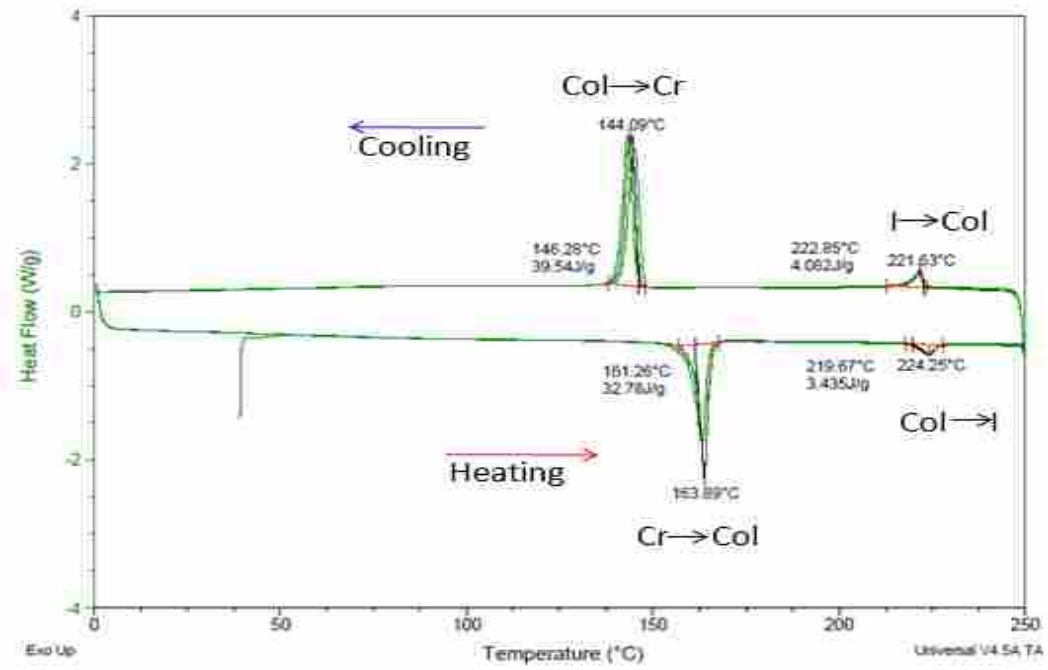

Figure 1-10: *A representative DSC of a liquid crystalline compound showing crystal (Cr) to columnar (Col) and columnar to isotropic liquid (I) transitions.*

With liquid crystalline materials, a DSC typically shows two transitions: a solid to liquid crystal transition and a liquid crystal to liquid transition. This data can be used

to corroborate the data observed via POM. Some, however, may also show transitions that may not be visible by microscopy, including transitions from a liquid crystal to a glassy phase or a transition from one distinct columnar phase to another distinct columnar phase.

1.3.3 Powder X-Ray Diffraction

Powder X-ray diffraction is a technique used for structural characterization of materials by using X-ray on powdered samples.[27] In this technique, an X-ray is passed though a sample in the liquid crystalline state. As it passes through the sample, the X-ray is scattered in multiple dimensions. It is then collected by a detector, averaged, and projected onto one dimension, leading to smooth diffraction rings around the axis of the beam.

X-ray diffraction can give the long range intercolumnar spacing and the symmetry of packing of a material in the columnar phase. This information can be used to help identify the type of phase demonstrated by the liquid crystalline material. For example, the (100) and (110) reflections, which are typically seen with a hexagonal columnar stacking arrangement, are measurements which can be used to calculate the distance between two columns in the columnar stack based on their trigonometric relationship (Figure 1-11).

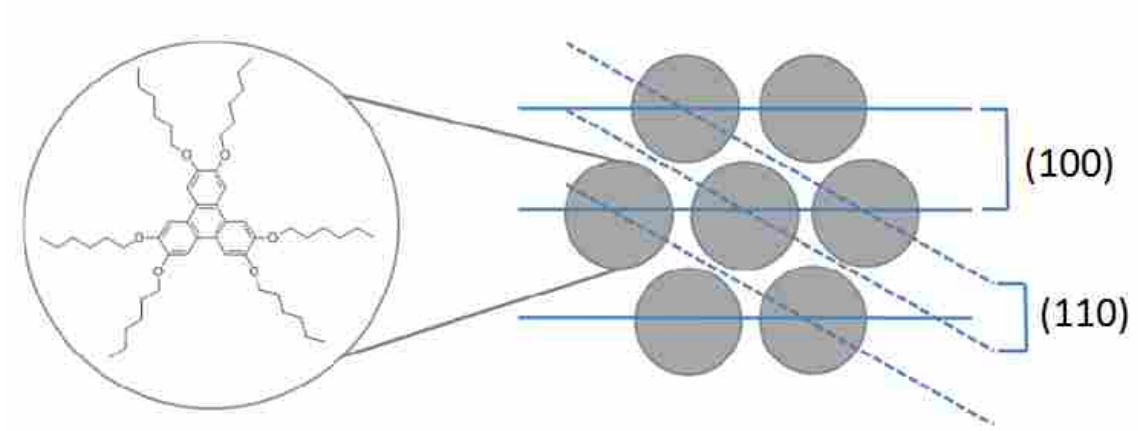

Figure 1-11: *A representation of the planes typically seen with a hexagonal columnar stacking arrangement.*[27]

1.3 Structures of Discotic Liquid Crystals

1.3.1 Polycyclic Aromatic Hydrocarbons

One of the simplest discotic molecules to demonstrate liquid crystalline behaviour contains a core consisting of a single benzene ring. First reported by Chandrasekhar and coworkers, hexaesterebenzene (HEB) derivatives have been shown to have a liquid crystalline phase (Figure 1-12).[11,28-29] Similarly, tetraesterbenzene (TEB) derivatives have also been shown to demonstrate a liquid crystalline phase, though over a much narrower temperature range (Figure 1-12).[28,30] Since these initial discoveries, these benzene-based mesogens have been broadly studied in order to better understand the mesophase behaviour and molecular interactions involved in stabilizing their columnar phases.[31-33]

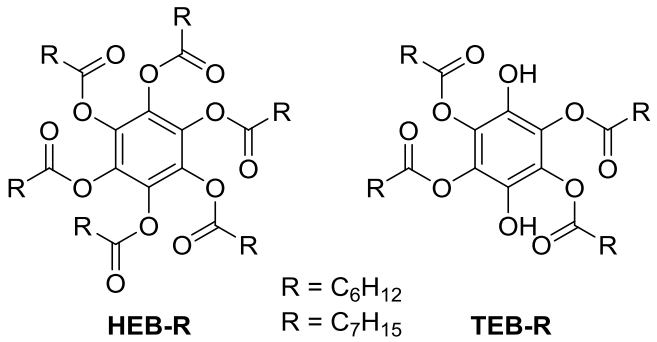

Figure 1-12: *Esterbenzene discotic molecules.*[11,28]

Table 1-1: *Phase transition temperatures of esterbenzenes.*

Structure	Phase Transition Temperature (^{o}C)	Reference
HEB-6	Cr 86 Col 86 I	11
HEB-7	Cr 80 Col 84 I	11
TEB-6	Cr 55 Col 57 I	28
TEB-7	Cr 68 Col 70 I	28

The majority of discotic mesogens, however, consist of a more complex core of polycyclic aromatic hydrocarbons (PAH). PAHs are a distinctive class of compounds that consist of multiple aromatic rings fused to one another and often form the core aromatic frameworks of liquid crystalline materials.

One of the most well-studied PAH cores are triphenylene molecules; with over 500 examples of triphenylene based discotic liquid crystals. First reported as a novel core for discotic liquid crystals in 1978,[34] triphenylenes have since garnered a significant amount of attention from liquid crystal scientists. Due to this, there are now a variety of triphenylene derivatives that are easily accessible, thermally and chemically stable, show a variety of mesophases, and have charge-transport properties that are promising for future applications.[35,36]

Another important PAH core for discotic liquid crystals is hexabenzocoronene (HBC) core. HBC is one of the largest and most symmetrical PAHs to act as a core for

a discotic liquid crystal.[37] HBC and its derivatives have been shown to have broad mesophases and potential applications in a variety of proposed devices including field effect transistors and photovoltaic cells.[38] Representative examples of triphenylene and hexabenzocoronene based discotic liquid crystals can be seen in Figure 1-13.

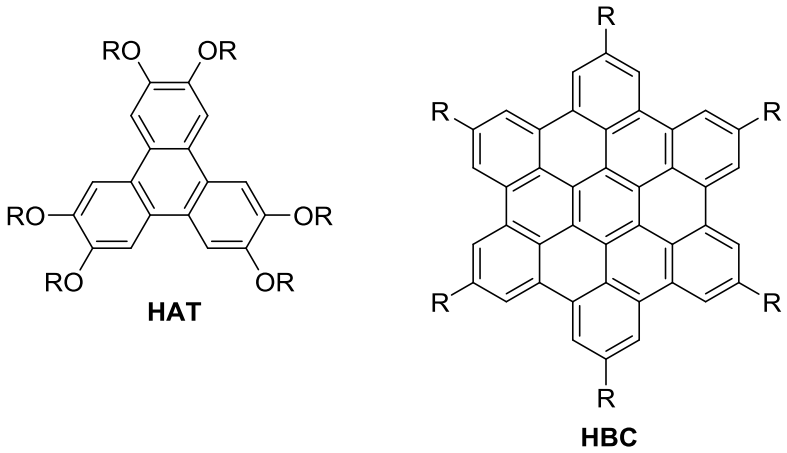

Figure 1-13: *Representative hexaalkoxytriphenylene (HAT) and hexabenzocoronene (HBC) liquid crystals.*

1.3.2 Important Properties of PAHs

Discotic mesogens typically contain a polycyclic aromatic hydrocarbon (PAH) core. PAHs have a number of useful properties that make them important in the synthesis of liquid crystalline compounds, including excellent charge transport properties which arise from the characteristically low HOMO-LUMO gap of this family of compounds.[39] In addition, when in columnar stacks, PAHs demonstrate effective π-π orbital overlap, leading to improved electron delocalization and charge mobility to occur along the axis of the column.[40] Essentially, due to the characteristically low HOMO-LUMO gap of polycyclic aromatic hydrocarbons, the PAH core of liquid crystalline molecules can be easily oxidized or reduced. Then, in the columnar stacking

arrangements, the molecules are positioned close enough that the electron can move along the column and carry the charge with it.

1.3.3 Structural Modifications to the PAH Core

To be useful in applications, however, liquid crystalline materials must display a columnar phase over a broad temperature range. Therefore, an understanding of the factors that influence mesophase temperature range is important for the design of new materials. Studies have shown that, in addition to the importance of the size and shape of the aromatic core, the nature of the substituents attached to the aromatic core also have a significant effect on the ability of a compound to form a liquid crystalline phase.[40-43]

A typical discotic liquid crystal consists of an aromatic core surrounded by several flexible side chains. It has been observed that varying the length of these flexible side chains can have a large influence on the overall temperature range at which the mesophase occurs.[42,44-46] Furthermore, it is believed that PAHs bearing electron withdrawing substituents result in increased dispersion interactions that promote π-stacking and, therefore, have an increased propensity to form columnar phases.[43]

The symmetrical triphenylene molecule, hexaalkoxytriphenylene (HAT) demonstrates the effect that changing the alkyl chain length and functional groups on the core of the molecule can have on the mesophase behaviour of a compound (Figure 1-14). An increase in the length of the alkoxy chains attached to the triphenylene core results in a decrease in the overall breadth of the liquid crystalline range (Table 1-2).[47] Similarly, a switch from alkoxy chains to ester linkages to give a hexaestertriphenylene

derivative (HET) results in a significant change to the mesophase behaviour even though the core size and overall length of the chains remains constant[47] (Table 1-2).

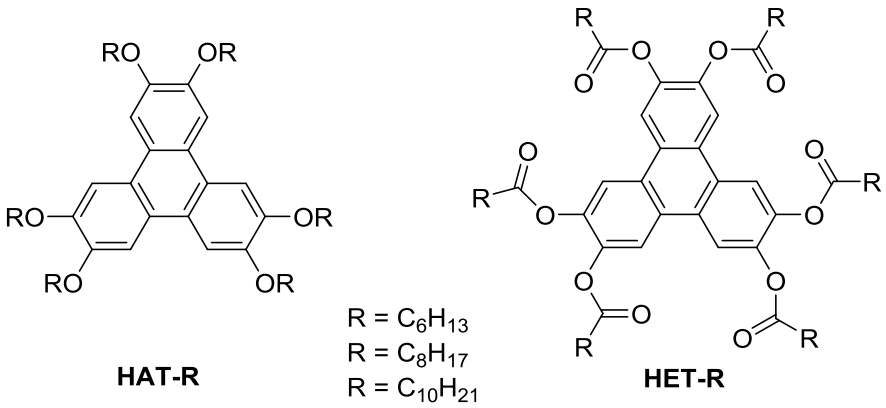

Figure 1-14: *Triphenylene-based discotic liquid crystals.*[47]

Table 1-2: *Phase transition temperatures of triphenylene discotic liquid crystals.*

Structure	Phase Transition Temperature (^{o}C)	Reference
HAT-6	Cr 68 Col 97 I	47
HAT-8	Cr 67 Col 86 I	47
HAT-10	Cr 58 Col 69 I	47
HET-6	Cr 108 Col 120 I	47
HET-8	Cr 62 Col 125 I	47
HET-10	Cr 67 Col 121 I	47

Furthering this trend is a series of triphenylene carboximides recently reported by Wu and coworkers (Figure 1-15). The imide substituents attached onto the triphenylene core combine an electron withdrawing nature with the flexbility of an alkyl chain. With this series, a significant change to the mesophase behaviour was again observed, with the imide substituents increasing the overall breadth and temperature range of the liquid crystalline phase[48] (Table 1-3).

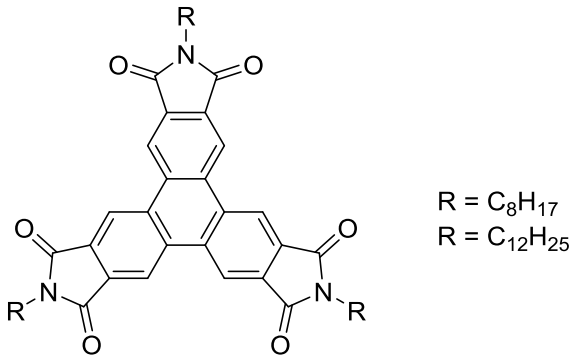

Figure 1-15: *Triphenylene carboximide discotic liquid crystals.*[48]

Table 1-3: *Phase transition temperatures of triphenylene carboximide discotic liquid crystals.*

Structure	Phase Transition Temperature (^{o}C)	Reference
TCx-8	Cr 158 Col 228 I	48
TCx-12	Cr 46 Col 218 I	48

1.5 Donor-Acceptor Liquid Crystals

Electron donor-acceptor columnar liquid crystals are a subclass of discotic liquid crystals. These columnar materials consist of an electron-rich 'donor' compound and an electron-poor 'acceptor' compound that self-assemble into alternating columnar stacks (Figure 1-16).[49]

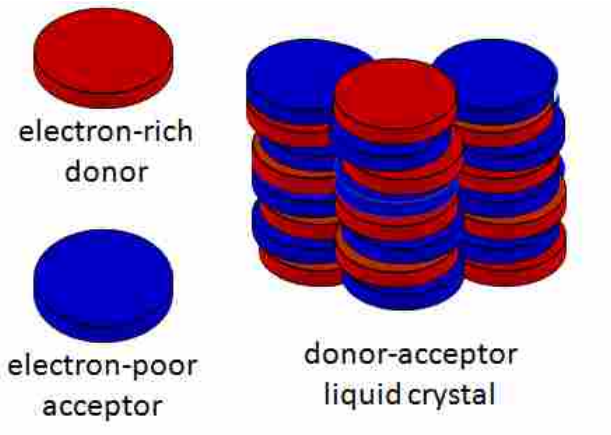

Figure 1-16: *Schematic representation of an electron donor-acceptor liquid crystal.*[49]

This electrostatic matching can lead to mixtures that have far different properties than either of the starting materials. The formation of a donor-acceptor liquid crystal can lead to stabilization and/or induction of a columnar mesophase, and has also been shown to improve charge mobility.[49-52] In addition, donor-acceptor liquid crystals often display a broad absorbance band that is unique to the mixture of components.[51] This absorbance band is referred to as a charge-transfer (CT) absorption band and results from the excitation of an electron from the highest occupied molecular orbital (HOMO) of the electron-rich donor to the lowest unoccupied molecular orbital (LUMO) of the electron-poor acceptor (Figure 1-17).[49] This absorption is found in the visible region and leads to the formation of highly-coloured materials.

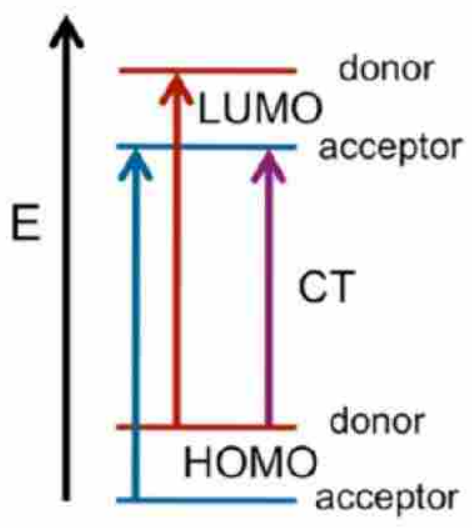

Figure 1-17: *Representation of the charge-transfer absorption characteristic to donor-acceptor liquid crystals.*[49]

Much of the initial work in this field was performed by Ringsdorf and coworkers in the early 1990s. They demonstrated that doping an electron-rich triphenylene derivative with electron-poor trinitrofluorenone as the electron acceptor in a 1:1 ratio stabilized the liquid crystalline phase of the triphenylene by means of charge-transfer

interactions between the donor and the acceptor.[53] Since then, these equimolar mixtures have been broadly studied for potential applications in opto-electronics and photovoltaics.[49,51, 54-56]

1.6 Applications of Columnar Liquid Crystals

Discotic liquid crystals have potential applications in a variety of organic electronics; including, liquid crystal displays (LCD), organic semiconductors, discotic solar cells, field effect transistors, and organic light emitting diodes (OLED).[57] In order to be useful in these applications, however, a thorough understanding of the structure-property relationships of these compounds are needed. Still, discotic liquid crystals are of particular interest in these fields due to their ability to maintain both order and fluidity in the liquid crystalline state. This gives these compounds properties similar to a single crystal, yet the mobility for the self-healing of defects.[58,59]

In columnar stacks, the molecules are positioned so spatially close to one another that there is overlap between the HOMO and LUMO of neighbouring molecules, allowing for charge transport to occur along the columnar axis. Therefore, these rigid aromatic cores surrounded by the insulating alkyl chains can be thought of as molecular wires with conductive channels - a molecular cable.[58-60] This property is important for applications in opto-electronics. In addition to their desirable charge transport properties, discotic liquid crystals also possess an intermediate band gap, making them ideal for use as organic semiconductors.

Organic semiconductors have recently attracted attention for potential use in photovoltaic solar cells. Currently, a variety of inorganic materials, including silicon are used for these applications. While they have adequate efficiencies, these materials are

expensive and difficult to prepare. In contrast, organic semiconductors are attractive for use in photovoltaics due to their relatively low cost and easy processability.[61,62] Unfortunately, however, the power conversion efficiencies of these materials are still relatively low at approximately 5%; so for discotic liquid crystals to compete, their efficiencies must be improved by an approximate factor of 2.[2]

Discotic liquid crystals also have potential applications of organic light emitting diodes. In these devices, an electric field is applied resulting in the movement of holes and electrons in their respective layers. When these layers combine at an interface, light is produced. Discotic liquid crystals have both been shown to have potential applications both in the electron transporting (n-type) and hole transporting (p-type) layers. Triphenylene derivatives, which posess high charge carrier mobility, are often used in the hole transporting layer,[63] while perylene derivatives are used in the electron transporting layer since they combine high charge carrier mobility with luminescent properties.[64] In order to be useful for applications, however, a more thorough understanding of the relationship between molecular structure and liquid crystalline properties is needed.

1.7 Previous Work

Hexaalkoxytriphenylenes (**1**) are some of the most extensively studied compounds that exhibit a columnar mesophase.[65-67] These compounds, however, exhibit a rather narrow columnar mesophase temperature range.[68] In comparison, a similar structure 10,13-dimethyl-2,3,6,7,11,12-hexakis(hexyloxy)dibenz[a,c]anthracene (**2**), which shows an elongation of one benzene ring and methyl substituents at the 10 and 13

positions, exhibits a columnar phase from 35-88 ^{o}C; suggesting that increasing the core size can effectively increase the columnar temperature range.[42]

Extending this idea, our group previously synthesized a hexaalkoxytrinaphthylene (**3**).[41] We anticipated that this molecule would display a broader columnar temperature range and possibly be a liquid crystal at ambient temperatures. Instead, the compound did not display any liquid crystalline behaviour.

In contrast, Ong *et al.* synthesized a heterocyclic analogue of compound **3**, hexakis-(decyloxy)diquinoxazlino[2,3-a:2′,3′-c]phenazine (**4**), which demonstrated a columnar phase from 86-215 ^{o}C.[69] Compounds **3** and **4** have aromatic cores of the same size, however, compound **4** contains electron withdrawing nitrogen atoms within the core while compound **3** does not. Similarly, the Williams group successfully synthesized hexaalkoxydibenzo[a,c]phenazine (**5**), which also displayed a broad liquid crystalline phase.[70] These results suggest that electron withdrawing groups are important to promote columnar behaviour.

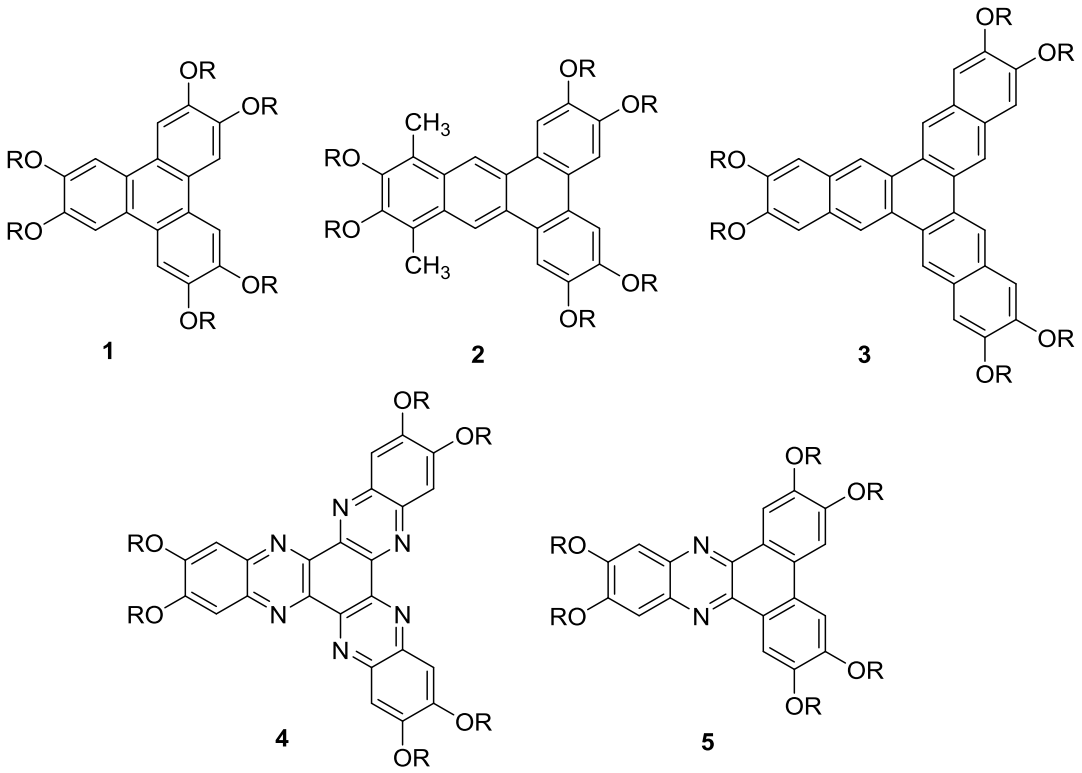

Figure 1-18: *Discotic triphenylenes and their extended analogues.*

Additional studies by Ichihara, Akopova, and Williams provide further evidence that electron withdrawing substituents can stabilize columnar mesophases (Figure 1-19).[71,72,43] Ichihara and co-workers prepared a series of cyano-substituted tetraalkoxytriphenylenes (**6**).[71] This compound differs from the parent hexaalkoxytriphenylene in that two of the alkoxy chains have been replaced with electron withdrawing cyano groups. Despite the loss of two flexible chains, however, these compounds still demonstrate columnar temperature ranges that are equal to or broader than those displayed by the parent hexaalkoxytripenylenes.[71] Akopova *et al.* prepared a series of substituted hexaalkoxytriphenylenes (**7**), which demonstrated a much broader mesophase when an electron withdrawing nitro group was present at the X position then when an electron donating amino group was present.[72] Similarly, the Williams group synthesized a series of substituted dibenzophenazines, where the

substituents were varied from electron donating to electron withdrawing (**8**). This series demonstrated a liquid crystalline phase only when electron withdrawing substituents were present; when electron donating substituents were present, no columnar mesophase was observed.[43] These results further support that theory that electron withdrawing groups are important to promote columnar behaviour.

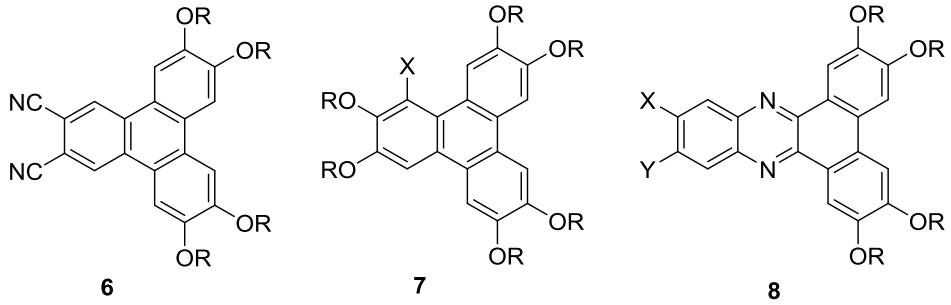

Figure 1-19: *Substituted discotic mesogens.*

1.7.1 Hexaalkoxydibenz[a,c]anthracene Derivatives

Based on these previous studies, our group synthesized a series of hexaalkoxydibenz[a,c]anthracenes using an approach developed in our laboratory (Figure 1-20). In this series, R and R' are alkyl chains of varying lengths and X and Y are various substituents, ranging from electron donating to electron withdrawing. When the X and Y positions were occupied by hydrogen atoms, no liquid crystalline phase was observed. However, when one or both of these positions were occupied by a substituent, a columnar phase was observed; with the identity of the substituent affecting the overall temperature range of the columnar mesophase.[73]

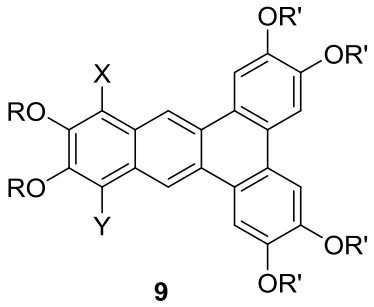

9

R = C_6H_{13}, C_8H_{17}, $C_{10}H_{21}$, $C_{12}H_{25}$
R' = C_6H_{13}, C_8H_{17}, $C_{10}H_{21}$, $C_{12}H_{25}$
X = Br, Cl, I, CN, NH_2, NO_2

Figure 1-20: *Previously synthesized hexaalkoxydibenz[a,c]anthracene series.*[73]

Interestingly, while this series did display a liquid crystalline phase with both electron donating and electron withdrawing substituents, it was observed that electron withdrawing groups stabilized the columnar phase. When the clearing point was plotted against the Hammett sigma values, a general trend was observed that the clearing point increased as the electron withdrawing nature of the substituent increased (Figure 1-21).[74] This trend fits well with the aforementioned studies performed by Akopova *et al.*[72] and the Williams group.[43]

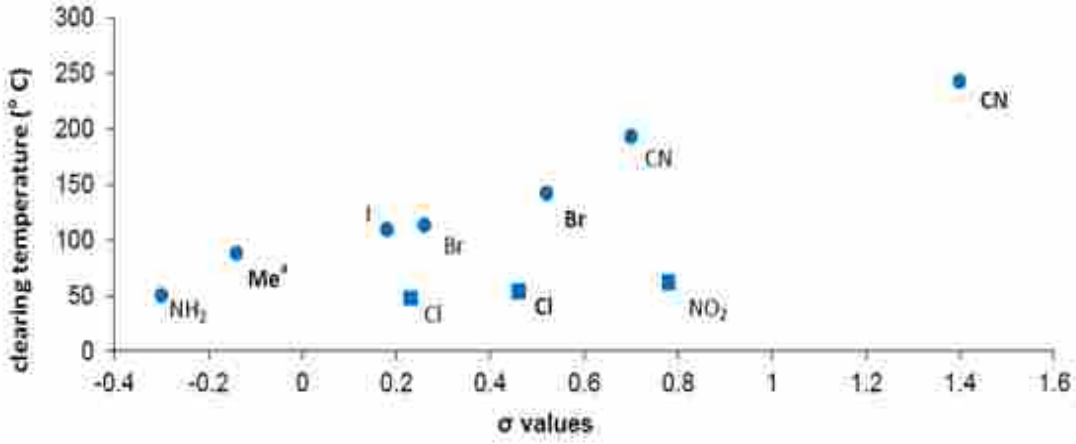

Figure 1-21: *Hammett plot of the clearing temperatures (on heating) compared to the Hammett sigma values.*[74] *The disubstituted compounds are* ***bolded*** *and are represented by the sum of their sigma values.*[74] [a]*Data is taken from Lau et al*[42]

1.7.2 Substituted 2,3,6,7-tetrakis(alkyloxy)dibenz[a,c]anthracenes

In addition to the aforementioned series, a series of substituted 2,3,6,7-tetrakis(alkyloxy)dibenz[a,c]anthracenes was also prepared, substituted with various substituents at the 11 and 12 positions and alkoxy chains at the 2, 3, 6, and 7 positions (Figure 1-22).

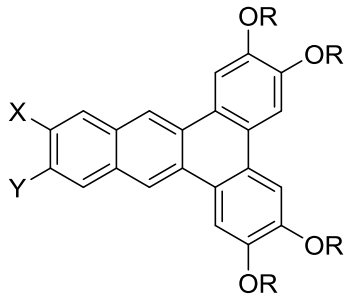

10

a X = Y = H, R = $C_{10}H_{21}$
b X = Y = MeO, R = $C_{10}H_{21}$
c X = Y = CN, R = C_8H_{17}
d X = Y = CN, R = $C_{10}H_{21}$
e X = Y = CN, R = $C_{12}H_{25}$
f X = CN, Y = H, R = $C_{10}H_{21}$
g X = CN, Y = H, R = $C_{12}H_{25}$

Figure 1-22: *Previously synthesized hexa-substituted dibenz[a,c]anthracene series.*[75]

With this series of compounds, a liquid crystalline phase was observed only when one or both of the lateral substituents were electron withdrawing cyano groups[14] (Figure 1-23). In contrast, when the lateral substituents were more electron donating groups, no liquid crystalline phase was observed.

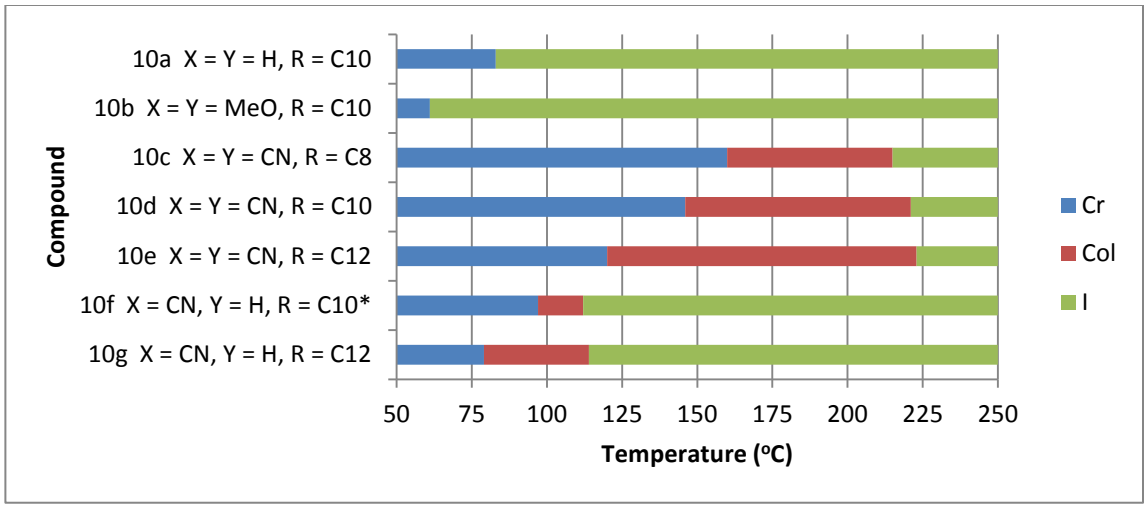

Figure 1-23: *Liquid crystal ranges of the hexa-substituted dibenz[a,c]anthracene series. The transitions are from DSC on heating.*[75] *I is an isotropic liquid, Col is a columnar phase and Cr is a crystal phase. *indicates that this is a monotropic phase that occurs only on cooling.*

This trend is consistent with our previous observation that electron withdrawing groups do stabilize the columnar mesophase. Along with the high clearing points, however, the solid to liquid crystal transition is relatively high as well; so, with this series, the solid phase is stabilized as well.[75]

1.8 Research Objectives

The objective of this research is to prepare a series of novel substituted dibenzanthracenes in order to better understand the relationship between chemical structure and liquid crystalline properties in this class of materials. Specifically, the first goals of this research are to expand the previously prepared series of hexa-substituted dibenzanthracenes by preparing ester-substituted derivatives; and, also, to prepare a novel series of imide-substituted dibenzanthracenes (Figure 1-24). By introducing substituents that combine an electron withdrawing nature, to pull electron density away from the core of the molecule, with the flexibility of an alkyl chain, we hope to see a broadening of the columnar mesophase via a lowering of the melting temperature.

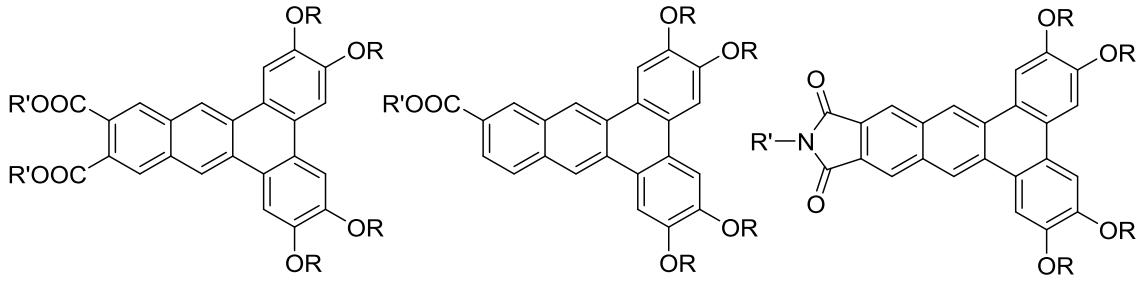

Figure 1-24: *Target dibenz[a,c]anthracenecarboxylates and dibenz[a,c]anthracenedicarboximide series.*

A second objective of this research is to prepare a novel series of electron donor-acceptor liquid crystals through the preparation of several different 1:1 mixtures of electron rich donors and electron poor acceptors. By combining donors such as hexaalkoxy[a,c]dibenzanthracene, hexaalkoxytriphenylene, hexaalkoxydibenzo[a,c]phenazine; with electron acceptors like trinitrofluorenone and tetracyanoquinodimethane (Figure 1-25) and studying their liquid crystalline properties, we hope to better understand the behaviour of these mixtures. Through the preparation of these donor-acceptor mixtures we hope both to induce a liquid crystalline phase in non-mesomorphic hexaalkoxydibenzanthracenes, and use the observed trends in behaviour to tune liquid crystalline temperature ranges. These results may lead to a better understanding of the arene-arene interactions that are occurring in these systems. In addition, these compounds may also be useful for their potential applications in the field of photovoltaics.

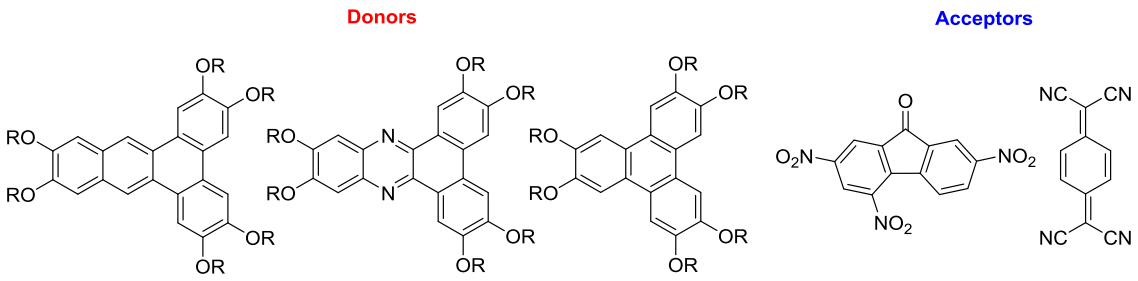

Figure 1-25: *Target electron donors and acceptors.*

Chapter 2 Synthesis and Mesomorphic Properties of Substituted Dibenzanthracenecarboxylates

2.1 Introduction

The previously synthesized hexa-substituted dibenzanthracene series (**10**) (Figure 2-1) displayed a liquid crystalline phase only when one or both of the lateral substituents were electron withdrawing cyano groups.[75] When the substituents were more electron donating methoxy groups or hydrogen atoms, a columnar phase was not observed. This fits well with results of previous studies[43,71-73] that have demonstrated the importance of electron withdrawing substituents to promote liquid crystalline behaviour.

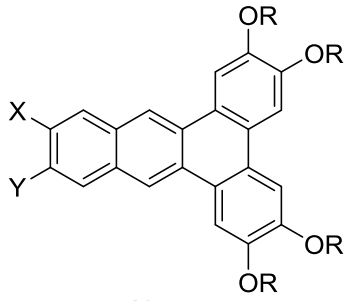

10

a X = Y = H, R = $C_{10}H_{21}$
b X = Y = MeO, R = $C_{10}H_{21}$
c X = Y = CN, R = C_8H_{17}
d X = Y = CN, R = $C_{10}H_{21}$
e X = Y = CN, R = $C_{12}H_{25}$
f X = CN, Y = H, R = $C_{10}H_{21}$
g X = CN, Y = H, R = $C_{12}H_{25}$

Figure 2-1: *Previously synthesized hexa-substituted dibenz[a,c]anthracene series.*[75]

With series **10**, when both of the lateral substituents were cyano groups, it was observed that, as the alkoxy chains became longer, the overall columnar temperature range increased via a lowering of the melting transition temperature (Figure 2-2).[75] A

similar trend was noticed with the mono-cyano derivatives although the columnar temperature ranges were much narrower; with the mono-cyano decyloxy (**10f**) derivative displaying a monotropic liquid crystalline phase only on cooling.[75]

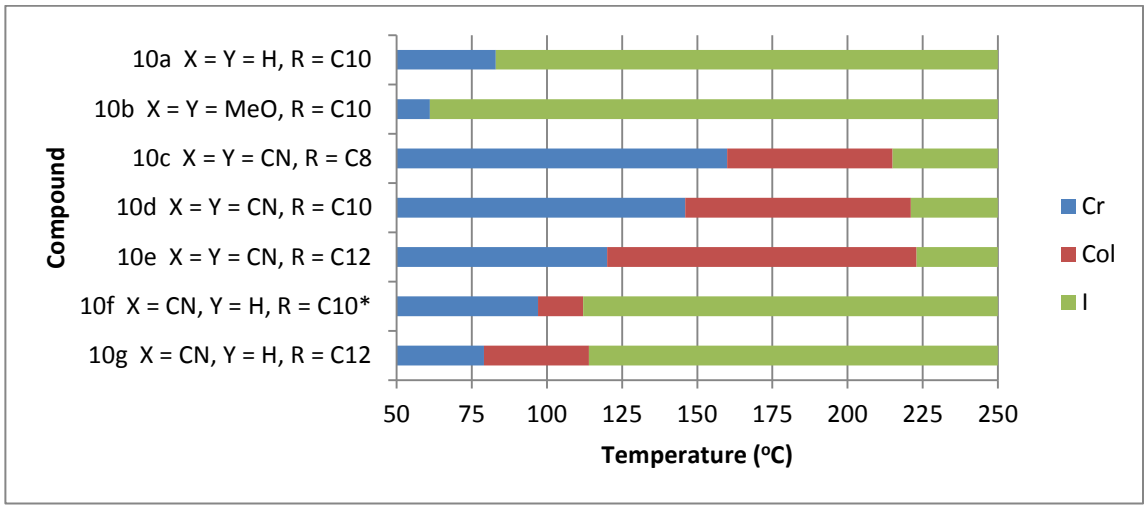

Figure 2-2: *Liquid crystal ranges of the hexa-substituted dibenz[a,c]anthracene series. The transitions are from DSC on heating.*[75] *I is an isotropic liquid, Col is a columnar phase and Cr is a crystal phase. *indicates that this is a monotropic phase that occurs only on cooling.*

Despite the observed trend, the melting transition temperatures for this series are all relatively high. This suggests that, with this series, the solid phase is also being stabilized. In an effort to lower the melting transition temperature while still maintaining liquid crystallinity, we aim to expand the series via the synthesis two additional derivatives that contain esters as the lateral substituents. Since esters are both moderately electron withdrawing and more flexible than the rigid cyano groups, we would expect to see a broadening of the columnar phase through a lowering of the melting transition temperature.

2.2 Synthetic Approach

To access the substituted 2,3,6,7-tetrakis(decyloxy)-11,12-dibenz[a,c]anthracenecarboxylate derivatives (**10h,i**) a modular approach was followed

(Scheme 2-1) that involved a Suzuki cross coupling of an aryl boronate (**13**) with a substituted dibromonaphthalene (**16**), followed by an oxidative ring closing.

Scheme 2-1: *Synthesis of dibenzanthracenecarboxylates **10h** and **10i***

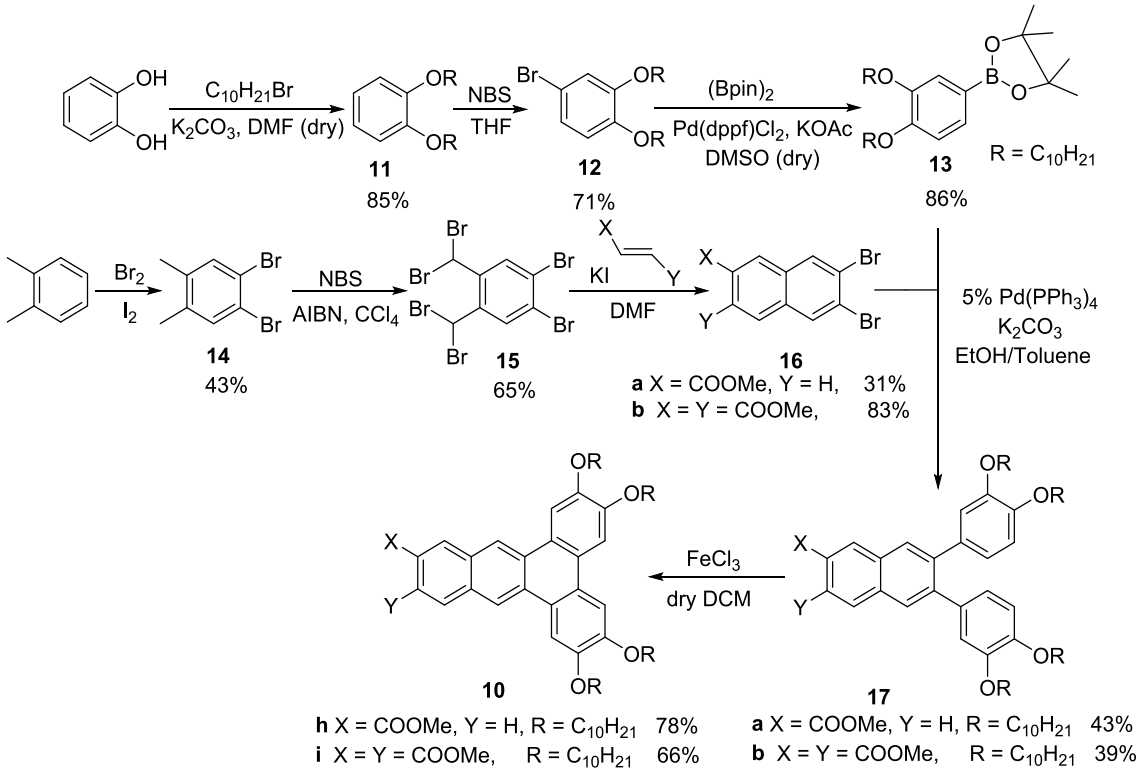

The aryl boronate necessary for the cross coupling was produced in three steps from commercially available catechol. First, catechol was alkylated[70] to produce 1,2-didecylbenzene in 85 % yield. This was followed by a bromination using N-bromosuccinimide in THF to afford **12** in a 71 % yield. The desired aryl boronate was achieved via a Miyaura borylation reaction using bis(pinacolato)diboron in the presence of potassium acetate and $Pd(dppf)Cl_2$ in anhydrous DMSO.

The substituted dibromonaphthalene was achieved in three steps from commercially available o-xylene. The o-xylene was first brominated using atomic bromine. The resulting product then underwent a benzylic bromination using N-bromosuccinimide and AIBN according to the procedure given by Dini *et al.*[7] to afford

15 in a moderate yield. The resulting product then underwent a Cava reaction with the desired alkene to produce substituted 6,7-dibromonaphthalenes **16a** and **16b** in 31 % and 83 % yields respectively.

Compounds **13** and **16** then underwent a Suzuki-Miyaura cross coupling to afford compounds **17a** and **17b**. An oxidative ring closing was then performed in dry DCM using 6 equivalents of iron (III) chloride for 30 minutes to afford the substituted 2,3,6,7-tetrakis(decyloxy)-11,12-dibenzanthracenecarboxylate derivatives (**10h,i**) in yields of 78 % and 66 % respectively.

2.3 Results

Both the mono-methyl ester dibenzanthracenecarboxylate (**10h**) and the di-methyl ester dibenzanthracenedicarboxylate (**10i**) were successfully synthesized. Unfortunately, neither derivative demonstrated a liquid crystalline phase (Figure 2-3).

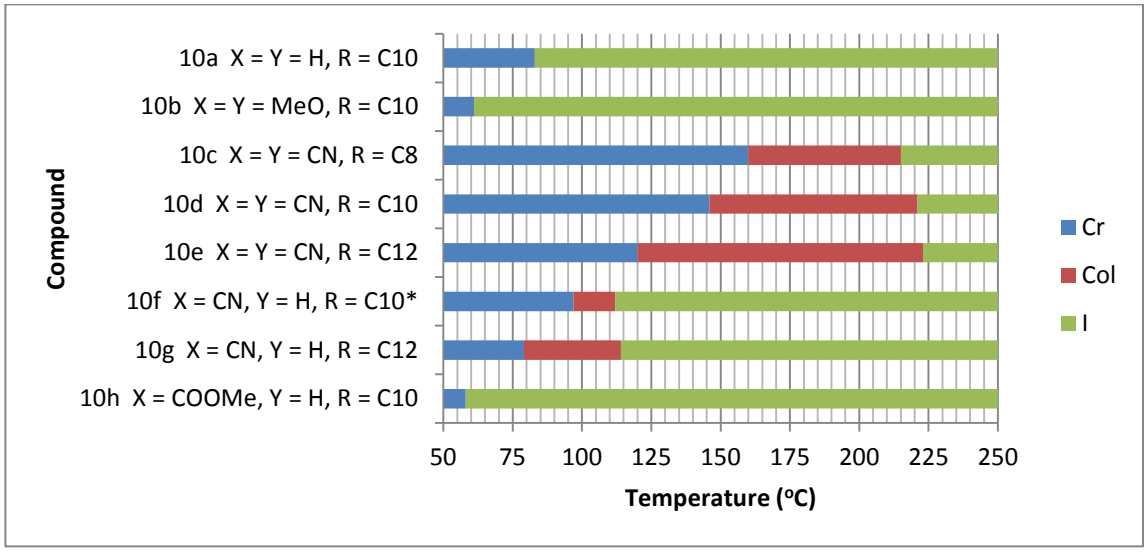

Figure 2-3: *Liquid crystal ranges of the hexa-substituted dibenz[a,c]anthracene series, including compound* ***10h****. Compound* ***10i*** *is not included due to its decomposition prior to melting. The transitions are from DSC on heating. I is an isotropic liquid, Col is a columnar phase and Cr is a crystal phase.*

The mono-methyl ester was observed to melt directly from a crystalline solid to an isotropic liquid at a temperature of 58 ^{o}C. The di-methyl ester dibenzanthracenedicarboxylate (**10i**) was also prepared; however, both the product of the Suzuki cross coupling (**17b**) and the target molecule (**10i**) contained a small impurity that could not be removed through column chromatography or multiple recrystallizations. During initial characterization studies of compound **10i**, however, the compound was observed to decompose prior to melting. This was confirmed by thermogravimetric analysis (Figure 2-4). In addition, NMR data taken before and after the decomposition of the dibenzanthracenedicarboxylate showed the loss of a singlet integrating for 6 protons. This singlet represents the 6 protons shared between the two methyl ester substituents. Based on this data, it is believed that the dibenzanthracenedicarboxylate is losing methanol to form either the dicarboxylic acid or the anhydride derivative, either of which would have a much higher melting point.

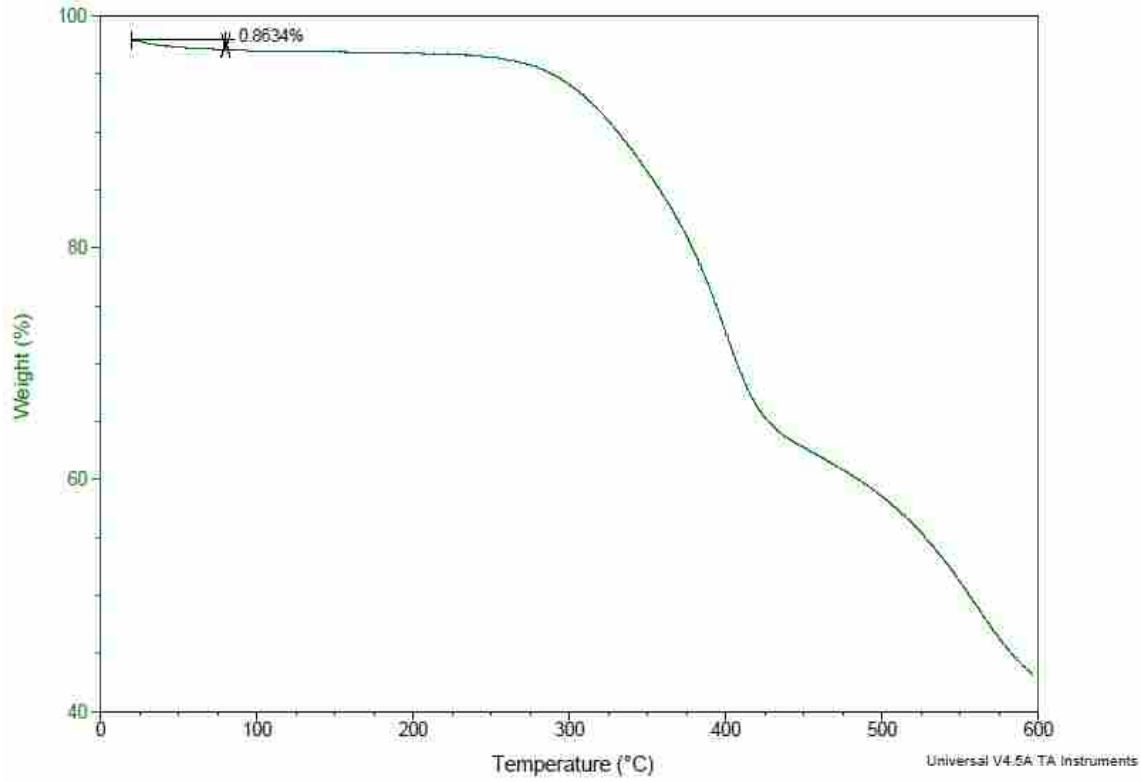

Figure 2-4: *Thermogravimetric analysis showing the decomposition of compound* ***10i****.*

Based on these results, combined with the fact that the compound did not show a columnar phase, **10i** was not purified or characterized any further.

2.4 Discussion

Based on the trends in behaviour that can be seen in Figure 2-3, it is clear that this series of molecules display liquid crystallinity only when the substituents are very electron withdrawing. It is, however, not too surprising that neither compounds **10h** nor **10i** did not display a columnar phase. The electron withdrawing substituents seem to be necessary to pull electron density away from the core of the molecule and make columnar stacking more favourable.[73] The ester substituents are only moderately electron withdrawing when compared to the cyano substituents and, since only methyl

esters were investigated, there is not a great deal of flexibility since there is no extended alkyl chain.

In comparison, Williams and co-workers have synthesized a series of mono-methyl ester dibenzophenazine derivatives (Figure 2-5).[77] Although these derivatives differ from the dibenzanthracene derivatives only by the introduction of two nitrogen atoms into the aromatic core, they display vastly different behaviour. In contrast to the mono-methyl ester dibenzanthracene derivative, which does not display a columnar phase, all of the mono-methyl ester dibenzophenazine derivatives display relatively broad columnar phases (Table 2-1).[77] This result further supports the theory that the methyl ester dibenzanthracene derivatives do not have enough electron-withdrawing character to stabilize a columnar phase.

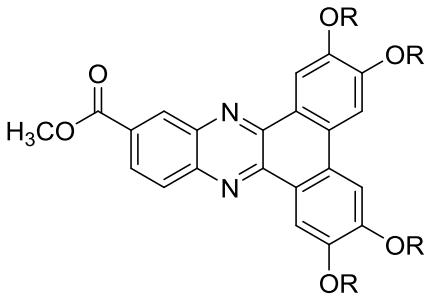

Figure 2-5: *Mono-methyl ester dibenzophenazine derivatives.*[77]

Table 2-1: *Phase transition temperatures of mono-methyl ester dibenzophenazine derivatives.*

Structure	Phase Transition Temperature (^{o}C)	Reference
R = C_6H_{13}	Cr 111 Col 200 I	77
R = C_8H_{17}	Cr 107 Col 161 I	77
R = $C_{10}H_{21}$	Cr 97 Col 136 I	77
R = $C_{12}H_{25}$	Cr 77 Col 106 I	77

In summary, this series of dibenzanthracene compounds (**10**) displays liquid crystallinity only when the lateral substituents are very electron withdrawing. The two methyl ester substituted derivatives were not electron withdrawing or flexible enough to

induce a columnar phase. Based on these results, it would be interesting to explore the effect of longer chain esters on this class of compounds or, as will be seen in Chapter 3, the effect of an alkyl-substituted imide substituent, which combines both an electron withdrawing substituent and a flexible alkyl chain.

2.5 Summary

Two dibenzanthracenecarboxylate derivatives (**10h, 10i**) were successfully synthesized using a modular approach developed in our lab for similar compounds. Unfortunately, neither derivative displayed any columnar behaviour. Series **10**, therefore, displays liquid crystallinity only when one or both of the lateral substituents are occupied by highly electron withdrawing cyano groups. These results show that small changes to the substituents on the aromatic core of the molecule can greatly affect the columnar properties of these compounds.

Chapter 3 Synthesis and Mesomorphic Properties of *N*-Substituted Dibenzanthracenedicarboximides

3.1 Introduction

The substituted 2,3,6,7-tetrakis(alkyloxy)dibenz[a,c]anthracene series (**10**) demonstrated that electron withdrawing substituents on the aromatic core promote liquid crystalline behaviour. With this series, however, in addition to a stabilization of the columnar phase, the solid phase was also stabilized; as evidence by the relatively high melting temperatures of the compounds in this series. We therefore sought to incorporate electron withdrawing groups that contain flexible alkyl chains onto the aromatic core in the hopes of producing materials possessing a broad columnar phase. Imides substituted with alkyl chains are promising candidates for these substitutents.

Imides, especially perylene bisimides, are widely used as electron deficient materials. Perylene bisimides and their derivatives have potential applications in molecular electronic devices, including light emitting diodes, photovoltaic cells, photochromic materials, molecular wires, and n-type semiconductors.[78-82] Furthermore, imides fused with conjugated systems like perylene, anthracene, and naphthalene have found uses as imide dyes for fluorescent imaging and dye-sensistized solar cells.[83,84] This class of compounds is particularly advantageous for these types of applications due to their high photochemical stability, ease of synthetic modification, and their charge transmission ability.[85-87]

Despite their uses as electron deficient materials, there are few examples of imides in mesogens. Still, there is some evidence that discotic frameworks substituted with imide derivatives show a stabilization of the columnar phase. Wu and co-workers

recently synthesized a series of triphenylene carboximides that display broad columnar phases (Figure 3-1).[48]

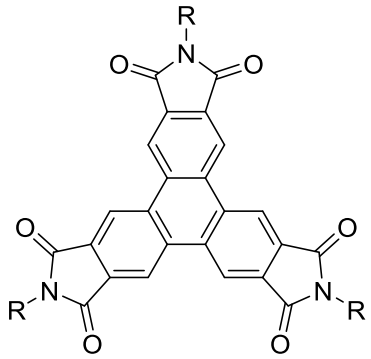

Figure 3-1: *Triphenylene carboximide discotic liquid crystals.*[48]

Table 3-1: *Phase transition temperatures of triphenylene carboximide discotic liquid crystals.*

Structure	Phase Transition Temperature (^{o}C)	Reference
R = C_8H_{17}	Cr 158 Col 228 I	48
R = $C_{12}H_{25}$	Cr 46 Col 218 I	48

To further probe the theory that subtituents that combine an electron withdrawing nature with the flexibility of an alkyl chain should stabilize the columnar phase, a series of novel *N*-substituted dibenzanthracenedicarboximides (Figure 3-2) will be synthesized via a synthetic approach similar to that employed for the dibenzanthracenecarboxylates described in Chapter 2. We anticipate that these compounds, substituted with alkoxy chains on one end of the molecule and alkyl-substituted imides on the other, will stabilize the columnar phase via a lowering of the solid to liquid crystal transition.

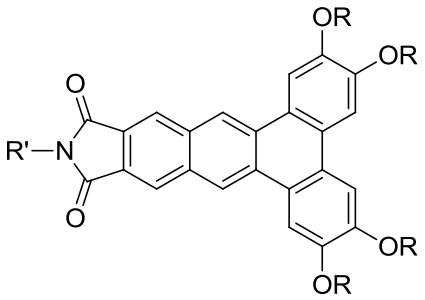

Figure 3-2: *Target N-substituted dibenzanthracenedicarboximide.*

3.2 Synthetic Approach

To access the *N*-substituted dibenz[a,c]anthracenedicarboximides a methodology similar to that used in the synthesis of the dibenz[a,c]anthracenecarboxylates described in Chapter 2 was employed.

The first step in preparing the target series was to synthesize the 6,7-dibromo-2-alkyl-benzo[f]isoindole-1,3-diones (**20a-d**) used in the modular approach (Scheme 3-1). Dimethyl 6,7-dibromo-2,3-naphthalenedicarboxylate (**16b**), prepared in Chapter 2, was converted to the dicarboxylic acid using a procedure adapted from Osawa and co-workers[88] in quantitative yields. The 6,7-dibromo-2,3-naphthalenedicaboxylic acid (**18**) was then converted to the anhydride using a procedure adapted from Baathulaa and co-workers[89] in good yield. To achieve the desired benzoisoindole-1,3-dione, the anhydride was refluxed with the appropriate amine to give compounds **20a-d** in yields of 77-90 %.

Scheme 3-1: *Synthesis of 2-alkyl benzoisoindole-1,3-diones* ***20a-d***

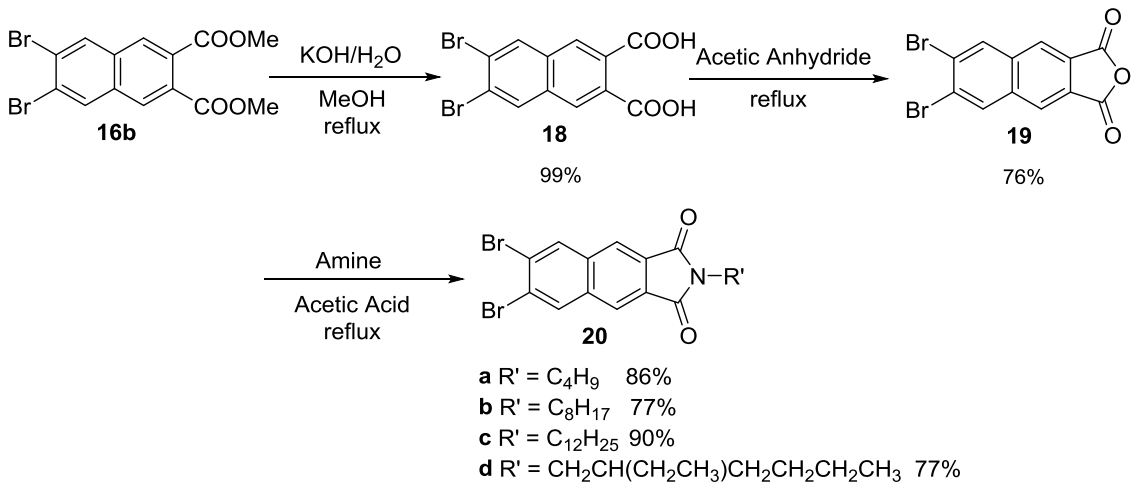

At this point, the modular approach described previously was employed (Scheme 3-2). The aryl boronates (**13a**,**b**) necessary for the cross coupling were prepared via the approach described in Chapter 2. Compounds **13** and **20** then underwent a Suzuki Miyaura cross coupling to afford compounds **21a**-**g**. Compounds **21a-c** were purified via column chromatography and a subsequent recrystallization. However, after column chromatography compounds **21d-g** were isolated as oils. Despite several attempts at recrystallization, these compounds would not solidify and were, therefore, used in the subsequent step without further purification. An oxidative ring closing was then performed in dry DCM using 6 equivalents of iron (III) chloride for 30 minutes to afford the *N*-alkyl-2,3,6,7-tetrakis(alkyloxy)-11,12-dibenz[a,c]anthracenedicarboximides (**22a**-**g**) in yields of 65-99 %.

Scheme 3-2: *Synthesis of N-alkyl-2,3,6,7-tetrakis(alkyloxy)-11,12-dibenz[a,c]anthracenedicarboximides* ***22a-g***

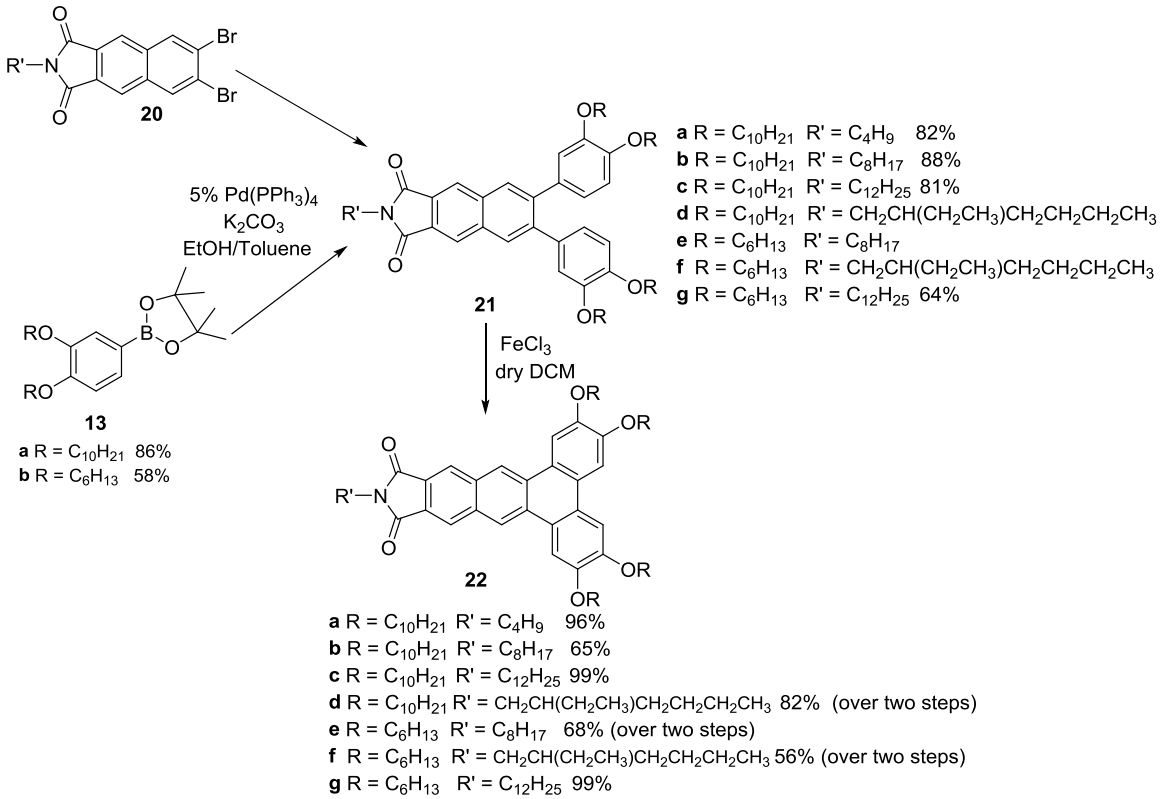

This methodology was applied to the formation of dibenz[a,c]anthracenedicarboximides with four different alkyl chain lengths (butyl, hexyl, octyl, and dodecyl) on the nitrogen atom and two different alkoxy chain lengths (hexyloxy and decyloxy) on the other side of the molecule. In total, 6 combinations of dibenz[a,c]anthracenedicarboximides (**22a-f**) were prepared, as can be seen in Scheme 3-2. A seventh derivative, **22g**, with hexyloxy chains and a dodecyl chain on the nitrogen atom was also prepared. In contrast to the other 6 derivatives, however, this compound was observed to decompose before melting. This result was confirmed by thermogravimetric analysis (TGA) and, therefore, was not studied further.

3.3 Results

3.3.1 Mesophase Characterization

The liquid crystalline properties of compounds **22a-f** were studied by polarized optical microscopy and DSC. All of the compounds in the series demonstrated a broad columnar phase. The micrographs in Figure 3-3 show the liquid crystal textures of compounds **22a-f** as seen by polarized optical microscopy. The observed textures are consistent with a hexagonal columnar phase.[70]

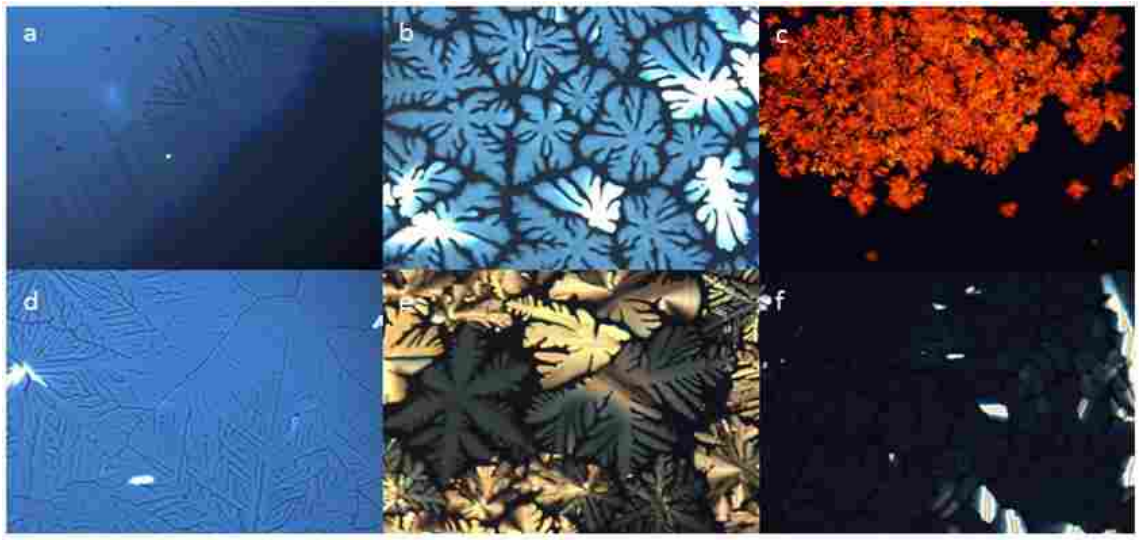

Figure 3-3: *Polarized optical micrographs of a) C4 imide/C10 alkoxy (**22a**) at 212 °C, b) C8 imide/C10 alkoxy (**22b**) at 220 °C, c) C12 imide/C10 alkoxy (**22c**) at 160 °C, d) Branched imide/C10 alkoxy (**22d**) at 221 °C, e) C8 imide/C6 alkoxy (**22e**) at 249 °C, f) Branched imide/C6 alkoxy (**22f**) at 284 °C. All micrographs were taken on cooling at a rate of 10 °C·min^{-1} and were taken at 200x magnification.*

Differential scanning calorimetry (DSC) was used to determine precise transition temperatures for this series. In all cases, the DSC for each of the compounds was performed at a constant temperature change of 5 ^{o}C·min^{-1} and the transition temperatures are reported on heating. The phase behaviour of compounds **22a-f** are summarized in Table 3-2.

Table 3-2: *Phase behaviour of compounds* ***22a-f*** *based on DSC with scan rate of 5 °C·min^{-1} on heating.*

Compound	R', R		Phase Transition Temperature (°C)
22a	R' = C_4H_9	R = $C_{10}H_{21}$	Cr 101 Col_h 214 I
22b	R' = C_8H_{17}	R = $C_{10}H_{21}$	Cr 64 Col_h 222 I
22c	R' = $C_{12}H_{25}$	R = $C_{10}H_{21}$	Cr 48 Col_h 206 I
22d	R' = Branched	R = $C_{10}H_{21}$	Cr 28 Col_h 223 I
22e	R' = C_8H_{17}	R = C_6H_{13}	Cr 131 Col_h 250 I
22f	R' = Branched	R = C_6H_{13}	Cr 87 Col_h 278 I

The phase behaviours of compounds **22a-f** have also been summarized graphically (Figure 3-4), for visual comparison of the varying alkyl chain lengths on the nitrogen atom and the alkoxy chains.

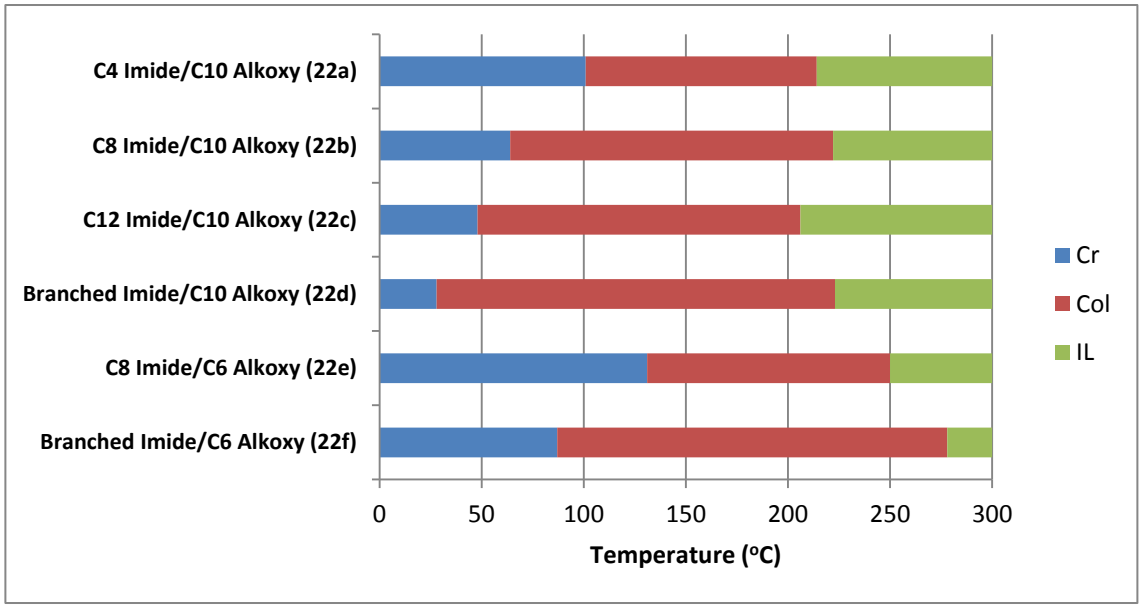

Figure3-4: *Liquid crystal ranges of compounds* ***22a-f****. The transitions are from DSC and are reported on heating at. I is an isotropic liquid, Col is a columnar phase and Cr indicated a crystalline solid phase.*

The series was also analyzed using powder X-ray diffraction by Kevin Bozek and Professor Vance Williams at Simon Fraser University. The data is summarized in Table 3-3 and a representative diffractogram is presented in Figure 3-5.

Table 3-3: *Diffractogram data of compounds* ***22a-f***

Compound	R', R	d-spacing (Å)	Miller Index (*hkl*)	Phase
22a	R' = C_4H_9 R = $C_{10}H_{21}$	21.5	(100)	Col_h (a = 24.8 Å)
22b	R' = C_8H_{17} R = $C_{10}H_{21}$	22.1	(100)	Col_h (a = 25.5 Å)
22c	R' = $C_{12}H_{25}$ R = $C_{10}H_{21}$	22.7	(100)	Col_h (a = 26.2 Å)
22d	R' = Branched R = $C_{10}H_{21}$	22.6	(100)	Col_h (a = 26.1 Å)
22e	R' = C_8H_{17} R = C_6H_{13}	19.2	(100)	Col_h (a = 22.1 Å)
22f	R' = Branched R = C_6H_{13}	19.0	(100)	Col_h (a = 21.9 Å)

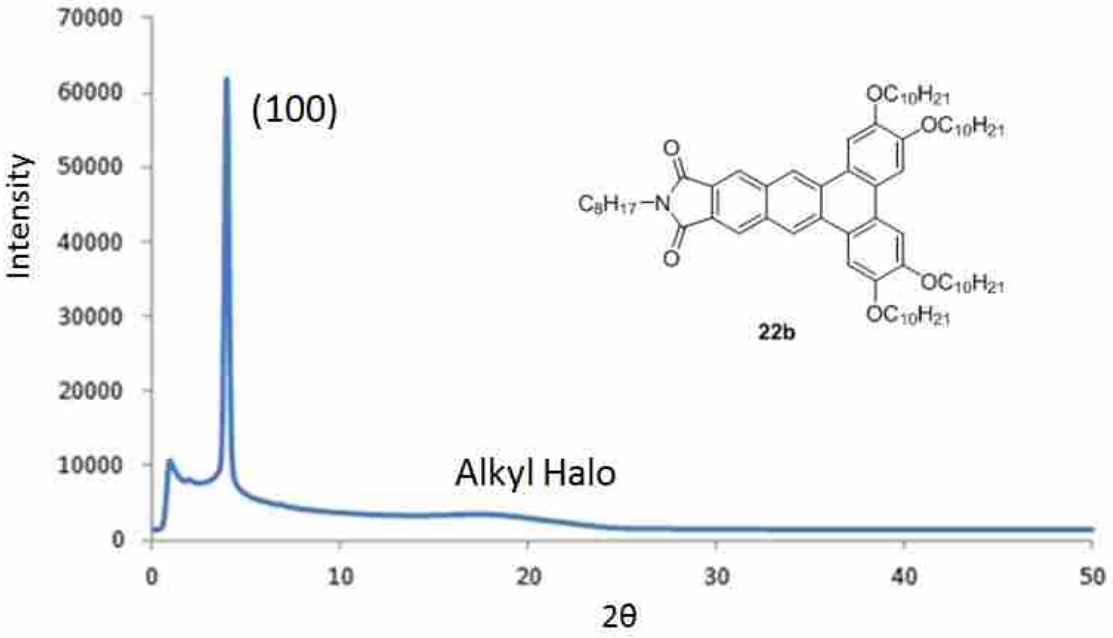

Figure 3-5: *Representative X-Ray diffractogram of compound* ***22b****.*

The (100) and (110) reflections can be used to calculate the distance between the columns in the columnar arrangement. With this series, the (110) reflection was not

observed. The (100) reflection, however, can be used to determine the type of phase demonstrated by the compound. The trigonometric relationship for a hexagonal columnar phase is $a = \frac{2}{\sqrt{3}}d$. Using this formula, the intercolumnar distances for each of the compounds were calculated to be between 21.9 Å and 26.2 Å. These intercolumnar distances, combined with the dendritic textures observed via polarized optical microscopy, indicate the compounds in series **22** are in the hexagonal columnar phase. This result is consistent with the observations from POM and DSC.

3.3.2 UV-Vis and Fluorescence

The solvatochromic behaviour of Series **22** was also examined. The branched chain derivative with the decyloxy chains (**22d**) was used to represent the series.

A 1x10^{-5} M solution of the imide was prepared in four different solvents, which varied in polarity. The UV-Vis spectra of these solutions are shown in Figure 3-6. A small red-shift in the absorbance maxima was observed as the solvent became more polar.

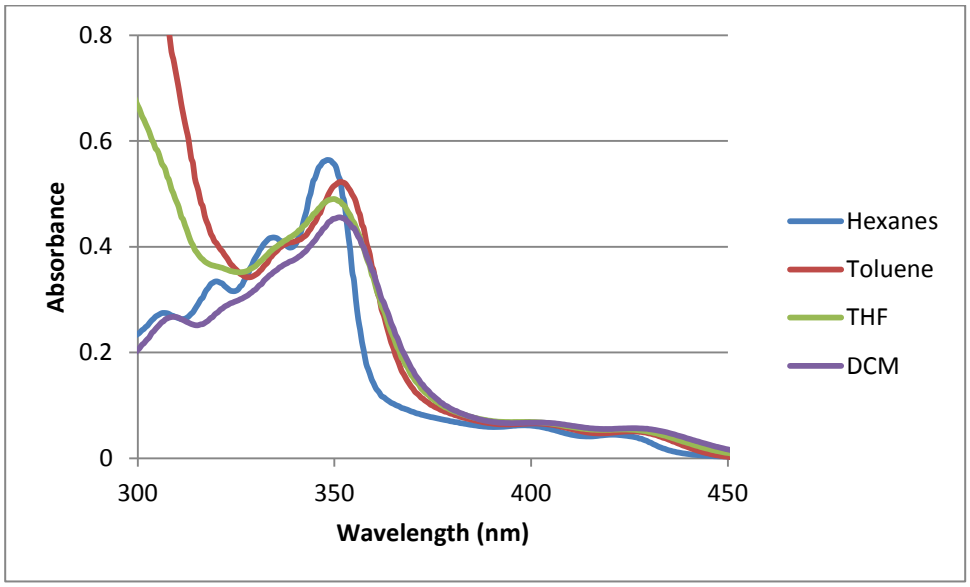

Figure 3-6: *UV-Vis spectra of 1x10^{-5} M solutions of **22d** in hexanes, toluene, THF, and DCM.*

Each of the solutions were then diluted 5-fold to prepare solutions with a concentration of $2x10^{-6}$ M. These solutions were then examined using the fluorometer to generate the emission spectra (Figure 3-7) and the excitation spectra (Figure 3-8) for each of the compounds in the series. With both the emission and the excitation spectra, as the solvent increases in polarity, the emission maxima in each spectra shifts to the right, suggesting the polar excited state is stabilized in more polar solvents. This result is consistent with the trend observed by UV-Vis.

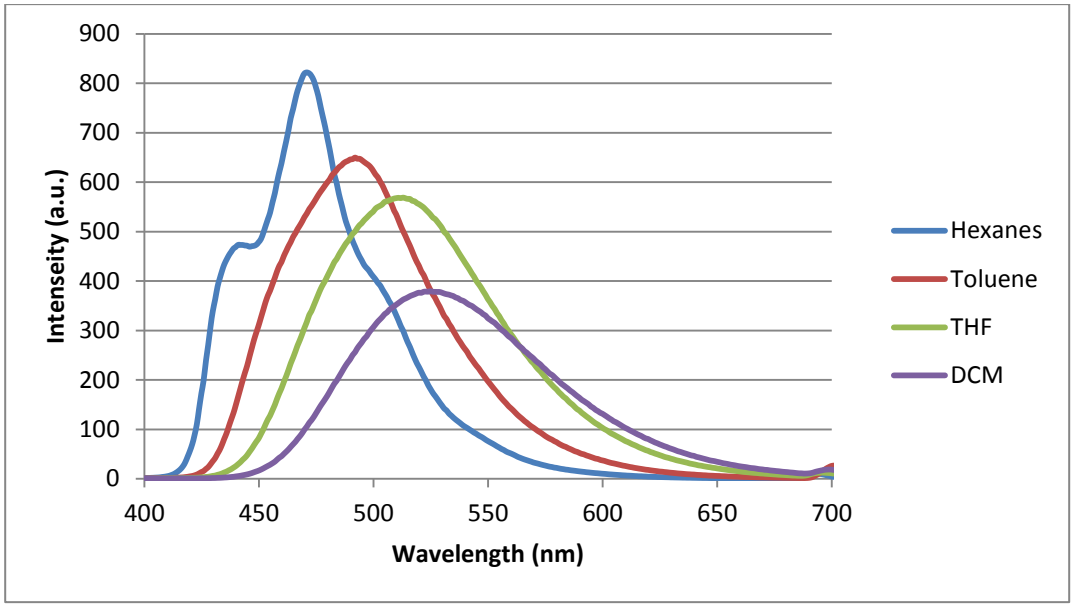

Figure 3-7: *Emission spectra of $2x10^{-6}$ M solutions of **22d** in hexanes, toluene, THF, and DCM (excitation at 340 nm)*

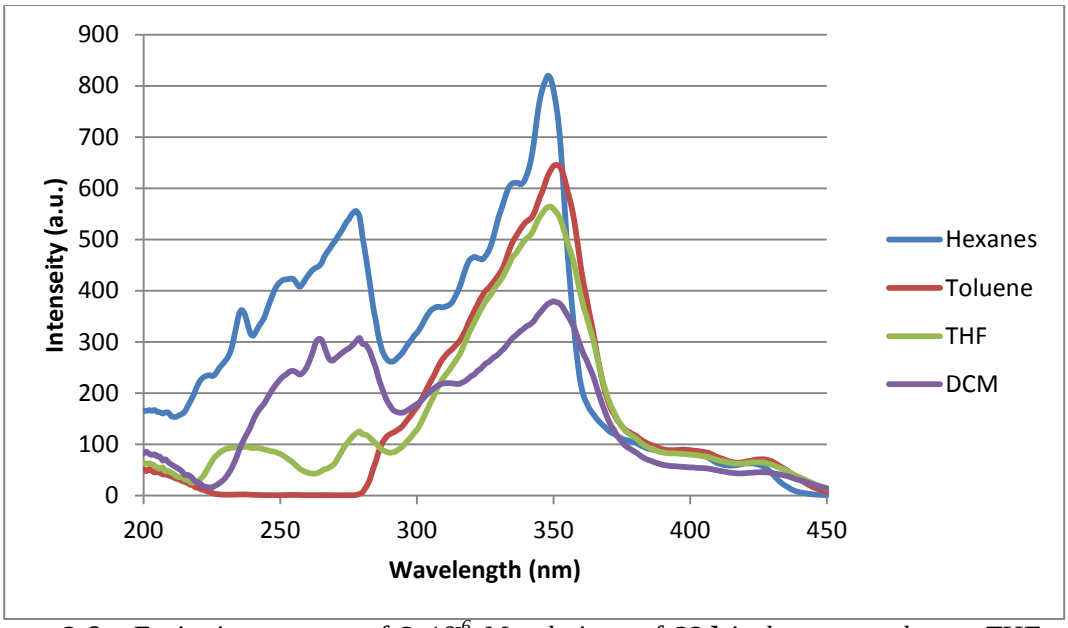

Figure 3-8: *Excitation spectra of 2x10^{-6} M solutions of **22d** in hexanes, toluene, THF, and DCM. The excitation spectra were generated at the maximum wavelength from each of the emission spectra (Figure 3-7).*

Solvatochromism, the phenomenon where a spectral shift occurs due to change in solvent polarity, results in solutions of solvatochromic compounds absorbing a different colour depending on the polarity of the solvent.[90-92] This can be observed when compound **22d** is viewed under an ultraviolet light; exhibiting blue fluorescence in hexanes, green in tetrahydrofuran (THF), and yellow in dichloromethane (DCM). This is referred to as positive solvatochromism; the excited state is more polar and the stabilization of this state leads to a red-shift of the spectra.[90-92]

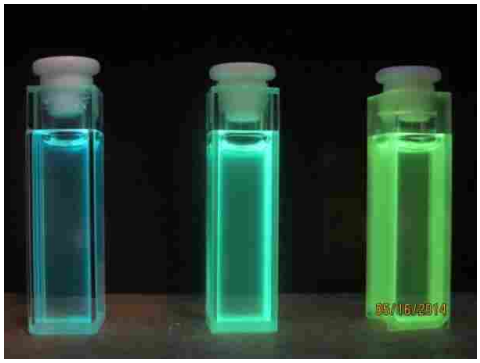

Figure 3-9: *Photograph of 2x10^{-6} M solutions of **22d** in hexanes, THF, and DCM when viewed under an ultraviolet light.*

3.4 Discussion

All six of the *N*-substituted dibenzanthracenedicarboximide derivatives (**22a-f**) displayed broad columnar phases with relatively low solid to liquid crystal transitions. Furthermore, when this series is compared to the substituted 2,3,6,7-tetrakis(alkyloxy)dibenzanthracene series, the observed melting transitions for compounds with similar chain lengths were significantly lower. A similar trend is found when hexaalkoxytriphenylenes[47] and Wu's triphenylene carboximide series[78] are compared. In this case, the triphenylene carboximides of similar chain lengths have much broader columnar phases than the corresponding hexaalkoxy triphenylenes.

Furthermore, when comparing the liquid crystalline behaviour of compounds **22a-f** it is evident that, as the chain on the nitrogen atom becomes longer and more flexible, there is a broadening of the columnar phase primarily by a lowering of the melting transition temperature. This trend is observed both with the decyloxy derivatives and the hexyloxy derivatives. With the four decyloxy derivatives, the melting transition temperature steadily declines as the chain length on the nitrogen is increased from butyl to octyl to dodecyl. The overall columnar phase broadens over these same compounds. Both trends culminate with the derivative with the branched chain on the nitrogen atom; which exhibits the broadest columnar phase and the lowest melting transition temperatures. This may be due to the branched chains affecting the formation of solid crystals, therefore destabilizing the solid phase. Interestingly, compounds **22b** and **22d**, which are each substituted with 8-carbon chains that are isomers of each other, exhibit different melting transitions, but very similar clearing points.

Similar trends are noticed with the hexyloxy derivatives, with the branched derivative (**22e**) having a lower melting transition temperature than the straight 8-carbon chain derivative (**22f**). Surprisingly, however, their clearing points are not very similar, despite the fact that they have isomeric chains. A hexyloxy derivative with a dodecyl chain in the nitrogen atom was also synthesized. This derivative, however, decomposed before melting (confirmed by thermogravimetric analysis) and was not studied further. Also of note is that, when the alkoxy chains were shortened to hexyloxy chains, the columnar temperature range was shortened and shifted to a higher overall temperature range.

The various trends observed with series **22** demonstrate that the introduction of imide groups onto the aromatic core of the molecule produces materials with broad columnar temperature ranges. This is likely due to the electron-withdrawing imides bearing flexible alkyl chains, allowing for the molecule to maintain its electron withdrawing character while also having increased flexibility around the aromatic core.

When the UV-Vis and fluorescence data was analyzed, it was observed that, as the solvent increased in polarity, the emission maxima shifted to the right, thus exhibiting positive solvatochromism. When the emission maxima is plotted against the dielectric constant of each solvent (a measurement of the polarity of the solvent), a linear relationship is observed with an R^2 value of 0.90. (Figure 3-10). These results suggest that the polar excited state is stabilized in polar solvents, leading to a red shift in emission.

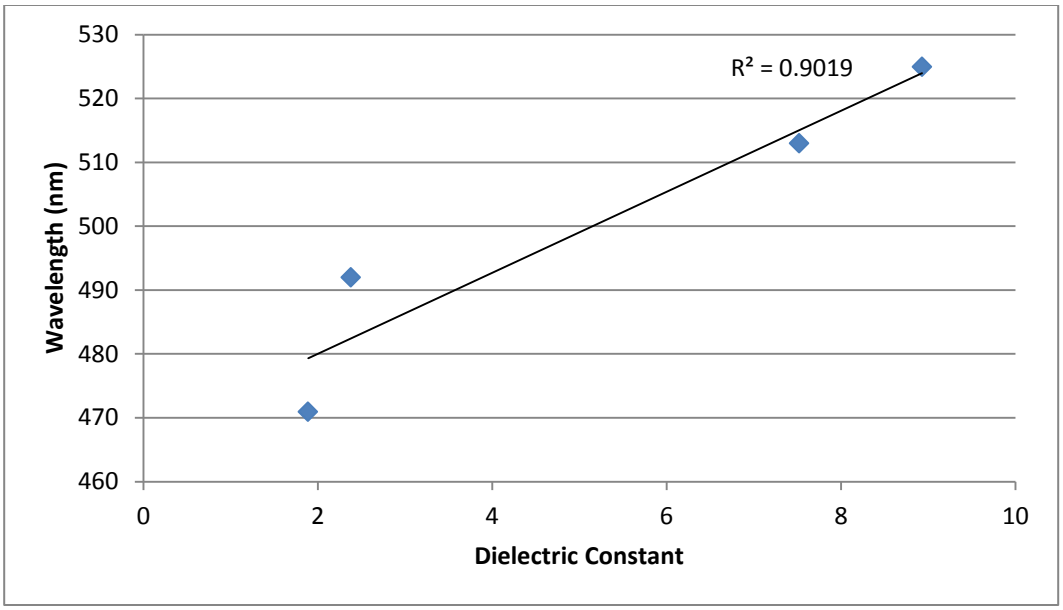

Figure 3-10: *Plot of the emission maxima of* ***22d*** *in each solvent compared to the dielectric constant of the solvent. All dielectric constants taken from Material Safety Data Sheets from Sigma Aldrich.*

3.5 Summary

A modular synthesis of a series of novel *N*-substituted 2,3,6,7-tetrakis(alkyloxy)-11,12-dibenz[a,c]anthracenedicarboximides (**22a-f**) has been reported. All six derivatives display broad columnar phases and relatively low melting temperatures when compared to structurally related liquid crystalline compounds. The melting transition temperature was found to decrease as the chain on the nitrogen atom became longer and more flexible. In addition, shorter alkoxy chains were found to shift the liquid crystalline range to higher overall temperatures. The series also displays solvatochromism, with a red-shift of the absorbance maxima as the solvent becomes more polar. These results show that substituents that combine an electron withdrawing nature and a flexible alkyl chain can stabilize the columnar phase of these types of compounds. In addition, this synthesis demonstrates the successful design of a series of

compounds that possess a broad columnar mesophase combined with a relatively low melting transition temperature.

Chapter 4 Electron Donor-Acceptor Liquid Crystals

4.1 Introduction

Electron donor-acceptor liquid crystals are a subclass of liquid crystals that consist of two complimentary components: the electron rich "donor" molecule and the electron poor "acceptor" molecule[49] (Figure 4-1). When the donor and the acceptor combine to form a liquid crystal, they can produce a material with far different properties than either of the individual materials. The formation of electron donor-acceptor liquid crystals can lead to broader columnar phase temperature ranges and/or the induction of a liquid crystalline phase with two non-mesogenic materials.[50-52]

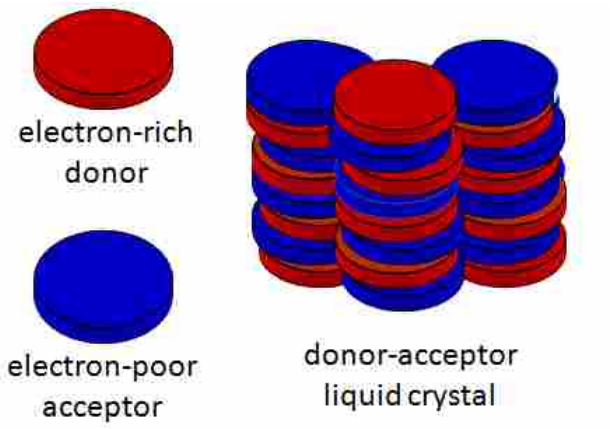

Figure 4-1: *Schematic representation of an electron donor-acceptor liquid crystal.*[49]

Initially, solid-state electron donor-acceptor mixtures garnered the most attention. For example, in 1960, a crystalline state was reported for a 1:1 mixture of benzene and hexafluorobenzene.[93] It was not until the early 1990s that a significant amount of work was performed on electron donor-acceptor liquid crystals. Much of the initial work on electron donor-acceptor liquid crystals was performed by Ringsdorf and co-workers who found that doping an electron-rich triphenylene derivative with electron-poor trinitrofluorenone in a 1:1 ratio stabilized the liquid crystalline phase of

the triphenylene (Figure 4-2).[53] Since then, this class of liquid crystals has been broadly studied for potential applications in organic photovoltaics due to their potential for a high degree of tunability.[56]

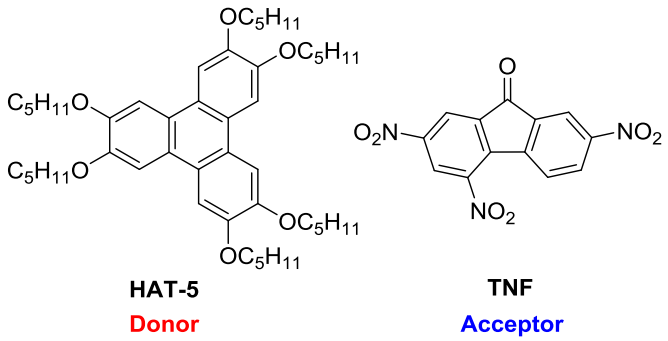

Figure 4-2: *Hexaalkoxytriphenylene donor and trinitrofluorenone acceptor used by Ringsdorf and co-workers.*[53]

More recently, the Reczek group demonstrated the tunability of electron donor-acceptor liquid crystals through the preparation of a novel series of compounds.[49] By combining a variety of bis-substituted naphthalene derivatives as electron donors with two different aromatic imides as electron acceptors (Figure 4-3) in a 1:1 molar ratio, Reczek and co-workers were able to create a variety of novel materials that possessed broad columnar phases and charge-transfer absorptions that spanned the entire visible spectrum.[49]

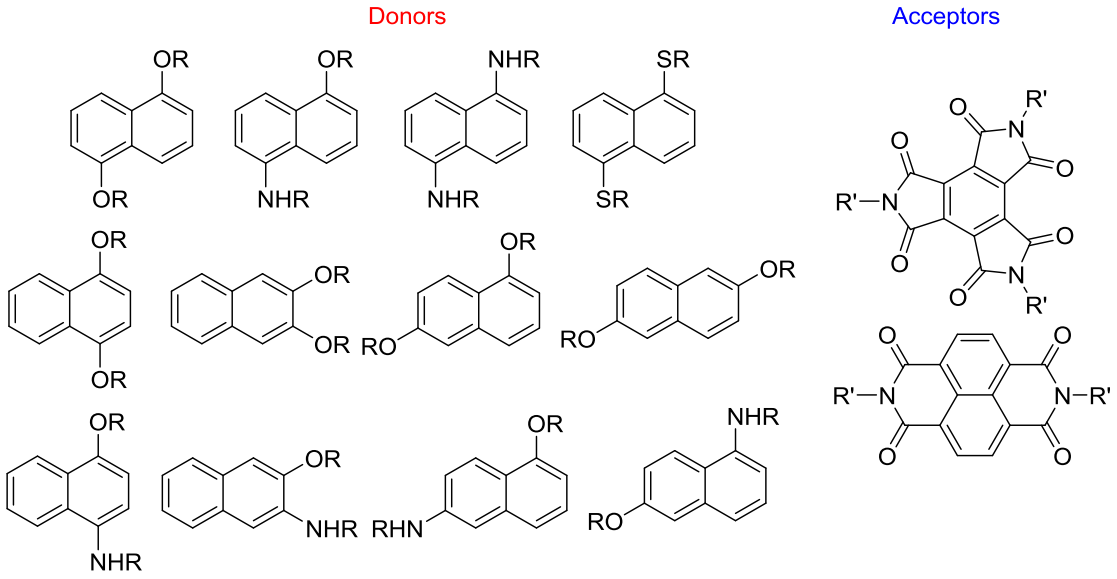

Figure 4-3: *Electron donors and acceptors prepared by Reczek and co-workers.*[49]

Initially, our goal was to induce a columnar mesophase in non-mesomorphic hexaalkoxydibenzanthracenes through the addition of trinitrofluorenone (TNF) as an electron acceptor (Figure 4-4). At the same time, however, we wanted to explore trends in the behaviour of structurally related dibenzanthracene and dibenzophenazine derivatives both with TNF and tetracyanoquinodimethane (TCNQ) acting as the acceptor (Figure 4-4). Furthermore, by exploring donor:acceptor ratios other than 1:1 with all of the mixtures, we should be able to further probe the relationship between the two components. Any observed trends may, ultimately, lead to a better understanding of the arene-arene interactions that are occurring in these types of compounds.

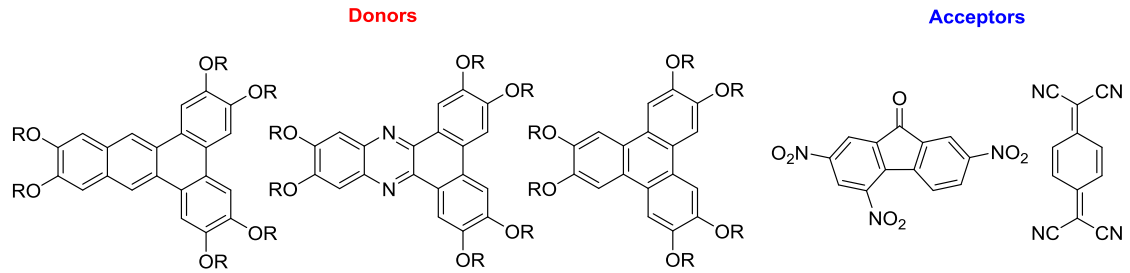

Figure 4-4: *Target electron donors and acceptors.*

4.2 Synthetic Approach and Mixture Preparation

The individual components for the mixtures were either prepared according to literature procedures[73,94-95] or, as with tetracyanoquinodimethane and 9-fluorenone, purchased from Sigma Aldrich.

To prepare the mixtures, stock solutions of the individual components were prepared in tetrahydrofuran (THF). The appropriate amount of each of the components was transferred to a small vial. The solvent was evaporated using a stream of nitrogen gas. Once dry, the mixture was heated to the melting point and then allowed to cool in order to ensure homogenous mixing. The samples were then tested using POM and DSC. The ratios of each of the components in the mixtures were confirmed using NMR spectroscopy.

4.3 Results

4.3.1 Hexaalkoxytriphenylene/Trinitrofluorenone Series

The first series prepared consisted of 2,3,6,7,10,11-hexakis(hexyloxy)triphenylene (HAT-6) as the electron donor and trinitrofluorenone (TNF) as the electron acceptor (Figure 4-5). The amount of TNF present in the mixture was varied from 10 % to 90 %. This series was prepared in order to support the findings of Ringsdorf and coworkers that a 1:1 mixture of these components was seen to broaden the columnar phase of the triphenylene.[53]

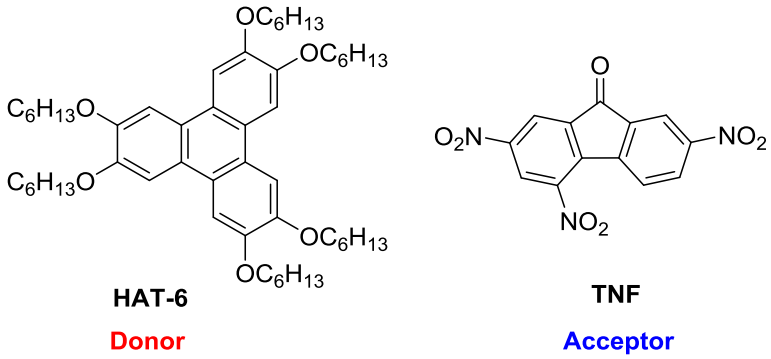

Figure 4-5: *Hexaalkoxytriphenylene (HAT-6) electron donor and trinitrofluorenone (TNF) electron acceptor.*

Upon initial mixing of the two components, a dark colour was observed, suggesting the formation of a charge-transfer complex.[51] When viewed under POM, the mixtures displayed a dendritic texture typical of a hexagonal columnar mesophase (Figure 4-6).

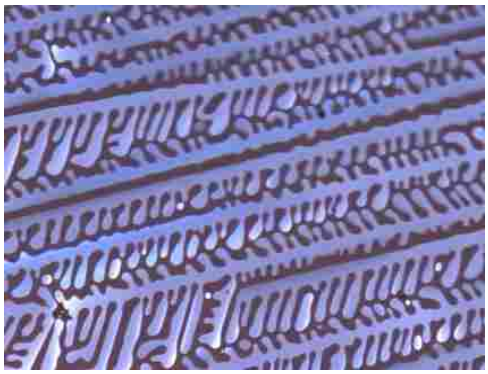

Figure 4-6: *Polarized optical micrograph of 1:1 HAT-6/TNF mixture at 212 °C on cooling at a rate of 10 °C·min^{-1} and taken at 200x magnification.*

As the molar ratio of the electron acceptor, TNF, was increased, there was also an observed increase in the clearing point of the liquid crystalline phase, with a maximum reached at the 1:1 mole ratio mixture. After this point, as the amount of TNF increased, the clearing point and overall breadth of the liquid crystalline phase were both seen to decrease. These results were confirmed by DSC (Figure 4-7). These results are consistent with the results of Ringsdorf *et al*.

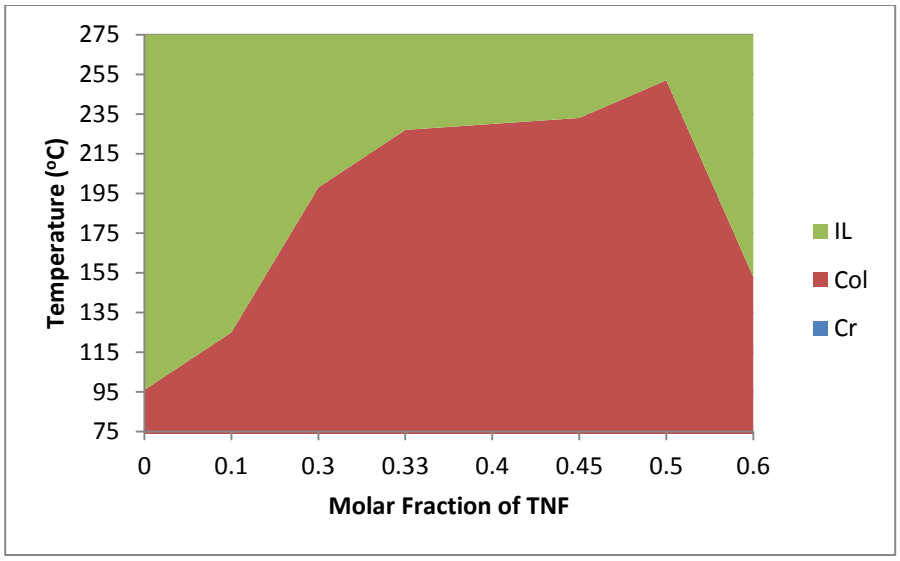

Figure 4-7: *Clearing points of HAT-6/TNF mixtures based on DSC with scan rate of 5 °C·min^{-1} on heating. I is an isotropic liquid, Col is a columnar phase and Cr indicated a crystalline solid phase.*

4.3.2 Hexaalkoxydibenzanthracene/Trinitrofluorenone Series

The next series that was prepared consisted of 2,3,6,7,11,12-hexakis(decyloxy)dibenz[a,c]anthracene (DBA) as the electron donor and TNF as the electron acceptor (Figure 4-8). The DBA does not have a liquid crystalline phase, melting directly from a crystalline solid to an isotropic liquid.[73] Therefore, it was expected that adding the TNF would result in the formation of a charge-transfer complex and induction of a liquid crystalline phase. In addition, it was also expected that the behaviour of this series would be very similar to the previous series since the main difference between the two donors is the addition of one ring onto the aromatic core.

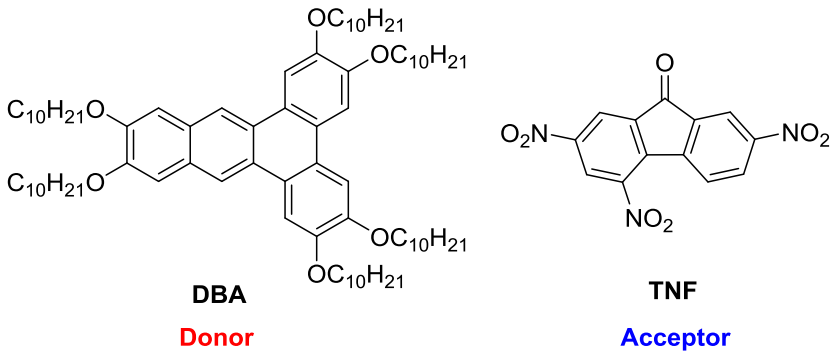

Figure 4-8: *Hexaalkoxydibenzanthracene (DBA) electron donor and trinitrofluorenone (TNF) electron acceptor.*

Once again, a dark colour was observed upon initial mixing of the two components, suggesting the formation of a charge-transfer complex. In addition, when viewed under POM, the mixtures displayed textures typical of a hexagonal columnar mesophase (Figure 4-9).

Figure 4-9: *Polarized optical micrograph of 30 % TNF / 70 % DBA mixture at 59 °C on cooling at a rate of 10 °C·min^{-1} and taken at 200x magnification.*

A liquid crystalline phase was successfully induced in the DBA upon small additions of TNF. The overall breadth of the liquid crystalline phase and the clearing point both increased as the molar ratio of TNF in the mixture was increased. In contrast to the HAT-6/TNF mixture, which displayed the highest clearing point at the 1:1 molar ratio mixture, the DBA/TNF series displayed the broadest liquid crystalline phase at approximately 33 % TNF (Figure 4-10). Upon further additions of TNF, the clearing

point decreased quickly with the liquid crystalline phase completely disappearing at approximately 45 % TNF. This would seem to suggest a preferred 2:1 molar ratio of electron donor to electron acceptor, rather than the preferred 1:1 ratio seen with the HAT-6/TNF series.

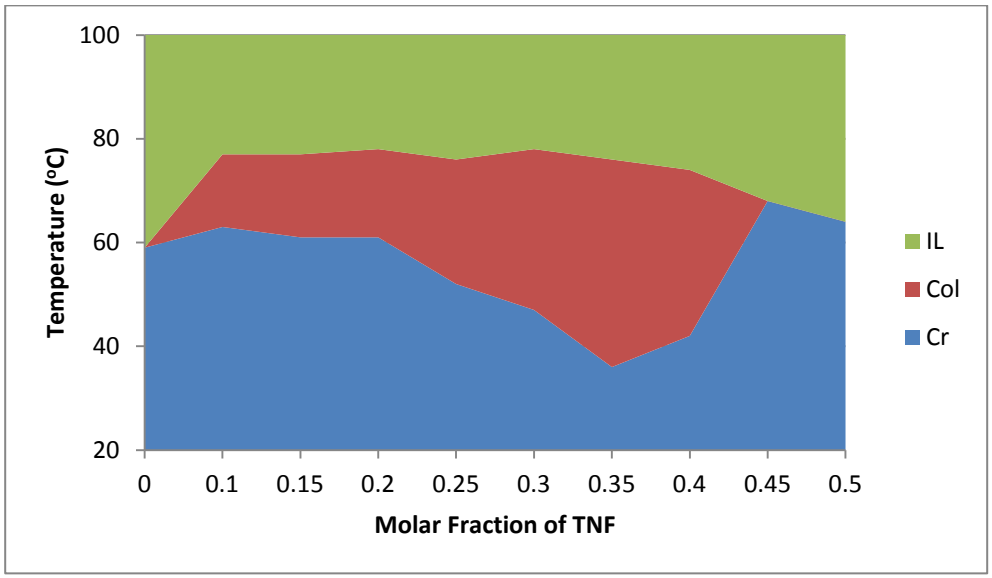

Figure 4-10: *Clearing points of DBA/TNF mixtures based on DSC with scan rate of 5 °C·min^{-1} on heating. I is an isotropic liquid, Col is a columnar phase and Cr indicated a crystalline solid phase.*

This behaviour was also observed in solution. The series was also prepared as solutions in THF and analyzed via UV-Vis spectroscopy. The results can be seen in Figure 4-11. The charge-transfer absorbance band was observed at 458 nm. The solution with the 2:1 molar ratio of DBA to TNF displayed the highest absorption of the series. This further supports the results gained from POM which seem to indicate a preferred 2:1 donor/acceptor molar ratio for this series.

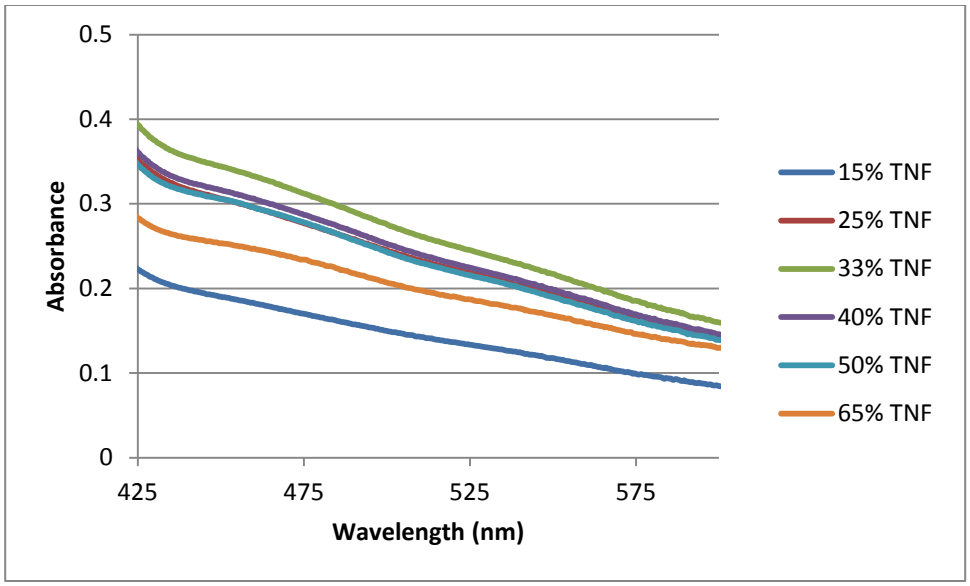

Figure 4-11: *UV-Vis absorption spectra for the DBA/TNF series. The charge transfer absorption can be seen at 458nm. $1x10^{-3}$ M solutions in hexanes.*

4.3.3 Dibenzophenazine/Trinitrofluorenone and Substituted Dibenzanthracene/Trinitrofluorenone Series

Two more series were prepared with electron donors that had similar structures to the hexaalkoxydibenzathracene of the previous series (Figure 4-12). In the first series, 2,3,6,7,11,12-hexakis(decyloxy)dibenzo[a,c]phenazine (DBP) acted as the electron donor and TNF acted as the electron acceptor. The DBP maintains the same shape as the DBA, but has a heteroaromatic core. The second series used TNF as the electron acceptor and the electron donor was 10,13-dibromo-2,3,6,7,11,12-hexakis(decyloxy)benzo[b]triphenylene (di-Br DBA). In this case, the di-Br DBA differed from the previous donor only by the introduction of two bromo substituents onto the aromatic ring. Due to the structural similarities of both donors to the DBA, it was hypothesized that they should display similar behaviour, favouring a 2:1 molar ratio of donor to acceptor. In contrast to the dibenzanthracene, however, both of these donors do display a liquid crystalline phase in their pure form.

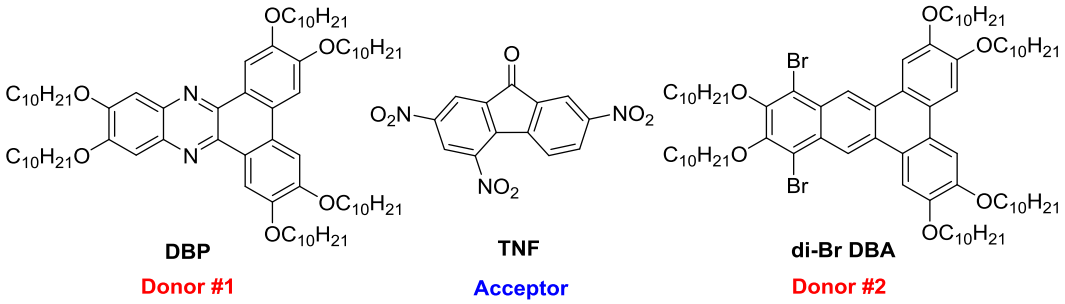

Figure 4-12: *Hexaalkoxydibenzophenazine (DBP) and di-bromo dibenzanthracene (di-Br DBA) electron donors and trinitrofluorenone (TNF) electron acceptor.*

With both series a charge-transfer complex was formed between the donor and acceptor; as evidenced by the dark colour displayed upon initial mixing. When viewed under POM, both series displayed textures typical of a hexagonal columnar mesophase (Figure 4-13).

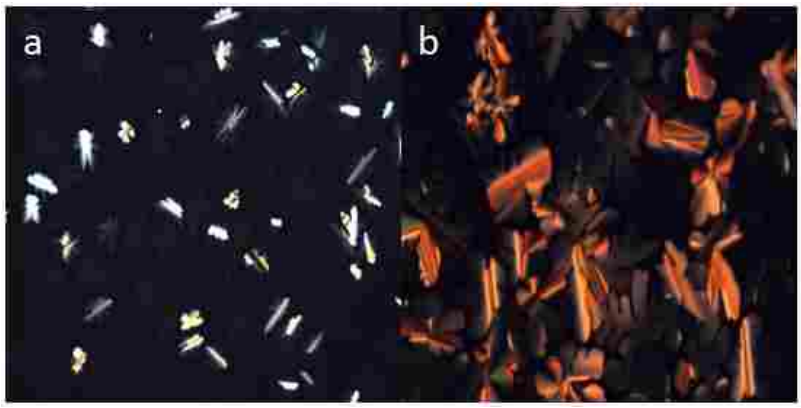

Figure 4-13: *Polarized optical micrographs of a) 20 % TNF / 80 % DBP mixture at 153 °C, b) 40 % TNF / 60 % di-Br DBA mixture at 206 °C. Both micrographs were taken on cooling at a rate of 10 °C·min^{-1} and were taken at 200x magnification.*

Both series displayed similar behaviour to the DBA/TNF series. After a small destabilization of the columnar phase upon small additions of TNF, the DBP/TNF series demonstrated an increase in clearing point and overall liquid crystalline temperature range until a maximum was reached at approximately 33 % TNF (Figure 4-14). The clearing point then decreased quickly, with the liquid crystalline phase disappearing completely at approximately 45 % TNF.

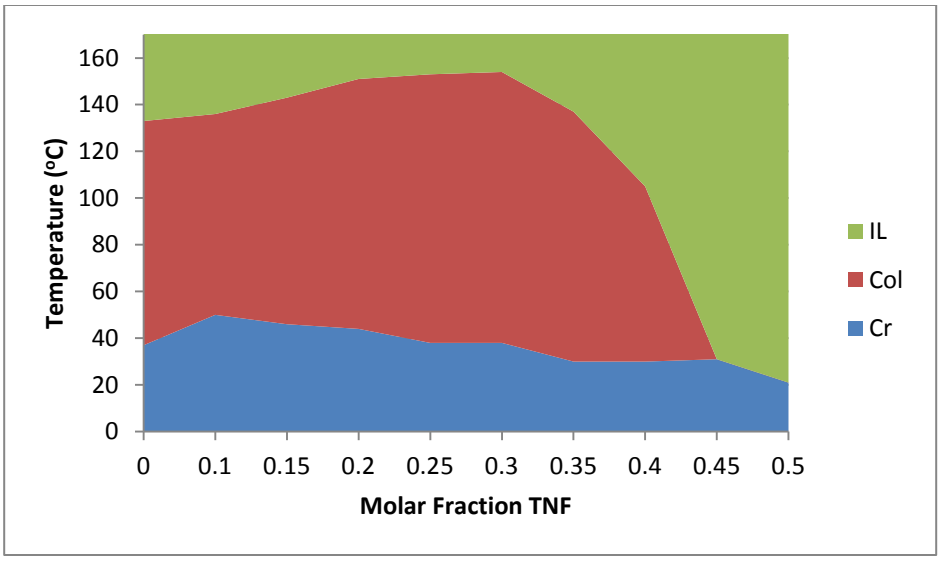

Figure 4-14: *Clearing points of DBP/TNF mixtures based on DSC with scan rate of 5 °C·min^{-1} on heating. I is an isotropic liquid, Col is a columnar phase and Cr indicated a crystalline solid phase.*

The di-Br DBA/TNF series displayed a very broad columnar phase over the entire series (Figure 4-15). The highest clearing points were observed between 30 % and 45 % TNF, with the 40 % TNF sample displaying the highest overall clearing point.

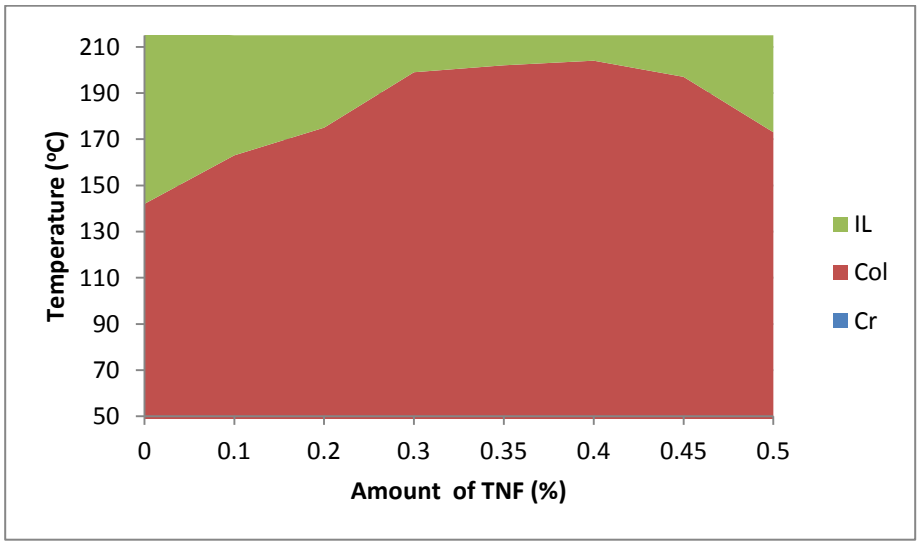

Figure 4-15: *Clearing points of di-Br DBA/TNF mixtures based on DSC with scan rate of 5 °C·min^{-1} on heating. I is an isotropic liquid, Col is a columnar phase and Cr indicated a crystalline solid phase.*

One interesting difference between the di-Br DBA/TNF series and the DBP/TNF series is the amount by which the columnar phase is stabilized. The difference in clearing point temperatures between the pure dibenzophenazine and the 2:1 DBP/TNF mixture is approximately 20 ^{o}C (Figure 4-14). In contrast, the difference in clearing point temperatures for the di-Br DBA/TNF series is approximately 90 ^{o}C (Figure 4-15). Therefore, the columnar phase of the bromo-substituted dibenzanthracene is stabilized to a much greater extent than the columnar phase of the dibenzophenazine upon the addition of trinitrofluorenone. This may perhaps be due to differences in the electronic nature of the cores. The core of the bromo-substituted dibenzanthracene is more electron-rich than the core of the dibenzophenazine, meaning that the trinitrofluorenone is able to accept more electron density and stabilize the columnar phase to a greater degree.

4.3.4 Dibenzanthracene/Dibenzophenazine Series and 1:1:1 Mixture

Based on these results, we were curious as to whether the DBA would display similar behaviour with a weaker electron acceptor. So, another series was prepared where the dibenzanthracene acted and the electron donor and the dibenzophenazine acted as the electron acceptor (Figure 4-16).

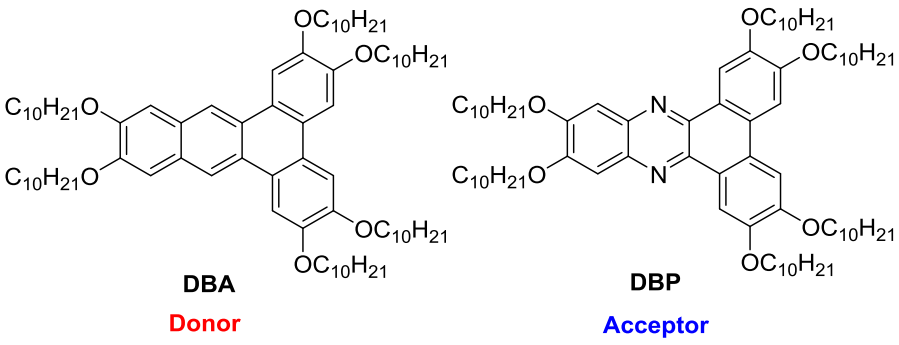

Figure 4-16: *Hexaalkoxydibenzanthracene (DBA) electron donor and hexaalkoxydibenzophenazine (DBP) electron acceptor.*

In contrast to each of the previous series, no dark colour was observed upon initial mixing of the two components, suggesting that a charge-transfer complex was not forming. Furthermore, once the phase behaviours were analyzed under POM and DSC, it was observed that, upon even small additions of DBA, the liquid crystalline phase of the DBP was being destabilized, with the clearing point dropping at a constant rate (Figure 4-17). In fact, this series did not even display a columnar phase at the 2:1 molar ratio of donor to acceptor, with the liquid crystalline phase disappearing at when the donor was present in approximately 40 % molar ratio.

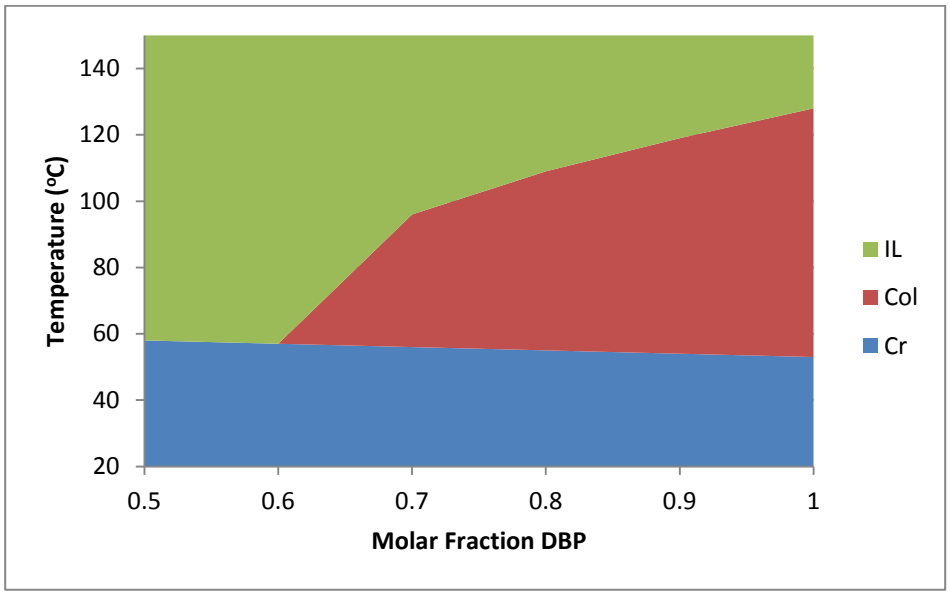

Figure 4-17: *Clearing points of DBA/DBP mixtures based on DSC with scan rate of 5 °C·min^{-1} on heating. I is an isotropic liquid, Col is a columnar phase and Cr indicated a crystalline solid phase.*

Based on this result, a 1:1:1 mixture was prepared that contained equimolar quantities of DBA, DBP, and TNF. Surprisingly, this mixture displayed a columnar phase between 30 and 75 ^{o}C, suggesting that the TNF was able to successfully stabilize the DBA/DBP mixture. When viewed via under the polarized optical microscope, however, this mixture displayed textures atypical of a hexagonal columnar mesophase

(Figure 4-18). Further studies, including X-ray diffraction will need to be performed in order to reconcile the type of phase that is being demonstrated by this mixture.

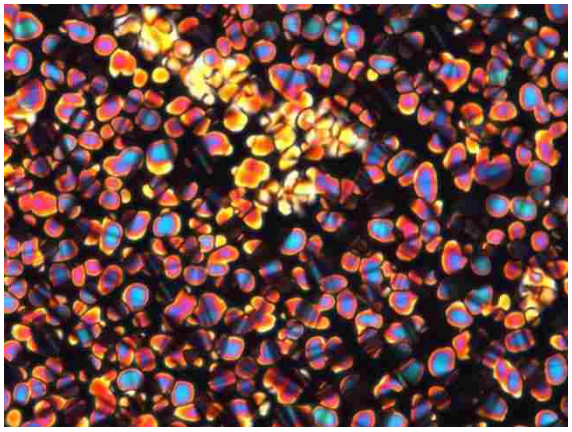

Figure 4-18: *Polarized optical micrograph of 1:1:1 DBA/DBP/TNF mixture at 80 °C on cooling at a rate of 10 °C·min^{-1} and taken at 500x magnification.*

4.3.5 Other Donors and Acceptors

Several other donor and acceptor series were also prepared and analyzed with varying degrees of success. Two series were prepared using tetracyanoquinodimethane (TCNQ) as the electron acceptor. One had the dibenzanthracene (DBA) acting as the electron donor, while the other had the dibenzophenazine (DBP) acting as the donor (Figure 4-19).

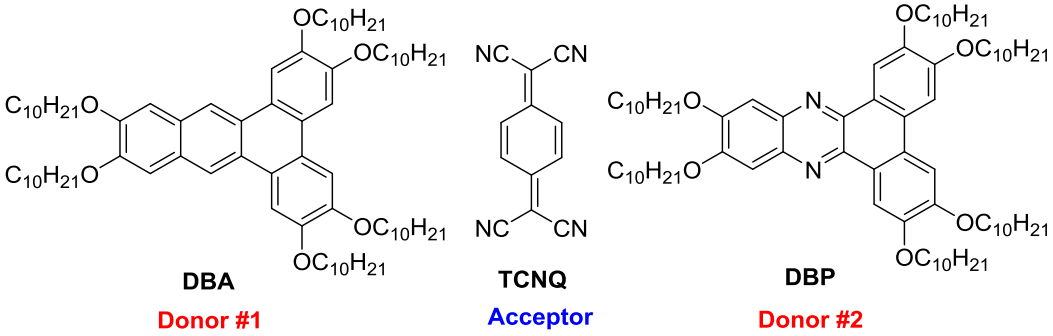

Figure 4-19: *Hexaalkoxydibenzanthracene (DBA) and hexaalkoxydibenzophenazine (DBP) electron donors and tetracyanoquinodimethane (TCNQ) electron acceptor.*

Unfortunately, the DBA/TCNQ series did not form miscible mixtures, with two distinct melting points observed with all of the samples. The DBP/TCNQ series only formed miscible mixtures up to a 1:1 molar ratio of donor to acceptor. Unfortunately, even small additions of TCNQ were seen to destabilize the columnar phase of the DBP.

A series using DBP as the electron donor and 9-fluorenone (9-F) as the electron acceptor was also prepared (Figure 4-20). Unfortunately, although these components did form miscible mixtures, no colour change was observed upon mixing, suggesting a charge-transfer complex between the donor and the acceptor was not formed. In addition, when analyzed using POM and DSC, it was observed that even small additions of the 9-fluorenone destabilized the columnar phase of the DBP.

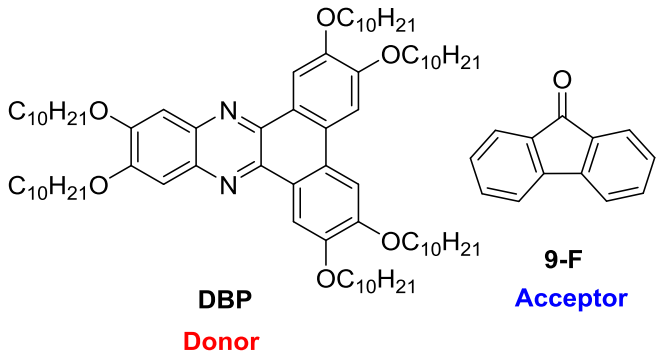

Figure 4-20: *Hexaalkoxydibenzophenazine (DBP) electron donor and 9-fluorenone (9-F) electron acceptor.*

4.4 Discussion

The hexaalkoxytriphenylene / trinitrofluorenone series displayed behaviour consistent with that noticed by Ringsdorf and co-workers. While the addition of even small amounts of TNF were seen to stabilize the columnar phase of the triphenylene, the 1:1 mixture had the broadest columnar phase with the highest overall clearing point. This result seems to support Ringsdorf's proposed theory that these components

assemble into columnar stacks of alternating donor and acceptor molecules.[53] A schematic representation of this stacking arrangement can be seen in Figure 4-21.

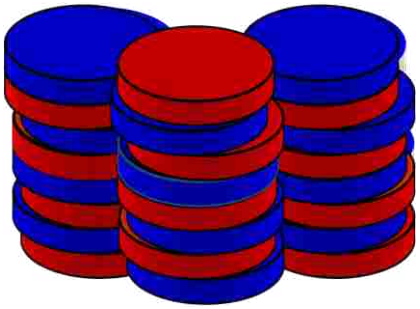

Figure 4-21: *Proposed stacking arrangement of the triphenylene / trinitrofuorenone series of alternating donor (red) and acceptor (blue) molecules.*

The structure of the hexaalkoxydibenzanthracene is very similar to that of the hexaalkoxytriphenylene, with the aromatic core being extended by only one benzene ring. Despite this, the pure forms of each display very different properties. While the triphenylene displays a liquid crystalline phase, the dibenzanthracene does not, melting directly from a crystalline solid to an isotropic liquid at 59 ^{o}C.[73] Despite this, it was hypothesized that, due to the structural similarities between the two donors, they would form similar complexes with the TNF and, therefore, display similar charge-transfer behaviour.

Surprisingly, the dibenzanthracene / trinitrofluorenone series displayed very different behaviour from the triphenylene / trinitrofluorenone series. The 1:1 molar ratio sample did not display a liquid crystalline phase at all. Instead, the 2:1 molar ratio mixture of donor to acceptor displayed the broadest liquid crystalline phase and highest clearing point. This would seem to suggest that the preferred stacking arrangement is not one of alternating stacks of donor and acceptor molecules. There are two possible stacking arrangements that may explain these results. The first proposed arrangement is

more of a 'sandwich' structure where there are two donor molecules for each acceptor molecule in the column. A schematic of this proposed stacking arrangement can be seen in Figure 4-22.

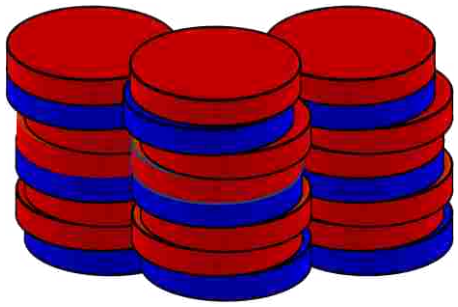

Figure 4-22: *Proposed 'sandwich' type stacking arrangement for the dibenzanthracene / trinitrofluorenone series. Donor molecules are in red and acceptor molecules are in blue.*

Another potential arrangement would be one where the hexaalkoxydibenzanthracene forms stacks by itself, with the trinitrofluorenone fitting in the spaces created by the long alkoxy chains. A schematic of this proposed stacking arrangement can be seen in Figure 4-23. This arrangement would allow for efficient packing of the molecules, possibly resulting in the induction of a columnar phase.

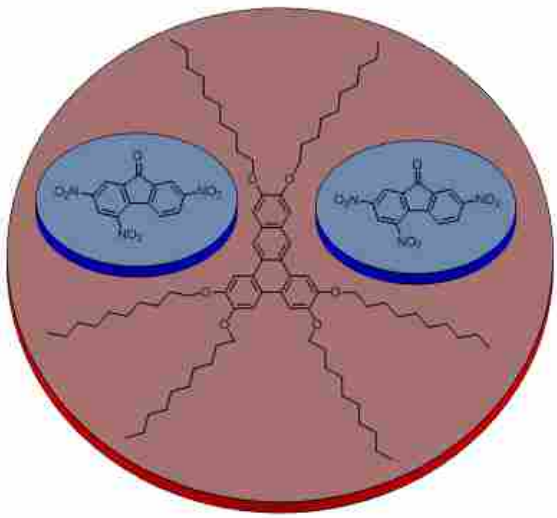

Figure 4-23: *Proposed stacking arrangement for the dibenzanthracene / trinitrofluorenone series where the acceptor molecules occupy the space created around the aromatic core by the long alkoxy chains. Donor molecules are in red and acceptor molecules are in blue.*

The sandwich-like 2:1 charge-transfer complex, however, is supported by the fact this behaviour is also seen in solution. When the absorbances of the different solutions are compared at 458 nm (the wavelength of the charge-transfer absorbance), it becomes apparent that the 2:1 mixture displays the highest absorbance of any of the different concentrations (Figure 4-24). It is surprising that the 20 % TNF solution also displays such a high absorbance at 458 nm while the 25 % TNF solution displays a slight minimum. This result was reproducible and may be the result of the 25 % sample (which would represent a 3:1 molar ratio of donor to acceptor) having a different and more unfavourable stacking pattern.

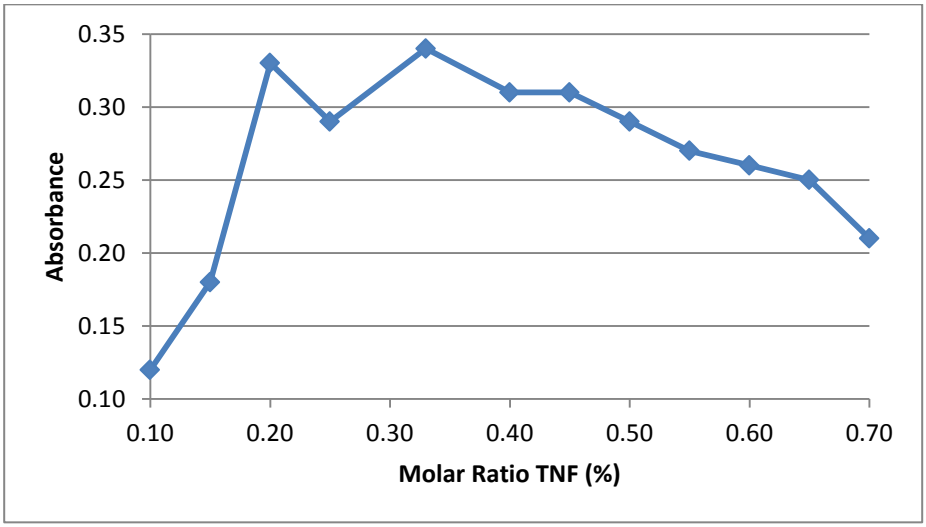

Figure 4-24: *Absorbance at 458 nm for each of the mixtures in the dibenzanthracene / trinitrofluorenone series.*

The results for the dibenzophenazine / trinitrofluorenone series and the bromo-substituted dibenzanthracene / trinitrofluorenone series also fit with the sandwich-like 2:1 stacking model. Both donors have structural similarities to the dibenzanthracene - the dibenzophenazine represents the same molecular structure, but has an aromatic core while the other donor adds two substituents onto the previously studied dibenzanthracene core. It is unsurprising, therefore, that both display similar behaviour

to the parent dibenzanthracene / trinitrofluorenone series with an approximate molar ratio of 2:1 donor to acceptor being favoured.

In addition, the fact that the bromo-substituted dibenzanthracene / trinitrofluorenone series displays similar behaviour to the parent dibenzanthracene / trinitrofluorenone series also supports the sandwich-type arrangement. If the other model were correct, we would expect this series to display different behaviour since the bromo substituents would take up some of the room in which the TNF molecules would be located (Figure 4-25).

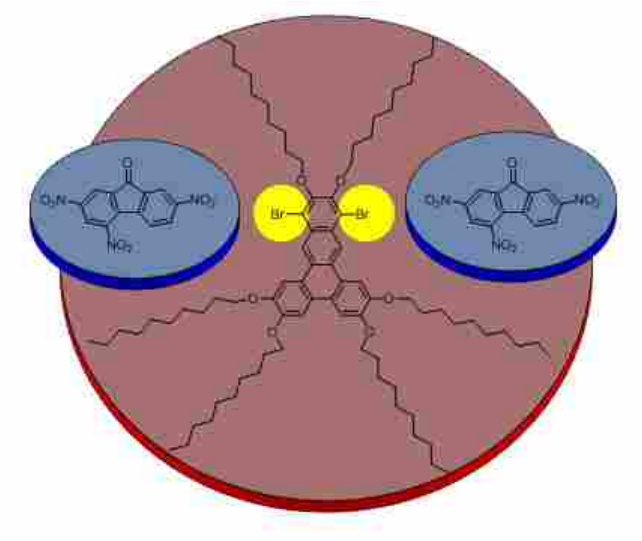

Figure 4-25: *Proposed stacking arrangement for the substituted dibenzanthracene / trinitrofluorenone series where the bromo substituents now occupy some of the space used by the TNF molecules. Donor molecules are in red and acceptor molecules are in blue.*

Although the above evidence seems to suggest that a 2:1 ratio of donor to acceptor in a sandwich-type packing arrangement is favoured for these types of molecules, further studies will be needed to provide further evidence for this theory. Computational studies on the donor molecules and acceptor molecules may help to provide an explanation for these trends in behaviour. Furthermore, X-ray diffraction studies may provide crystallographic evidence supporting the proposed stacking

arrangement. In addition, performing further studies on similar dibenzathracenes and dibenzophenzines where the substituents on the aromatic core are altered, may help to determine how prevalent this type of behaviour is in similar molecules.

4.5 Summary

Several series of novel electron donor-acceptor liquid crystals have been prepared. The hexaalkoxytriphenylene / trinitrofluorenone series displayed a favoured 1:1 molar ratio of donor to acceptor, which is consistent with previous reports and suggests a favoured stacking arrangement of alternating donor and acceptor molecules. In contrast, the hexaalkoxydibenzanthracene / trinitrofluroenone series demonstrated a preferred 2:1 molar ratio of electron donor to electron acceptor in both the solid state and in solution. Electron donors with similar structures, including a hexaalkoxydibenzophenazine and a substituted dibenzanthracene also displayed similar behaviour. These results would seem to suggest a preferred sandwich-like 2:1 stacking arrangement, with two donor molecules for each acceptor molecule in the columnar stacks. This type of stacking arrangement has not been reported in the literature before. Further evidence, including computational and crystallographic studies will be needed to further support this proposed stacking arrangement.

Chapter 5 Conclusions and Future Work

Two methyl ester substituted dibenzanthracenecarboxylates (**10h,i**) have been prepared using a modular approach (Figure 5-1). Unfortunately, although structurally similar compounds, substituted with electron withdrawing cyano groups displayed a mesomorphic phase, neither of the dibenzanthracenecarboxylates displayed a liquid crystalline phase. This may be the result of the methyl ester substituents not having enough electron withdrawing character to pull electron density away from the core of the molecule.

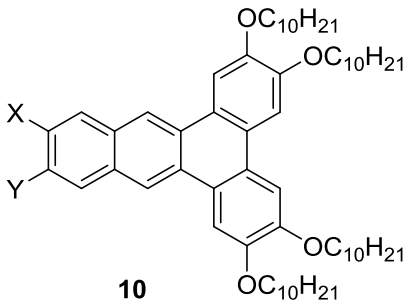

10

h X = COOMe, Y = H
i X = Y = COOMe

Figure 5-1: *Target dibenzanthracenecarboxylate molecules.*

Based on this result, a series of novel *N*-substituted dibenzanthracenedicarboximides (**22a-g**) were also prepared using a similar approach (Figure 5-2). By incorporating electron-withdrawing groups that contain flexible alkyl chains onto the aromatic core, we hoped to create electron deficient materials with broad columnar phases. With the exception of one compound that decomposed prior to melting, six of the derivatives did display broad columnar phases with relatively low melting transition temperatures. It was shown that, the longer and more flexible the alkyl chain on the nitrogen atom, the broader the columnar phase. Furthermore, these

compounds display positive solvatochromism, with a red-shifting of the emission maxima as the solvent becomes more polar.

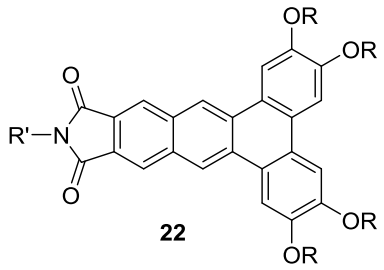

22

a R = $C_{10}H_{21}$ R' = C_4H_9
b R = $C_{10}H_{21}$ R' = C_8H_{17}
c R = $C_{10}H_{21}$ R' = $C_{12}H_{25}$
d R = $C_{10}H_{21}$ R' = $CH_2CH(CH_2CH_3)CH_2CH_2CH_2CH_3$
e R = C_6H_{13} R' = C_8H_{17}
f R = C_6H_{13} R' = $CH_2CH(CH_2CH_3)CH_2CH_2CH_2CH_3$
g R = C_6H_{13} R' = $C_{12}H_{25}$

Figure 5-2: *Target dibenzanthracenedicarboximide series.*

Future directions of this research could include post-synthetic modification of the aromatic core of these compounds in order to achieve a more accurate and revealing structure-property relationship.

Several novel electron donor-acceptor liquid crystalline series were also prepared (Figure 5-3). While the initial triphenylene / trinitrofluorenone series displayed the expected preferred 1:1 molar ratio, the structurally similar dibenzanthracene / trinitrofluorenone series displayed a preferred ratio of 2:1 donor to acceptor. Electron donors with similar structures also demonstrated this type of behaviour.

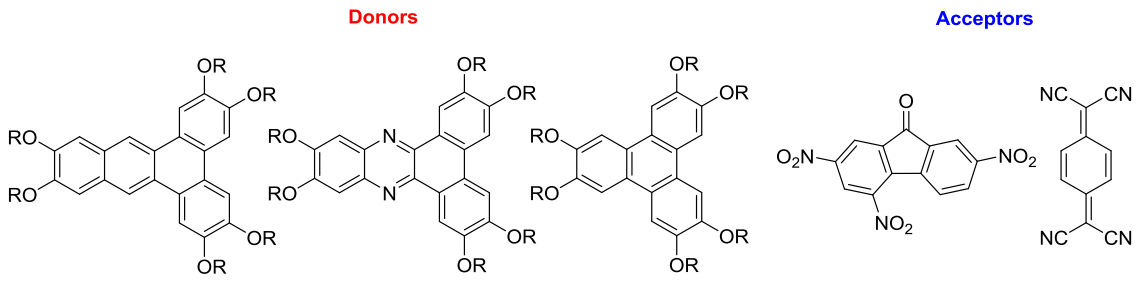

Figure 5-3: *Target electron donors and acceptors.*

These results suggest that a sandwich-like 2:1 stacking arrangement is preferred by this class of electron donors. This stacking arrangement has not previously been reported in the literature. Further computational and crystallographic studies are needed to confirm this proposed theory. Future directions for this research could include preparing additional electron donor-acceptor series which use dibenzanthracene and dibenzophenazine compounds that differ in the number and type of substituents on the aromatic core. Ultimately, a better understanding of this behaviour will allow us to tune liquid crystalline properties and develop materials with potential applications in organic electronics.

Chapter 6 Experimental Procedures

6.1 General

6.1.1 NMR Spectroscopy

^{1}H and ^{13}C spectra were recorded on a Varian 300 MHz (1H) Unity Inova NMR Spectrometer or a Agilent Technologies 400 MHz Spectrometer (as indicated) using the indicated deuterated solvents purchased from CIL Int. Chemical shifts are reported in δ scale downfield from the peak for tetramethylsilane.

In some cases not all aliphatic and/or aromatic ^{13}C peaks are observed in substituted dibenzanthracenedicarboxylates or dibenzanthracenedicarboximides and their precursors due to overlapping signals.

6.1.2 High Resolution Mass Spectrometry

High resolution mass spectra were recorded at the Centre Régional de Spectrométrie de Masse à l'Université de Montréal using an Agilent LC-MSD TOF spectrometer.

6.1.3 Mesophase Characterization

Polarized optical microscopy studies were performed using an Olympus BX-51 polarized optical microscope equipped with a Linkam LTS 350 heating stage and a digital camera. Differential scanning calorimetry studies were carried out using a TA Instruments DSC Q200 with a scanning rate of 5 °C/min. Variable temperature X-Ray diffraction measurements were carried out by Kevin Bozek and Professor Vance Williams at Simon Fraser University.

6.1.4 Chemicals and Solvents

All reagents and starting materials were purchased from Sigma-Aldrich and used as purchased, with the exception of TCNQ, which was recrystallized from acetonitrile prior to use. Anhydrous solvents were dispensed using a custom-built solvent system from Glasscontour (Irvine, CA) which used purification columns packed with activated alumina and supported copper catalyst. Oven-dried glassware was used for all reactions that were performed under nitrogen. The following compounds were prepared according to literature procedures: 1,2-bis(decyloxy)benzene,[96] 1,2-bis(hexyloxy)benzene,[96] 1,2-dibromo-4,5-bis(dibromomethyl)benzene,[76] trinitrofluorenone,[94] 2,3,6,7-tetrakis(tetradecyloxy)-9,10-phenanthrenedione,[97] 4,5-bis(decyloxy)-1,2-benzenediamine,[95] 2,3,6,7,11,12-hexakis(decyloxy)dibenzo[a,c]phenazine,[95] 2,3-dibromo-6,7-bis(decyloxy)naphthalene,[41,98] 2,3,6,7,11,12-hexakis(decyloxy)dibenz[a,c]anthracene,[73] and 10,13-dibromo-2,3,6,7,11,12-hexakis(decyloxy)benzo[b]triphenylene.[73]

6.2 Synthesis

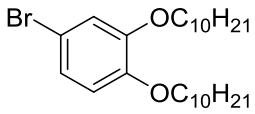

1-bromo-3,4-bis(decyloxy)benzene (12a)[99] 1,2-bis(decyloxy)benzene (10.0 g, 25.6 mmol) and THF (75 mL) were combined in a round bottom flask and cooled to 0 ^{o}C under N_2. NBS (5.02 g, 28.2 mmol) was added to the reaction mixture over a period of approximately 5 minutes. The solution was allowed to gradually warm to room temperature and was stirred for 4 days. 75 mL of water was added and the product was extracted using ethyl acetate (3x75 mL). The organic phase was washed with water

(2x50 mL) and brine (1x50 mL). The organic phase was dried with $MgSO_4$ and the solvent was removed under reduced pressure. The crude product was recrystallized from ethanol to yield **12a** as a beige solid (10.7 g, 89 %). ^{1}H NMR (300 MHz, $CDCl_3$) δ: 0.89 (m, 6H), 1.27 (m, 28H), 1.81 (m, 4H), 3.95 (m, 4H), 6.75 (d, 1H, J = 9 Hz), 6.97 (m, 2H). NMR data compared to literature values.[22]

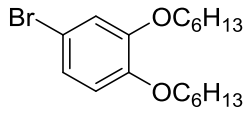

1-bromo-3,4-bis(hexyloxy)benzene (12b):[99] 1,2-bis(hexyloxy)benzene (13.0 g, 46.6 mmol) and THF (200 mL) were combined in a round bottom flask and cooled to 0 ^oC under N_2. NBS (9.14 g, 51.4 mmol) was added to the reaction mixture over a period of approximately 5 minutes. The solution was allowed to gradually warm to room temperature and was stirred for a period of 4 days. 100 mL of water was added and the product was extracted using ethyl acetate (3x100 mL). The organic phase was washed with water (2x75 mL) and brine (1x75 mL). The organic phase was dried with $MgSO_4$ and the solvent was removed under reduced pressure. The crude product was recrystallized from ethanol to yield **12b** as a yellow oil (10.0 g, 62 %). ^{1}H NMR (400 MHz, $CDCl_3$) δ: 0.91 (m, 8H), 1.35 (m, 26H), 1.78 (m, 4H), 3.94 (m, 4H), 6.72 (d, 1H, J = 8 Hz), 6.98 (m, 2H). NMR data compared to literature values.[22]

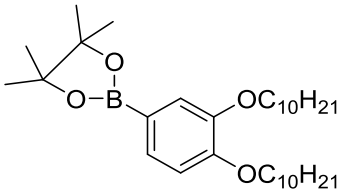

1-pinacolatoboron-3,4-bis(decyloxy)benzene (13a):[99] 1-bromo-3,4-bis(decyloxy)benzene (10.0 g, 21.3 mmol), bis(pinacolato)diboron (5.99 g, 23.6 mmol), Pd(dppf)Cl_2 (0.47 g, 0.63 mmol) and potassium acetate (6.27 g, 63.9 mmol) were combined in a round bottom flask and purged with N_2. Anhydrous DMSO (125 mL) was added to the flask using a canula. The solution was then heated to 80 ^oC and left to stir under N_2 for 3 days. The solution was then cooled to room temperature, followed by the addition of 75 mL dichloromethane and washed with water (2x50 mL) and brine (1x50 mL). The organic phase was dried with $MgSO_4$ and the solvent was removed under reduced pressure to yield a brown oil as the crude product. The crude product was purified via column chromatography (98:2 hexanes/ethyl acetate) to yield **13a** as a yellow oil (9.47 g, 86 %). ^1H NMR (300 MHz, $CDCl_3$) δ: 0.89 (m, 6H), 1.27 (m, 28H), 1.81 (m, 4H), 4.02 (m, 4H), 6.87 (d, 1H, J = 8 Hz), 7.30 (s, 1H), 7.40 (d, 1H, J = 8 Hz). NMR data compared to literature values.[22]

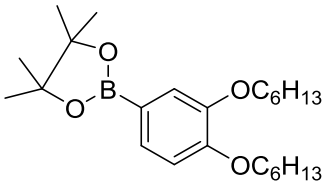

1-pinacolatoboron-3,4-bis(hexyloxy)benzene (13b):[99] 1-bromo-3,4-bis(hexyloxy)benzene (10.0 g, 27.9 mmol), bis(pinacolato)diboron (7.87 g, 31.0 mmol), Pd(dppf)Cl_2 (0.61 g, 0.84 mmol) and potassium acetate (8.24 g, 83.9 mmol) were

combined in a round bottom flask and purged with N_2. Anhydrous DMSO (125 mL) was added to the flask using a canula. The solution was then heated to 80 ^oC and left to stir under N_2 for 5 days. The solution was then cooled to room temperature, followed by the addition of 75 mL dichloromethane and washed with water (2x50 mL) and brine (1x50 mL). The organic phase was dried with $MgSO_4$ and the solvent was removed under reduced pressure to yield a brown oil as the crude product. The crude product was purified via column chromatography (98:2 hexanes/ethyl acetate) to yield **13b** as a dark yellow oil (6.59 g, 58 %). ^1H NMR (400 MHz, $CDCl_3$) δ: 0.89 (m, 6H), 1.31 (m, 12H), 1.78 (m, 4H), 3.99 (m, 4H), 6.84 (d, 1H, J = 8 Hz), 7.26 (s, 1H), 7.36 (d, 1H, J = 7 Hz). NMR data compared to literature values.[22]

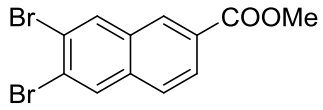

Methyl 6,7-dibromo-2-naphthalenecarboxylate (16a): 1,2-Dibromo-4,5-bis(dibromomethyl)benzene (5.00 g, 8.63 mmol) and potassium iodide (2.29 g, 13.80 mmol) were combined in a round bottom flask and purged with N_2. Dry DMF (50 mL) was added to the flask and the reaction mixture was heated to 80 ^oC. Methyl acrylate (0.89 g, 10.35 mmol) was added and the mixture was heated at 80 ^oC under N_2 for 23 hrs. The reaction mixture was then poured into 100 mL of water. 120 mL of sodium thiosulfate was added and the resulting precipitate was collected by suction filtration. The crude product was purified via column chromatography (9:1 hexanes/ethyl acetate) and the resulting product was recrystallized from hexanes to yield **16a** as a yellow solid (0.91 g, 31 %). ^1H NMR (400 MHz, $CDCl_3$) δ: 3.99 (s, 3H), 7.76 (d, 1H, J = 8 Hz), 8.10

(d, 1H, J = 7 Hz), 8.19 (s, 1H), 8.24 (s, 1H), 8.49 (s, 1H). ^{13}C NMR (100 MHz, $CDCl_3$) δ: 52.4, 123.0, 124.8, 126.5, 127.1, 128.6, 129.8, 132.0, 132.1, 133.3, 134.7, 166.5. HRMS (ASAP) calc'd for $C_{12}H_8O_2Br_2$ *m/z* 341.8902, found 341.8891.

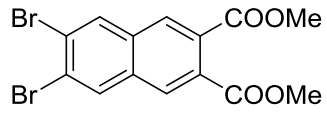

Dimethyl 6,7-dibromo-2,3-naphthalenedicarboxylate (16b): 1,2-Dibromo-4,5-bis(dibromomethyl)benzene (5.00 g, 8.63 mmol) and potassium iodide (2.29 g, 13.80 mmol) were combined in a round bottom flask and purged with N_2. Dry DMF (50 mL) was added to the flask and the reaction mixture was heated to 80 ^{o}C. Dimethyl fumarate (1.49 g, 10.35 mmol) was added and the mixture was heated at 80 ^{o}C under N_2 for 23 hours. The reaction mixture was then poured into 100 mL of water. 120 mL of sodium thiosulfate was added and the resulting precipitate was suction filtered. The crude product was purified via column chromatography (9:1 hexanes/ethyl acetate) and the resulting product was recrystallized from ethyl acetate/hexanes to yield **16b** as a beige solid (2.87 g, 83 %). ^{1}H NMR (400 MHz, $CDCl_3$) δ: 3.97 (s, 6H), 8.14 (s, 2H), 8.23 (s, 2H). ^{13}C NMR (100 MHz, $CDCl_3$) δ: 52.8, 125.4, 128.9, 129.7, 132.7, 132.8, 167.4. HRMS (ASAP) calc'd for $C_{14}H_{10}O_4Br_2$ *m/z* 399.8946, found 399.8951.

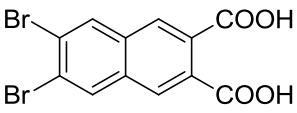

6,7-dibromo-2,3-naphthalenedicarboxylic acid (18): Dimethyl 6,7-dibromo-2,3-naphthalenedicarboxylate (4.00 g, 9.95 mmol) was dissolved in methanol (500 mL) with

heating in a round bottom flask fitted with a reflux condenser. Potassium hydroxide (19.5 g, 348 mmol) was added as a solution in water (500 mL). The solution was heated at reflux for 18 hours. The reaction mixture was then concentrated slightly to remove the methanol. Any remaining starting material was extracted from the remaining solution using ethyl acetate. The aqueous layer was then acidified using aqueous HCl, resulting in the formation of a white precipitate. The precipitate was collected via suction filtration to yield **18** as a white solid (0.37 g, 99 %). The resulting product was used without further purification. ^{1}H NMR (300 MHz, DMSO) δ: 8.62 (s, 2H), 8.54 (s, 2H).

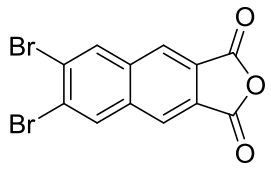

6,7-dibromo-naphtho[2,3-c]furan-1,3-dione (19): 6,7-dibromo-2,3-naphthalenedicarboxylic acid (3.72 g, 9.94 mmol) was dissolved in acetic anhydride (500 mL) in a round bottom flask. The solution was heated to reflux and allowed to stir for a period of 7 hours. The solution was then cooled to room temperature and poured over crushed ice, resulting in the formation of a precipitate. The precipitate was collected via suction filtration to yield **19** as a beige solid (2.70 g, 76 %). ^{1}H NMR (400 MHz, $CDCl_3$) δ: 8.75 (s, 2H), 8.84 (s, 2H). ^{13}C NMR (100 MHz, $CDCl_3$) δ: 126.4, 126.7, 128.0, 135.0, 135.4, 163.4. HRMS (ASAP) calc'd for $C_{12}H_4O_3Br_2$ *m/z* 353.8527, found 353.8531.

General procedure for the synthesis of 6,7-dibromo-2-alkyl-benzo[f]isoindole-1,3-diones (20): 6,7-dibromo-naphtho[2,3-c]furan-1,3-dione (1 eq) and the desired amine (1.5 eq) were dissolved in 100 mL of glacial acetic acid (excess). The mixture was heated to reflux under N_2 for 18 hours. The solution was cooled to room temperature and the solvent was removed under reduced pressure. The crude products were purified according to the conditions listed.

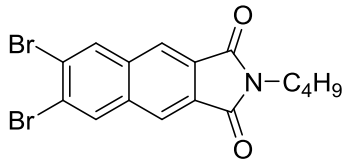

6,7-dibromo-2-butyl-benzo[f]isoindole-1,3-dione (20a): 6,7-dibromo-naphtho[2,3-c]furan-1,3-dione (0.80 g, 2.24 mmol), butylamine (0.25 g, 3.37 mmol) and glacial acetic acid (100 mL) were used. The crude product was purified via column chromatography (9:1 hexanes/ethyl acetate) and the resulting product was recrystallized from dichloromethane/hexanes to yield **20a** as a beige solid (0.79 g, 86 %). ^{1}H NMR (400 MHz, $CDCl_3$) δ: 0.97 (m, 3H), 1.41 (m, 2H), 1.71 (m, 2H) 3.76 (t, 2H, J = 7 Hz), 8.22 (s, 2H), 8.35 (s, 2H). ^{13}C NMR (100 MHz, $CDCl_3$) δ: 13.6, 20.1, 30.5, 38.2, 123.2, 126.1, 129.0, 134.1, 134.7, 167.3. HRMS (ASAP) calc'd for $C_{16}H_{13}NO_2Br_2$ *m/z* 408.9308, found 408.9313.

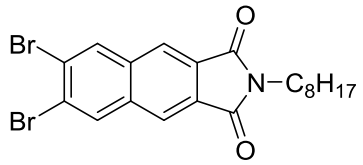

6,7-dibromo-2-octyl-benzo[f]isoindole-1,3-dione (20b): 6,7-dibromo-naphtho[2,3-c]furan-1,3-dione (0.30 g, 0.84 mmol), octylamine (0.16 g, 1.26 mmol) and glacial acetic acid (100 mL) were used. The crude product was purified via column chromatography (9:1 hexanes/ethyl acetate) and the resulting product was recrystallized from dichloromethane/hexanes to yield **20b** as a beige solid (0.30 g, 77 %). ^{1}H NMR (400 MHz, $CDCl_3$) δ: 0.87 (m, 3H), 1.31 (m, 10H), 1.71 (m, 2H) 3.75 (t, 2H, J = 7 Hz), 8.22 (s, 2H), 8.35 (s, 2H). ^{13}C NMR (100 MHz, $CDCl_3$) δ: 14.0, 22.5, 26.8, 28.4, 29.1, 31.7, 38.5, 123.2, 126.1, 129.1, 134.1, 134.7, 167.3.

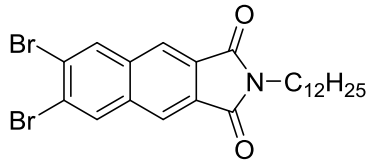

6,7-dibromo-2-dodecyl-benzo[f]isoindole-1,3-dione (20c): 6,7-dibromo-naphtho[2,3-c]furan-1,3-dione (0.65 g, 1.82 mmol), dodecylamine (0.51 g, 2.73 mmol) and glacial acetic acid (100 mL) were used. The crude product was purified via column chromatography (9:1 hexanes/ethyl acetate) and the resulting product was recrystallized from acetone to yield **20c** as a beige solid (0.86 g, 90 %). ^{1}H NMR (400 MHz, $CDCl_3$) δ: 0.88 (m, 3H), 1.25 (m, 18H), 1.71 (m, 2H) 3.75 (t, 2H, J = 7 Hz), 8.22 (s, 2H), 8.35 (s, 2H). ^{13}C NMR (100 MHz, $CDCl_3$) δ: 14.0, 22.6, 26.8, 28.4, 29.1, 29.3, 29.4, 29.53, 29.58, 29.59, 31.8, 38.5, 123.2, 126.1, 129.1, 134.1, 134.7, 167.3.

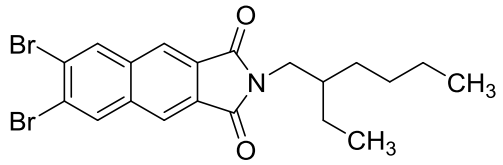

6,7-dibromo-2-(2-ethyl-1-hexylimide)-benzo[f]isoindole-1,3-dione (20d): 6,7-dibromo-naphtho[2,3-c]furan-1,3-dione (0.75 g, 2.11 mmol), 2-ethyl-1-hexylamine (0.41 g, 3.16 mmol) and glacial acetic acid (100 mL) were used. The crude product was purified via column chromatography (9:1 hexanes/ethyl acetate) and the resulting product was recrystallized from dichloromethane/hexanes to yield **20d** as a beige solid (0.76 g, 77 %). ^{1}H NMR (400 MHz, $CDCl_3$) δ: 0.91 (m, 6H), 1.35 (m, 8H), 1.88 (m, 1H) 3.66 (d, 2H, J = 8 Hz), 8.22 (s, 2H), 8.35 (s, 2H). ^{13}C NMR (100 MHz, $CDCl_3$) δ: 10.3, 14.0, 22.9, 23.8, 28.4, 30.5, 38.2, 42.3, 123.2, 126.1, 129.0, 134.1, 134.8, 167.6.

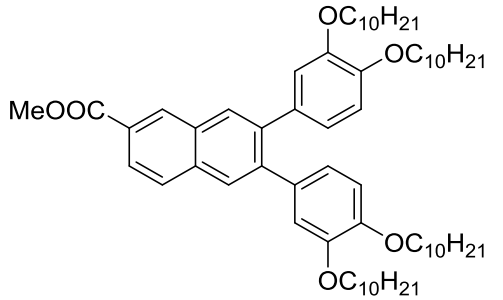

Methyl 6,7-bis(3',4'-didecyloxyphenyl)-2-naphthalenecarboxylate (17a): Methyl 6,7-dibromo-2-naphthalenecarboxylate (0.25 g, 0.73 mmol), 1-pinacolatoboron-3,4-bis(decyloxy)benzene (0.95 g, 1.83 mmol), aq. 2.0 M K_2CO_3 (2.50 mL), ethanol (2.50 mL), and toluene (10.0 mL) were combined in a round bottom flask and purged with N_2. $Pd(PPh_3)_4$ (0.042 g, 0.036 mmol), was added and the mixture was heated to 80 ^{o}C and left to stir under N_2 for a period of 3 days. The solution was cooled to room temperature, followed by the addition of 20 mL dichloromethane, and washed with

water (2x20 mL) and brine (1x50 mL). The organic phase was dried with $MgSO_4$ and the solvent was removed under reduced pressure. The crude product was purified via column chromatography (60:40 hexanes/dichloromethane) and the resulting product was recrystallized from ethanol to yield **17a** as a yellow solid (0.31 g, 43 %). ^{1}H NMR (400 MHz, $CDCl_3$) δ: 0.88 (m, 12H), 1.47 (m, 56H), 1.67 (m, 4H), 1.82 (m, 4H), 3.71 (m, 4H), 3.98 (m, 7H), 6.67 (s, 2H), 6.82 (m, 4H), 7.89 (m, 2H), 7.97 (s, 1H), 8.07 (d, 1H, J = 9 Hz), 8.63 (s, 1H). ^{13}C NMR (100 MHz, $CDCl_3$) δ: 14.0, 22.6, 26.01, 26.05, 29.1, 29.35, 29.38, 29.41, 29.47, 29.5, 29.61, 29.64, 29.69, 31.9, 52.2, 69.1, 69.2, 113.2, 115.9, 122.0, 125.3, 127.4, 127.7, 128.7, 130.2, 130.7, 131.6, 133.7, 133.8, 134.6, 139.8, 141.4, 148.1, 148.2, 148.4, 167.2. HRMS (ASAP) calc'd for $C_{64}H_{98}O_6$ *m/z* 962.7363, found 962.7353.

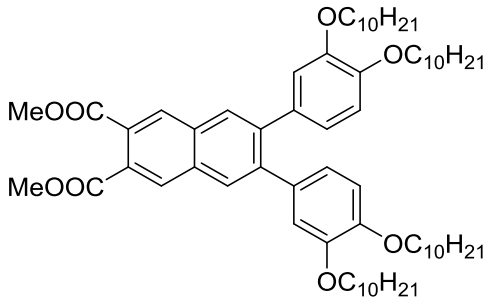

Dimethyl 6,7-bis(3',4'-didecyloxyphenyl)-2,3-naphthalenedicarboxylate (17b): Dimethyl 6,7-dibromo-2,3-naphthalenedicarboxylate (0.50 g, 1.24 mmol), 1-pinacolatoboron-3,4-bis(decyloxy)benzene (1.62 g, 3.13 mmol), aq. 2.0 M K_2CO_3 (5.00 mL), ethanol (5.00 mL), and toluene (20.0 mL) were combined in a round bottom flask and purged with N_2. $Pd(PPh_3)_4$ (0.072 g, 0.062 mmol), was added and the mixture was heated to 80 ^{o}C and stirred under N_2 for 3 days. The solution was cooled to room temperature, followed by the addition of 20 mL dichloromethane, and washed with

water (2x20 mL) and brine (1x50 mL). The organic phase was dried with $MgSO_4$ and the solvent was removed under reduced pressure. The crude product was purified via column chromatography (95:5 hexanes/ethyl acetate) to give a yellow oil. The resulting product was used in the next step without further purification (0.49 g, 39 %).

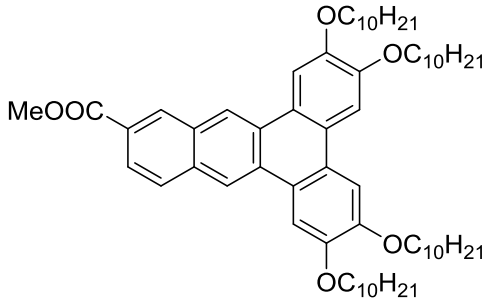

Methyl 2,3,6,7-tetrakis(decyloxy)-11-dibenz[a,c]anthracenecarboxylate (10h): Methyl 6,7-bis(3',4'-didecyloxyphenyl)-2-naphthalenecarboxylate (0.14 g, 0.14 mmol), and $FeCl_3$ (0.14 g, 0.87 mmol), were dissolved in dichloromethane (25.0 mL). The solution was stirred at room temperature under N_2 for 30 minutes. The solution was poured into methanol (100 mL), followed by the addition of water (50 mL). The product was extracted using dichloromethane (3x50 mL). The organic layer was dried using $MgSO_4$ and purified via a short silica column (100 % dichloromethane). The solvent was removed under reduced pressure. The crude product was recrystallized from acetone/methanol to yield **10h** as a yellow solid (0.10 g, 78 %). ^{1}H NMR (400 MHz, $CDCl_3$) δ: 0.89 (m, 12H), 1.41 (m, 46H), 1.58 (m, 10H), 1.98 (m, 8H), 4.03 (s, 3H), 4.28 (m, 8H), 7.79 (s, 2H), 8.10 (m, 4H), 8.87 (s, 1H), 8.90 (s, 1H), 9.01 (s, 1H). ^{13}C NMR (100 MHz, $CDCl_3$) δ: 14.0, 22.6, 26.1, 29.3, 29.4, 29.5, 29.60, 29.68, 31.9, 52.2, 69.4, 69.5, 69.6, 69.7, 107.3, 107.5, 107.9, 120.9, 123.0, 123.2, 123.3, 124.3,

124.5, 124.8, 126.8, 128.0, 128.7, 130.1, 130.3, 131.5, 133.1, 149.1, 149.2, 149.9, 150.2, 167.3. HRMS (ASAP) calc'd for $C_{64}H_{96}O_6$ *m/z* 960.7207, found 960.7195.

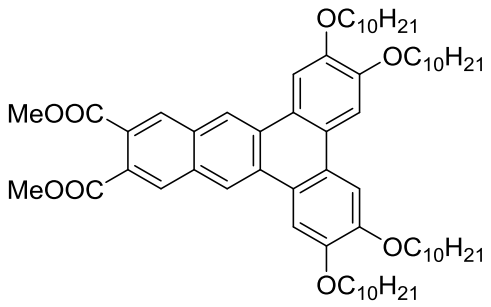

Dimethyl 2,3,6,7-tetrakis(decyloxy)-11,12-dibenz[a,c]anthracenedicarboxylate (10i): Dimethyl 6,7-dibromo-2,3-naphthalenedicarboxylate (0.36 g, 0.35 mmol), and $FeCl_3$ (0.34 g, 2.11 mmol), were dissolved in dichloromethane (50.0 mL). The solution was stirred at room temperature under N_2 for 30 minutes. The solution was poured into methanol (100 mL), and the resulting precipitate was collected via suction filtration. The crude product was dissolved in DCM and purified via a short silica column (100 % dichloromethane). The solvent was removed under reduced pressure. The crude product was recrystallized from acetone/methanol to yield **10i** as a yellow solid. Based on the lack of mesophase, the resulting product was not purified further.

General procedure for the synthesis of the *N*-substituted-6,7-bis(3',4'-dialkyloxy)-2,3-naphthalenedicarboximides (21): The 6,7-dibromo-2-alkyl-benzo[f]isoindole-1,3-dione (1 eq), 1-pinacolatoboron-3,4-bis(alkyloxy)benzene (2.52 eq), 5.00 mL of aq. 2.0 M K_2CO_3 (10.3 eq), 5.00 mL of ethanol (10.3 eq), and 20.0 mL of toluene (excess) were combined in a round bottom flask and degassed with N_2. $Pd(PPh_3)_4$ (5 mol %) was added and the mixture was heated to 80 ^oC and left to stir under N_2 for 3 days. The

solution was cooled to room temperature, followed by the addition of 20 mL dichloromethane, and washed with water (2x20 mL) and brine (1x50 mL). The organic phase was dried with $MgSO_4$ and the solvent was removed under reduced pressure. The crude products were purified according to the conditions listed.

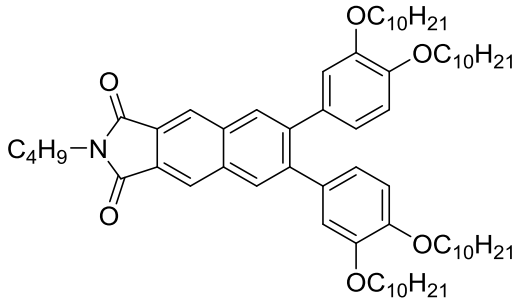

***N*-butyl-6,7-bis(3',4'-didecyloxyphenyl)-2,3-naphthalenedicarboximide (21a):** 6,7-dibromo-2-butyl-benzo[f]isoindole-1,3-dione (0.39 g, 0.97 mmol), 1-pinacolatoboron-3,4-bis(decyloxy)benzene (1.26 g, 2.52 mmol), $Pd(PPh_3)_4$ (0.056 g, 0.048 mmol), aq. 2.0 M K_2CO_3 (5.25 mL), ethanol (5.25 mL), and toluene (22.0 mL) were used. The crude product was purified via column chromatography (60:40 hexanes/dichloromethane) and the resulting product was recrystallized from acetone to yield **21a** as a white solid (0.82 g, 82 %). ^{1}H NMR (400 MHz, $CDCl_3$) δ: 0.88 (m, 12H), 0.96 (m, 3H), 1.28 (m, 58H), 1.67 (m, 6H), 1.82 (m, 4H), 3.71 (m, 4H), 3.77 (m, 2H), 3.98 (m, 4H), 6.66 (s, 2H), 6.84 (m, 4H), 8.04 (s, 2H), 8.33 (s, 2H). ^{13}C NMR (100 MHz, $CDCl_3$) δ: 13.6, 14.0, 20.1, 22.6, 26.00, 26.05, 29.0, 29.30, 29.34, 29.38, 29.40, 29.46, 29.5, 29.61, 29.63, 29.68, 29.7, 30.6, 31.9, 38.0, 69.1, 113.2, 115.7, 122.0, 124.1, 127.9, 131.1, 132.9, 134.4, 142.3, 148.5, 148.6, 168.2. HRMS (ASAP) calc'd for $C_{68}H_{103}NO_6$ *m/z* 1029.7806, found 1029.7785.

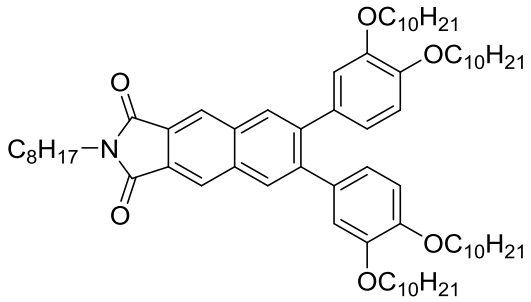

***N*-octyl-6,7-bis(3',4'-didecyloxyphenyl)-2,3-naphthalenedicarboximide (21b):** 6,7-dibromo-2-octyl-benzo[f]isoindole-1,3-dione (0.23 g, 0.49 mmol), 1-pinacolatoboron-3,4-bis(decyloxy)benzene (0.64 g, 1.24 mmol), $Pd(PPh_3)_4$ (0.028 g, 0.024 mmol), aq. 2.0 M K_2CO_3 (2.50 mL), ethanol (2.50 mL), and toluene (10.0 mL) were used. The crude product was purified via column chromatography (70:30 hexanes/dichloromethane) and the resulting product was recrystallized from acetone to yield **21b** as a yellow solid (0.47 g, 88 %). ^{1}H NMR (400 MHz, $CDCl_3$) δ: 0.88 (m, 15H), 1.28 (m, 66H), 1.67 (m, 6H), 1.82 (m, 4H), 3.73 (m, 6H), 3.98 (m, 4H), 6.67 (s, 2H), 6.84 (m, 4H), 8.04 (s, 2H), 8.33 (s, 2H). ^{13}C NMR (100 MHz, $CDCl_3$) δ: 14.0, 22.61, 22.67, 26.00, 26.04, 26.9, 28.5, 29.0, 29.15, 29.17, 29.30, 29.34, 29.38, 29.40, 29.46, 29.5, 29.61, 29.63, 29.68, 31.7, 31.9, 38.3, 69.1, 113.2, 115.7, 122.0, 124.1, 127.9, 131.1, 132.9, 134.4, 142.3, 148.53, 148.59, 168.2. HRMS (ASAP) calc'd for $C_{72}H_{111}NO_6$ *m/z* 1085.8411, found 1085.8406.

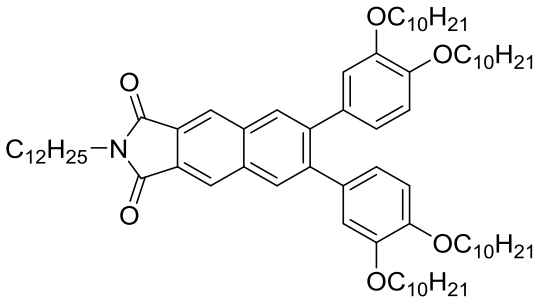

***N*-dodecyl-6,7-bis(3',4'-didecyloxyphenyl)-2,3-naphthalenedicarboximide (21c):** 6,7-dibromo-2-dodecyl-benzo[f]isoindole-1,3-dione (0.46 g, 0.87 mmol), 1-pinacolatoboron-3,4-bis(decyloxy)benzene (1.14 g, 2.20 mmol), $Pd(PPh_3)_4$ (0.050 g, 0.043 mmol), aq. 2.0 M K_2CO_3 (5.00 mL), ethanol (5.00 mL), and toluene (20.0 mL) were used. The crude product was purified via column chromatography (60:40 hexanes/dichloromethane) and the resulting product was recrystallized from acetone to yield **21c** as a yellow solid (0.81 g, 81 %). ^{1}H NMR (400 MHz, $CDCl_3$) δ: 0.88 (m, 15H), 1.28 (m, 74H), 1.67 (m, 6H), 1.82 (m, 4H), 3.73 (m, 6H), 3.98 (m, 4H), 6.67 (s, 2H), 6.84 (m, 4H), 8.04 (s, 2H), 8.33 (s, 2H). ^{13}C NMR (100 MHz, $CDCl_3$) δ: 11.5, 20.0, 20.1, 23.43, 23.47, 24.3, 26.0, 26.5, 26.6, 26.72, 26.75, 26.78, 26.81, 26.84, 26.89, 27.02, 27.04, 27.07, 27.12, 27.17, 29.32, 29.34, 35.7, 66.6, 110.6, 113.1, 119.4, 121.6, 125.3, 128.5, 130.4, 131.9, 139.7, 145.9, 146.0, 165.6. HRMS (ASAP) calc'd for $C_{79}H_{119}NO_6$ *m/z* 1141.9037, found 1141.9016.

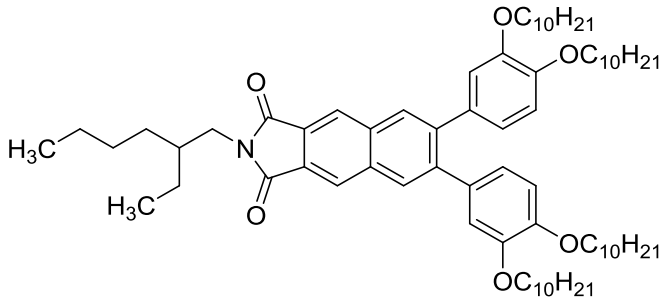

***N*-2-ethyl-1-hexyl-6,7-bis(3',4'-didecyloxyphenyl)-2,3-naphthalenedicarboximide (21d):** 6,7-dibromo-2-(2-ethyl-1-hexyl)-benzo[f]isoindole-1,3-dione (0.43 g, 0.92 mmol), 1-pinacolatoboron-3,4-bis(decyloxy)benzene (1.19 g, 2.31 mmol), $Pd(PPh_3)_4$ (0.051 g, 0.046 mmol), aq. 2.0 M K_2CO_3 (5.00 mL), ethanol (5.00 mL), and toluene (20.0 mL) were used. The crude product was purified via column chromatography (60:40 hexanes/dichloromethane) to yield a yellow oil. The resulting product was used in the next step without further purification (0.85 g, 85 %).

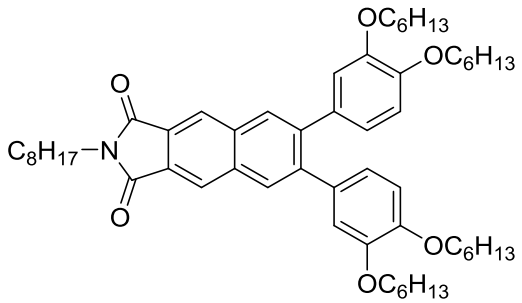

***N*-octyl-6,7-bis(3',4'-dihexyloxyphenyl)-2,3-naphthalenedicarboximide (21e):** 6,7-dibromo-2-octyl-benzo[f]isoindole-1,3-dione (0.40 g, 0.85 mmol), 1-pinacolatoboron-3,4-bis(hexyloxy)benzene (0.87 g, 2.15 mmol), $Pd(PPh_3)_4$ (0.050 g, 0.043 mmol), aq. 2.0 M K_2CO_3 (5.25 mL), ethanol (5.25 mL), and toluene (21.0 mL) were used. The crude product was purified via column chromatography (60:40 hexanes/dichloromethane) to

yield a yellow oil. The resulting product was used in the next step without further purification (0.57 g, 78 %).

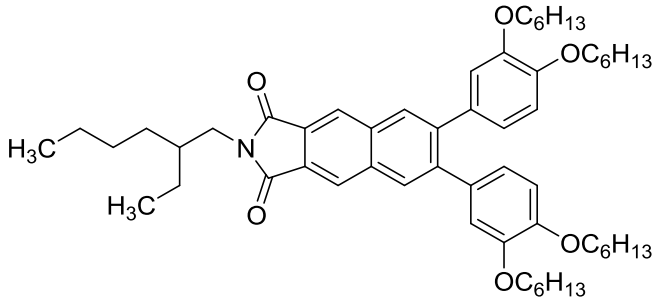

***N*-2-ethyl-1-hexyl-6,7-bis(3',4'-dihexyloxyphenyl)-2,3-naphthalenedicarboximide (21f):** 6,7-dibromo-2-(2-ethyl-1-hexyl)-benzo[f]isoindole-1,3-dione (0.30 g, 0.84 mmol), 1-pinacolatoboron-3,4-bis(hexyloxy)benzene (0.86 g, 2.12 mmol), $Pd(PPh_3)_4$ (0.050 g, 0.042 mmol), aq. 2.0 M K_2CO_3 (5.00 mL), ethanol (5.00 mL), and toluene (20.0 mL) were used. The crude product was purified via column chromatography (60:40 hexanes/dichloromethane) to yield a yellow oil. The resulting product was used in the next step without further purification (0.71 g, 96 %).

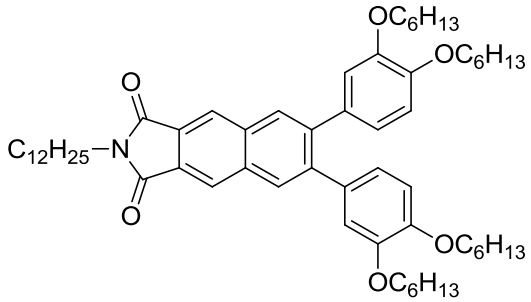

***N*-dodecyl-6,7-bis(3',4'-dihexyloxyphenyl)-2,3-naphthalenedicarboximide (21g):** 6,7-dibromo-2-dodecyl-benzo[f]isoindole-1,3-dione (0.30 g, 0.57 mmol), 1-pinacolatoboron-3,4-bis(hexyloxy)benzene (0.58 g, 1.44 mmol), $Pd(PPh_3)_4$ (0.030 g,

0.028 mmol), aq. 2.0 M K_2CO_3 (3.50 mL), ethanol (3.50 mL), and toluene (14.0 mL) were used. The crude product was purified via column chromatography (60:40 hexanes/dichloromethane) and the resulting product was recrystallized from ethanol to yield **21g** as a light yellow solid (0.34 g, 64 %). ^{1}H NMR (400 MHz, $CDCl_3$) δ: 0.89 (m, 15H), 1.33 (m, 38H), 1.50 (m, 4H), 1.68 (m, 6H), 1.82 (m, 4H), 3.73 (m, 6H), 3.99 (t, 4H, J = 7H), 6.67 (s, 2H), 6.84 (m, 4H), 8.04 (s, 2H), 8.33 (s, 2H). ^{13}C NMR (100 MHz, $CDCl_3$) δ: 13.9, 14.0, 22.5, 22.6, 25.64, 25.69, 26.9, 28.5, 29.0, 29.21, 29.24, 29.3, 29.4, 29.55, 29.59, 29.6, 31.5, 31.6, 31.8, 38.3, 69.1, 113.2, 115.7, 122.0, 124.1, 127.9, 131.1, 132.9, 134.4, 142.3, 148.53, 148.59, 168.2. HRMS (ASAP) calc'd for $C_{60}H_{87}NO_6$ *m/z* 917.6549, found 917.6533.

General procedure for the synthesis of the *N*-substituted-2,3,6,7-tetrakis(alkyloxy)-11,12-dibenz[a,c]anthracenedicarboximides (22): The desired naphthalenedicarboxyimide (1 eq) and $FeCl_3$ (6 eq) were dissolved in 50.0 mL of dichloromethane (excess). The solution was stirred at room temperature under N_2 for 30 minutes. The solution was poured into methanol (100 mL), followed by the addition of water (50 mL). The product was extracted using dichloromethane (3x50 mL). The organic layer was dried using $MgSO_4$ and purified via a short silica column (100 % dichloromethane). The solvent was removed under reduced pressure, followed by recrystallization via the conditions listed.

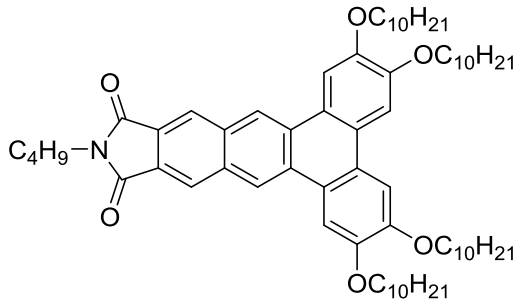

***N*-butyl-2,3,6,7-tetrakis(decyloxy)-11,12-dibenz[a,c]anthracenedicarboximide (22a):** *N*-butyl-6,7-bis(3',4'-didecyloxyphenyl)-2,3-naphthalenedicarboximide (0.25 g, 0.24 mmol), $FeCl_3$ (0.23 g, 1.45 mmol), and dichloromethane (50.0 mL) were used. The crude product was recrystallized from dichloromethane/hexanes to yield **22a** as a yellow solid (0.24 g, 96 %). ^{1}H NMR (400 MHz, $CDCl_3$) δ: 0.89 (m, 12H), 0.97 (m, 3H), 1.23 (m, 35H), 1.61 (m, 16H), 1.75 (m, 2H), 1.99 (m, 8H), 3.73 (m, 9H), 3.78 (m, 2H), 4.30 (m, 8H), 7.81 (s, 1H), 8.13 (s, 1H), 8.54 (s, 1H), 9.04 (s, 1H). ^{13}C NMR (100 MHz, $CDCl_3$) δ: 13.6, 14.0, 18.4, 20.2, 22.6, 25.3, 26.1, 29.36, 29.39, 29.5, 29.60, 29.67, 30.6, 31.9, 38.0, 58.4, 69.5, 69.6, 107.2, 107.6, 122.6, 123.9, 124.8, 125.0, 127.0, 130.4, 132.5, 149.3, 150.6, 168.1. HRMS (ASAP) calc'd for $C_{68}H_{101}NO_6$ *m/z* 1027.7659, found 1027.7629.

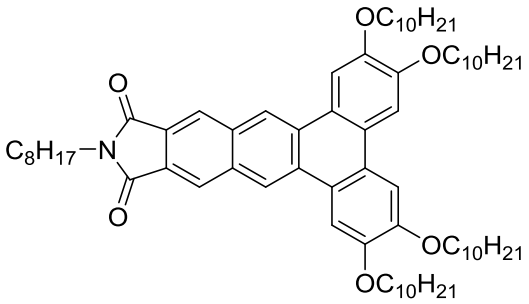

***N*-octyl-2,3,6,7-tetrakis(decyloxy)-11,12-dibenz[a,c]anthracenedicarboximide (22b):** *N*-octyl-6,7-bis(3',4'-didecyloxyphenyl)-2,3-naphthalenedicarboximide (0.23 g, 0.21 mmol), $FeCl_3$ (0.21 g, 1.29 mmol), and dichloromethane (50.0 mL) were used. The crude product was recrystallized from ethyl acetate/ethanol to yield **22b** as a yellow solid (0.15 g, 65 %). ^{1}H NMR (400 MHz, $CDCl_3$) δ: 0.89 (m, 18H), 1.23 (m, 45H), 1.61 (m, 14H), 1.76 (m, 4H), 1.97 (m, 10H), 3.78 (m, 2H), 4.31 (m, 8H), 7.81 (s, 1H), 8.13 (s, 1H), 8.55 (s, 1H), 9.05 (s, 1H). ^{13}C NMR (100 MHz, $CDCl_3$) δ: 14.06, 14.09, 22.61, 22.67, 26.1, 26.9, 28.6, 29.1, 29.2, 29.3, 29.5, 29.60, 29.68, 31.7, 31.9, 38.3, 69.5, 69.6, 107.1, 107.6, 122.6, 123.9, 124.8, 125.0, 127.0, 130.4, 132.5, 149.3, 150.6, 168.1. HRMS (ASAP) calc'd for $C_{72}H_{109}NO_6$ *m/z* 1083.8255, found 1083.8242.

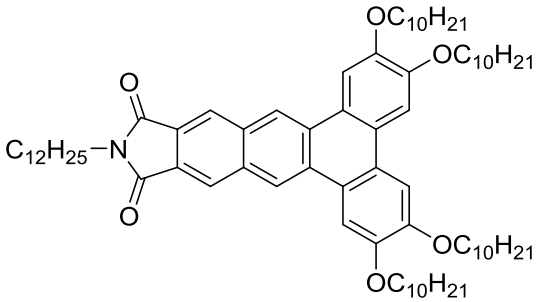

***N*-dodecyl-2,3,6,7-tetrakis(decyloxy)-11,12-dibenz[a,c]anthracenedicarboximide (22c):** *N*-dodecyl-6,7-bis(3',4'-didecyloxyphenyl)-2,3-naphthalenedicarboximide (0.25 g, 0.22 mmol), $FeCl_3$ (0.21 g, 1.31mmol), and dichloromethane (50.0 mL) were used.

The crude product was recrystallized from dichloromethane/ethanol to yield **22c** as a yellow solid (0.25 g, 99 %). ^{1}H NMR (400 MHz, $CDCl_3$) δ: 0.88 (m, 15H), 1.23 (m, 56H), 1.61 (m, 16H), 1.75 (m, 3H), 1.99 (m, 9H), 3.78 (t, 2H, J = 7 Hz), 4.31 (m, 8H), 7.81 (s, 1H), 8.12 (s, 1H), 8.54 (s, 1H), 9.03 (s, 1H). ^{13}C NMR (100 MHz, $CDCl_3$) δ: 14.0, 22.6, 26.1, 26.9, 28.6, 29.2, 29.32, 29.37, 29.50, 29.56, 29.60, 29.68, 29.7, 31.8, 31.9, 69.5, 69.6, 107.1, 107.6, 122.6, 123.9, 124.8, 125.0, 127.1, 130.4, 132.5, 149.3, 150.6, 168.1. HRMS (ASAP) calc'd for $C_{76}H_{117}NO_6$ *m/z* 1139.8881, found 1139.8850.

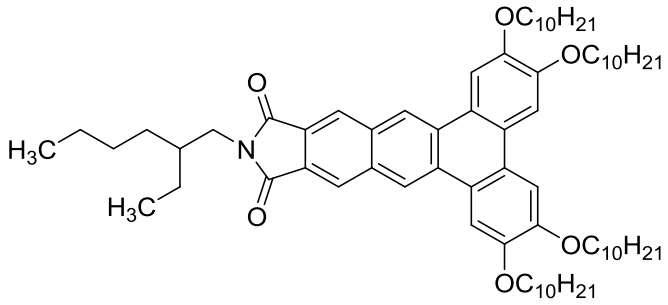

***N*-2-ethyl-1-hexyl-2,3,6,7-tetrakis(decyloxy)-11,12-dibenz[a,c]anthracenedicarboximide (22d):** *N*-2-ethyl-1-hexyl-6,7-bis(3',4'-didecyloxyphenyl)-2,3-naphthalenedicarboximide (0.25 g, 0.23 mmol), $FeCl_3$ (0.22 g, 1.38 mmol), and dichloromethane (50.0 mL) were used. The crude product was recrystallized from dichloromethane/ethanol to yield **22d** as a yellow solid (0.24 g, 97 %). ^{1}H NMR (400 MHz, $CDCl_3$) δ: 0.89 (m, 18H), 1.29 (m, 55H), 1.62 (m, 9H), 1.98 (m, 9H), 3.69 (d, 2H, J = 7 Hz), 4.30 (m, 8H), 7.79 (s, 1H), 8.09 (s, 1H), 8.50 (s, 1H), 8.99 (s, 1H). ^{13}C NMR (100 MHz, $CDCl_3$) δ: 10.4, 14.0, 14.1, 22.6, 23.0, 23.9, 26.1, 28.5, 29.3, 29.4, 29.5, 29.61, 29.68, 29.7, 30.6, 31.9, 38.2, 42.2, 69.5, 69.6, 107.1, 107.6, 122.6, 123.8, 124.7, 125.0, 126.9, 130.4, 132.4, 149.3, 150.5, 168.4. HRMS (ASAP) calc'd for $C_{72}H_{109}NO_6$ *m/z* 1083.8255, found 1083.8247.

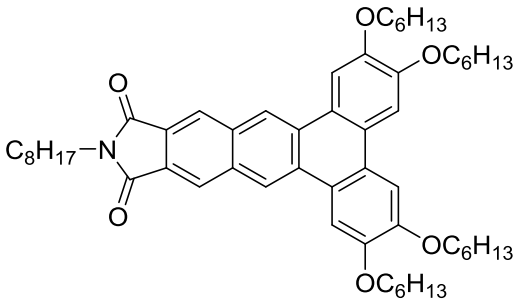

***N*-octyl-2,3,6,7-tetrakis(hexyloxy)-11,12-dibenz[a,c]anthracenedicarboximide (22e):** *N*-octyl-6,7-bis(3',4'-dihexyloxyphenyl)-2,3-naphthalenedicarboximide (0.23 g, 0.26 mmol), $FeCl_3$ (0.26 g, 1.59 mmol), and dichloromethane (50.0 mL) were used. The crude product was recrystallized from dichloromethane/ethanol to yield **22e** as a yellow solid (0.19 g, 87 %). ^{1}H NMR (400 MHz, $CDCl_3$) δ: 0.90 (m, 15H), 1.29 (m, 22H), 1.63 (m, 12H), 1.74 (m, 2H), 1.99 (m, 8H), 3.77 (t, 2H, J = 8 Hz), 4.28 (m, 8H), 7.77 (s, 1H), 8.04 (s, 1H), 8.46 (s, 1H), 8.93 (s, 1H). ^{13}C NMR (100 MHz, $CDCl_3$) δ: 14.03, 14.05, 22.61, 22.64, 22.65, 25.8, 27.0, 28.6, 29.1, 29.2, 29.3, 31.6, 31.7, 38.3, 69.4, 69.5, 107.0, 107.5, 122.5, 123.79, 124.72, 124.9, 127.0, 130.3, 132.4, 149.2, 150.5, 168.1. HRMS (ASAP) calc'd for $C_{56}H_{77}NO_6$ *m/z* 859.5754, found 859.5751.

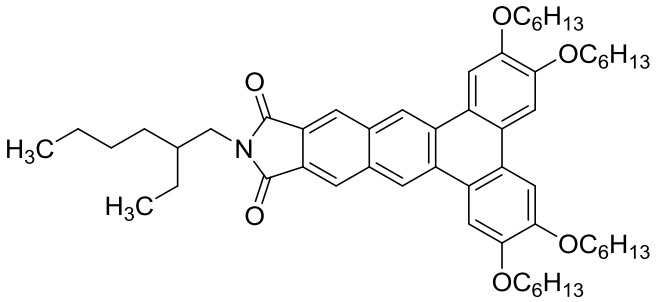

***N*-2-ethyl-1-hexyl-2,3,6,7-tetrakis(hexyloxy)-11,12-dibenz[a,c]anthracenedicarboximide (22f):** *N*-2-ethyl-1-hexyl-6,7-bis(3',4'-didecyloxyphenyl)-2,3-naphthalenedicarboximide (0.20 g, 0.23 mmol), $FeCl_3$ (0.22 g, 1.36 mmol), and

dichloromethane (50.0 mL) were used. The crude product was recrystallized from ethanol to yield **22f** as a yellow solid (0.12 g, 58 %). ^{1}H NMR (400 MHz, $CDCl_3$) δ: 0.90 (m, 18H), 1.38 (m, 19H), 1.62 (m, 13H), 1.98 (m, 9H), 3.69 (d, 2H, J = 7 Hz), 4.31 (m, 8H), 7.80 (s, 1H), 8.12 (s, 1H), 8.53 (s, 1H), 9.03 (s, 1H). ^{13}C NMR (100 MHz, $CDCl_3$) δ: 10.4, 14.03, 14.05, 22.6, 23.0, 23.9, 25.81, 25.83, 28.5, 29.33, 29.34, 30.6, 31.6, 38.3, 42.2, 69.5, 69.6, 107.1, 107.6, 122.6, 123.9, 124.7, 125.0, 127.0, 130.4, 132.5, 149.3, 150.6, 168.4. HRMS (ASAP) calc'd for $C_{56}H_{77}NO_6$ *m/z* 859.5778, found 859.5751.

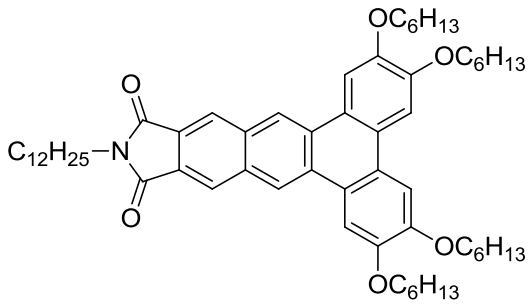

***N*-dodecyl-2,3,6,7-tetrakis(hexyloxy)-11,12-dibenz[a,c]anthracenedicarboximide (22g):** *N*-dodecyl-6,7-bis(3',4'-dihexyloxyphenyl)-2,3-naphthalenedicarboximide (0.20 g, 0.21 mmol), $FeCl_3$ (0.21 g, 1.28 mmol), and dichloromethane (50.0 mL) were used. The crude product was recrystallized from acetone to yield **22g** as a yellow solid (0.19 g, 99 %). ^{1}H NMR (400 MHz, $CDCl_3$) δ: 0.89 (m, 15H), 1.26 (m, 20H), 1.64 (m, 24H), 1.75 (m, 2H), 1.96 (m, 8H), 3.78 (t, 2H, J = 7 Hz), 4.29 (m, 8H), 7.81 (s, 1H), 8.14 (s, 1H), 8.55 (s, 1H), 9.06 (s, 1H). ^{13}C NMR (100 MHz, $CDCl_3$) δ: 14.02, 14.05, 14.09, 22.63, 22.64, 25.8, 26.9, 28.6, 29.2, 29.3, 29.50, 29.56, 29.59, 31.6, 31.8, 38.7, 69.5, 69.6, 107.1, 107.6, 122.6, 123.9, 124.8, 125.0, 127.1, 130.5, 132.5, 149.3, 150.6, 168.1. HRMS (ASAP) calc'd for $C_{60}H_{85}NO_6$ *m/z* 915.6396, found 915.6377.

References

(1) Slucken, T.J. et. al, *Crystals That Flow: Classic Papers from the history of liquid crystals*, Taylor & Francis, London, 2004.

(2) Kumar, S., *Chemistry of discotic liquid crystals : from monomers to polymers*. CRC Press: Boca Raton, 2011.

(3) Reinitzer, F. *Monatshefte für Chemie / Chemical Monthly* **1888,** *9*, 421-441.

(4) Lehmann, O. Über fliessende Krystalle. *Z. Phys. Chem.* **1889,** *4*, 462-472.

(5) Vorlander, D. *Ber. Dtsch. Chem. Ges.* **1907,** *40*, 1970-1972.

(6) Sergeyev, S.; Pisula, W.; Geerts, Y.H. *Chem. Soc. Rev.* **2007**, *36*, 1902.

(7) Ishihara, A. *J. Chem. Phys.* **1951,** *19*, 1142-1147.

(8) Alben, R. *Phys. Rev. Lett.* **1973,** *30*, 778-781.

(9) Straley, J. P. *Phys. Rev. A* **1974,** *10*, 1881-1887.

(10) Runnels, L. K.; Colvin, C., *Liquid Crystals*. Gordon and Breach: New York, 1972; Vol. 3.

(11) Chandrasekhar, S.; Sadashiva, B.K.; Suresh, K.A. *Pramana* **1977**, 9, 471 – 480.

(12) Xiao, S. X.; Myers, M.; Miao, Q.; Sanaur, S.; Pang, K. L.; Steigerwald, M. L.; Nuckolls, C. *Angew. Chem. Int. Ed.* **2005,** *44*, 7390-7394.

(13) Schmidt-Mende, L.; Fechtenkotter, A.; Mullen, K.; Moons, E.; Friend, R. H.; MacKenzie, J. D. *Science* **2001,** *293*, 1119-1122.

(14) Nelson, J. *Science* **2001,** *293*, 1059-1060.

(15) Laschat, S. *et al. Angew. Chem. Int. Ed.* **2007**, *46*, 4832.

(16) Collings, P. J.; Hird, M. In Introduction to Liquid Crystals, Gray, G. W., Goodby, J. W. and Fukuda, A., Eds.; Taylor & Francis Group: London, UK, 1997; pp 1-92, 147-194.

(17) Bisoyi, H.K.; Kumar, S. *Chem. Soc. Rev.* **2010**, *39*, 264-285.

(18) Lamgner, M.; Praefcke, K.; Kruerke, D.; Heppke, G. *J. Mater. Chem.* **1995**, *5*, 693-699.

(19) Praefcke, K., *Physical Properties of Liquid Crystals: Nematics*. INSPEC: London, U.K., 2001.

(20) Kouwer, P.H.J.; Jager, W.F.; Mijs, W.J.; Picken, S.J. *Macromolecules.* **2001**, *34*, 7582-7584.

(21) Sakashita, H.; Nishitani, A.; Sumiya, Y.; Terauchi, H.; Ohta, K.; Yamamoto, I. *Mol. Cryst. Liq. Cryst.* **1988**, *163*, 211-219.

(22) Steinke, N.; Frey, W.; Baro, A.; Laschat, S.; Drees, C.; Nimtz, M.; Hagele, C.; Giesselmann, F. *Chem.-Eur. J.* **2006,** *12*, 1026-1035.

(23) Pecchia, A.; Movaghar, B.; Kelsall, R.W.; Bourlange, A.; Evans, S.; Howson, M.; Shen, T.; Boden, N. *Microelectron. Eng.* **2000**, *51-52*, 633-644.

(24) Hatsusaka, K.; Ohto, K.; Yamamoto, I.; Shirai, H. *J. Mater. Chem.* **2001**, *11*, 423-433.

(25) Ichihara, M.; Suzuki, A.; Hatsusaka, K.; Ohta, K. *Liq. Cryst.* **2007**, *34*, 555-567.

(26) Dean, J. A., *Analytical chemistry handbook*. McGraw-Hill: New York, 1995.

(27) West, A. R., *Basic solid state chemistry*. 2nd ed.; John Wiley & Sons: New York, 1999; p xvi, 480 p.

(28) Chandrasekhar, S.; Sadashiva, B.K.; Suresh, K.A. *Mol. Cryst. Liq. Cryst.* **2003**, *397*, 295-305.

(29) Chandrasekhar, S.; Sadashiva, B.K.; Suresh, K.A.; Madhusudana, N.V.; Kumar, S.; Shashidhar, R.; Venkatesh, G. *J. Phys.* **1979**, *C3*, 120-124.

(30) Lillya, C.P.; Thakur, R. *Mol. Cryst. Liq. Cryst.* **1989**, *170*, 179-183.

(31) Goozner, R. E.; Labes, M. M. *Mol. Cryst. Liq. Cryst.* **1979,** *56*, 75-81.

(32) Frank, F. C.; Chandrasekhar, S. *J. Phys.-Paris* **1980,** *41*, 1285-1288.

(33) Usol'tseva, N.; Praefcke, K.; Smirnova, A.; Blunk, D. *Liq. Cryst.* **1999,** *26*, 1723-1734.

(34) Billard, J.; Dubois, J.C.; Tinh, N.H.; Zann, A. *J. Chim.* **1978**, *2*, 535-540.

(35) Kumar, S. *Liq. Cryst.* **2004**, *31*, 1037-1059.

(36) Kumar, S. *Liq. Cryst.* **2005**, *32*, 1089-1113.

(37) Berresheim, A.J.; Muller, M.; Mullen, K. *Chem. Rev.* **1999**, *99*, 1747-1786.

(38) Mende, L.S.; Fechtenkotter, A.; Mullen, K.; Moons, E.; Friend, R.H.; Mackenzie, J.D. *Science.* **2001**, *293*, 1119-1122.

(39) Bendikov, M.; Wudl, F.; Perepichka, D. *Chem. Rev.* **2004**, *104*, 4891-4945.

(40) van de Craats, A.M.; Warman, J.M. *Adv. Mater.* **2001**, *13*, 130-133.

(41) Lynett, P.T.; Maly, K.E. *Org. Lett.* **2009**, 11, 3726-3729.

(42) Lau, K.; Foster, J.; Williams, V. *Chem. Commun.* **2003**, 2172-2173.

(43) Foster, E. J.; Jones, R. B.; Lavigueur, C.; Williams, V. E. *J. Am. Chem. Soc.* **2006**, *128*, 8569-8574.

(44) Praefke, K.; Eckert, A.; Blunk, D. *Liq. Cryst.* **1997**, *22*, 113-119.

(45) Kumar, S.; Manickam, M. *Mol. Liq. Cryst.* **1998**, *309*, 291-295.

(46) Bushby, R.J.; Boder, N.; Kilner, G.A.; Lozman, O.R.; Lu, Z.B.; Liu, Q.; Thornton-Pett, M. *J. Mater. Chem.* **2003**, *13*, 470-474.

(47) Destrade, C.; Mondon, M., C.; Malthete, J. *J. Phys. Colloques* **1979,** *40*, C3-17-C3-21.

(48) Yin, J.; Hemi, Q.; Zhang, K.; Luo, J.; Zhang, X.; Chi, C.; Wu, J. *Org. Lett.* **2009**, *11*, 3028-3031.

(49) Reczek, J.J.; Leight, K.R.; Esarey, B.E.; Murray, A.E. *Chem. Mater.* **2012,** *24*, 3318-3328.

(50) Bengs, H.; Ebert, M.; Karthaus, O.; Kohne, B.; Praefke, K.; Ringsdorf, H.; Wendorf, J.; Wusterfeld, R. *Adv. Mater.* **1990**, *2*, 141-144.

(51) Wang, J.Y.; Yan, J.; Ding, L.; Ma, Y.; Pei, J. *Adv. Funct. Mater.* **2009**, 1746-1752.

(52) Liu, K.; Wang, C.; Li, Z.; Zhang, X. *Angew. Chem. Int. Ed.* **2011**, *50*, 4952-4956.

(53) Ringsdorf, H.; Wustefeld, R.; Zerta, E.; Ebert, M.; Wendorff, J. H. *Angew. Chem., Int. Ed. Engl*. **1989**, *28*, 914−918.

(54) Alvey, P.M.; Reczek, J.J.; Lynch, V.; Iverson, B.L. *J. Org. Chem.* **2010**, *75*, 7682-7690.

(55) Reczek, J.J.; Villazor, K.R.; Lynch, V.; Swager, T.M.; Iverson, B.L. *J. Am. Chem. Soc*. **2006**, *128*, 7995−8002.

(56) Pisula, W.; Kastler, M.; Wasserfallen, D.; Robertson, J.W.F.; Nolde, F.; Kohl, C.; Müllen, K. *Angew. Chem., Int. Ed.* **2006**, *45*, 819−823.

(57) Bahadur, B. e., *Liquid Crystals: Applications and Uses*. World Scientific: Singapore, 1990; Vol. 1-3.

(58) Boden, N.; Bushby, R. J.; Clements, J.; Movaghar, B. *J. Mater. Chem.* **1999,** *9*, 2081-2086.

(59) Scott, J. C. *Nature* **1994,** *371*, 102.

(60) Mori, H. *J. Disp. Technol.* **2005,** *1*, 179-186.

(61) Brabec, C. J., *Organic photovoltaics : concepts and realization*. Springer: New York, 2003; p xii, 297 p.

(62) de Freitas, J. N.; Nogueira, A. F.; De Paoli, M. A. *J. Mater. Chem.* **2009,** *19*, 5279-5294.

(63) Bacher, A.; Bleyl, I.; Erdelen, C. H. **1997,** *9*, 1031-1035.

(64) Stapff, I. H.; Stumpflen, V.; Wendorff, J. H.; Spohn, D. B.; Mobius, D. L*iq. Cryst.* **1997,** *23*, 613-617.

(65) Boden, N.; Borner, R. C.; Bushby, R. J.; Cammidge, A. N.; Jesudason, M. V. *Liq. Cryst.* **1993,** *15*, 851-858.

(66) Christ, T.; Glusen, B.; Greiner, A.; Kettner, A.; Sander, R.; Stumpflen, V.; Tsukruk, V.; Wendorff, J. H. *Adv. Mater.* **1997,** *9*, 48-52.

(67) Paraschiv, I.; Giesbers, M.; van Lagen, B.; Grozema, F. C.; Abellon, R. D.; Siebbeles, L. D. A.; Marcelis, A. T. M.; Zuilhof, H.; Sudholter, E. J. R. *Chem. Mater.* **2006,** *18*, 968-974.

(68) Laschat, S.; Baro, A.; Steinke, N.; Giesselmann, F.; Hagele, C.; Scalia, G.; Judele, R.; Kapatsina, E.; Sauer, S.; Schreivogel, A.; Tosoni, M. *Angew. Chem. Int. Ed.* **2007,** *46*, 4832-4887.

(69) Ong, C. W.; Liao, S. C.; Chang, T. H.; Hsu, H. F. *J. Org. Chem.* **2004,** *69*, 3181-3185.

(70) Voisin, E.; Foster, E. J.; Rakotomalala, M.; Williams, V. E. *Chem. Mater.* **2009,** *21*, 3251-3261.

(71) Ichihara, M.; Suzuki, H.; Mohr, B.; Ohta, K. *Liq. Cryst.* **2007**, *34*, 401-410.

(72) Akopova, O.B.; Bronnikova, A.A.; Kruvchinskii, A.; Kotovich, L.N.; Shabyshev, L.S.; Valkova, L.A. *J. Struct. Chem.* **1998**, *3*, 376-383.

(73) Paquette, J.A.; Yardley, C.J.; Psutka, K.M.; Cochran, M.A.; Calderon, O.; Williams, V.E.; Maly, K.E. *Chem. Commun.* **2012**, *48,* 8210-8212.

(74) Paquette, J.A. MSc. Thesis, Wilfrid Laurier University, 2012.

(75) Psutka, K.; Williams, J.; Paquette, J.; Schneider, A.; Maly, K. *Manuscript in preparation.*

(76) Dini, D.; Calvete, M.; Hanack, M.; Pong, R.; Flom, S.; Shirk, J. *J. Phys. Chem. B.* **2006,** *110,* 12230-12239.

(77) Foster, E.J.; Lavigueur, C.; Ying-Chieh, K.; Williams, V.E. *J. Mater. Chem.* **2005**, *15*, 4062-4068.

(78) Ventura, B.; Langhals, H.; Böck, B.; Flamigni, L. *Chem. Commun*. **2012**, *48,* 4226-4228.

(79) Tian, H.; Liu, P.H.; Zhu, W.; Gao, E.; Wu, D.J.; Cai, S. *J. Mater. Chem*. **2000**, *10,* 2708-2715.

(80) Berberich, M.; Krause, A.M.; Orlandi, M.; Scandola, F.; Würthner, F. *Angew. Chem. Int. Ed*. **2008**, *47,* 6616-6619.

(81) Wilson, T.M.; Tauber, M.J.; Wasielewski, M.R. *J. Am. Chem. Soc*. **2009**, *131,* 8952-8957.

(82) Katz, H. E.; Johnson, J.; Lovinger, A. J.; Li, W. *J. Am. Chem. Soc.* **2000**, *122*, 7787-7792.

(83) Bullock, J. E.; Vagnini, M. T.; Ramanan, C.; Co, D. T.; Wilson, T. M.; Dicke, J. W.; Marks, T. J.; Wasielewski, M. R. *J. Phys. Chem. B* **2010,** *114*, 1794−1802.

(84) Erten-Ela, S.; Turkmen, G. *Renew. Energy* **2011**, *36*, 1821−1825.

(85) Boobalan, G.; Imran, P.S.; Nagarajan, S. *Chin. Chem. Lett.* **2012**, *23*, 149-153.

(86) Langhals, H.; Kirner, S. *Eur. J. Org. Chem.* **2000**, *2*, 365-380.

(87) Zhan, X.; Facchetti, A.; Barlow, S.; Marks, T. J.; Ratner, M. A.; Wasielewski, M.R.; Marder, S.R. *Adv. Mater*. **2011**, *23*, 268−284.

(88) Osawa, T.; Kajitani, T.; Hashizume, D.; Ohsumi, H.; Sasaki, S.; Takata, M.; Koizumi, Y.; Saeki, A.; Seki, S.; Fukushime, T.; Aida, T. *Angew. Chem.* **2012**, *51*, 7990-7993.

(89) Baathulaa, K.; Xu, Y.; Qian, X. *J. Photochem. Photobiol. A.* **2010**, *216*, 24-34.

(90) Reichardt, C. *Chem. Rev.* **1994**, *94*, 2319-2358.

(91) Buncel, E.; Rajagopal, S. *Acc. Chem. Res.* **1990**, *23*, 226-231.

(92) Marini, A.; Mun oz-Losa, A.; Biancardi, A.; Mennucci, B. *J. Phys. Chem. B* **2010**, *114*, 17128-17135.

(93) Patrick, C. R.; Prosser, G. S. *Nature (London)* **1960**, 1021.

(94) Percec, V.; Imam, M.; Peterca, M.; Wilson, D.; Graf, R.; Spiess, H.; Balagurusamy, V.; Heiney, P. *J. Am. Chem. Soc.* **2009,** *131*, 7662-7677.

(95) Ong, C.W.; Hwang, J.Y.; Tzeng, M.C.; Liao, S.C.; Hsu, H.F.; Chang, T.H. *J. Mater. Chem*. **2007**, *17*, 1785–1790.

(96) Mohr, B.; Wegner, G.; Ohta, K. *J. Chem. Soc. Chem. Comm.* **1995**, 995-996.

(97) Mohr, B.; Enkelmann,V.; Wegner,G. *J. Org. Chem.* **1994**, *59*, 635–638.

(98) Chen, Z.H.; Swager, T.M. *Org. Lett.*, **2007**, *9*, 997–1000.

(99) Yeh, M. ; Su, Y. ; Tzeng, M.; Ong, C.W.; Kajitani, T.; Enozawa, H.; Takata, M.; Koizum, Y.; Saeki, A.; Seki, S.; Fukushima, T. *Angew. Chem. Int. Ed.* **2013**, *52*, 1031-1034.